THE UNIVERSITY OF MICHIGAN

INDUSTRY PROGRAM OF THE COLLEGE OF ENGINEERING

THE STUDY OF PARTICLE-LIQUID COCURRENT DOWNWARD FLOW THROUGH A TUBE WITH A RESTRICTING ORIFICE END FOR APPLICATION TO A MOBILE FUEL NUCLEAR REACTOR SYSTEM

Wan Yong Chon

A dissertation submitted in partial fulfillment
of the requirements for the degree of
Doctor of Philosophy in The
University of Michigan
1960

September, 1960

IP-460

ensm
UMR1156

Doctoral Committee:

Associate Professor Frederick G. Hammitt, Chairman
Professor Robert C. F. Bartels
Professor Lloyd E. Brownell
Professor John A. Clark
Professor Henry J. Gomberg
Dr. Wayne H. Jens, Atomic Power Development Associates, Inc.
Evan C. Kovacic, Atomic Power Development Associates, Inc.
Professor Richard K. Osborn

ACKNOWLEDGMENTS

The author wishes to express his sincere appreciation to Dr. Frederick G. Hammitt, Chairman of the Doctoral Committee, for his constant guidance and encouragement. Deep appreciation is devoted to Dr. Henry J. Gomberg, head of the Nuclear Engineering Department and a member of the committee, without whose absolute support the author could not have continued and completed his work.

The utmost gratitude is extended to Mr. Evan C. Kovacic, who gave the author the original suggestion of this problem, the opportunity of obtaining the sponsorship of Atomic Power Development Associates, Inc., (APDA) and further, was a constant source of encouragement and helpful advice throughout the investigation.

Dr. Wayne H. Jens, Assistant Technical Director of APDA, has showed constant interest and invarient support to this investigation, and is thus to be acknowledged.

The author naturally extends his appreciation to Dr. R. C. F. Bartels, Dr. L. E. Brownell, Dr. John A. Clark, and Dr. Richard K. Osborn for their untiring guidance as members of the Doctoral Committee during the investigation.

The whole work is dedicated by the author to his wife, Keum Sook Chon, and his mother, Songok-Oh Chon, since without their firm moral supports and courageous sacrifices in many ways and for many years, this work would never be completed toward the end.

TABLE OF CONTENTS

Page

LIST OF TABLES

LIST OF FIGURES

NOMENCLATURE

a	Intercept coefficient, dimensionless
b	Slope coefficient, dimensionless
c	Drag coefficient, dimensionless
D_o	Orifice diameter, cm
D_p	Particle diameter, cm
f	Friction factor, dimensionless
f_m	Modified friction factor, dimensionless
F_a	Empirical factor, dimensionless
F	Ratio of variance, dimensionless
F_{excess}	Excess flow rate, $\frac{cc}{min}$
F_s	Particle flow rate, $\frac{cc}{min}$
F_ℓ	Liquid flow rate, $\frac{cc}{min}$
g	Gravity constant, 981 cm/sec^2
G	Mass flow rate, $g/sec\text{-}cm^2$
K	Empirical coefficients, dimensionless
L	Length of tube, cm
l,m,n	Numbers, dimensionless
P	Pressure, g/cm^2, $"H_2O$
r	Correlation coefficient, dimensionless
R	Ratio, the tube diameter to orifice diameter, dimensionless
Re	Reynolds number, dimensionless
Re_m	Modified Reynolds number, dimensionless
Re_o	In-orifice modified Reynolds number, dimensionless
U	Velocity, cm/sec
ϵ	Void fraction, dimensionless

ϕ_s	Shape factor, dimensionless
ρ	Density, g/cm^3
ρ_F	Fluid density, g/cm^3
μ	Absolute viscosity, g/sec-cm
σ	Variance, arbitrary unit
Σ	Summation notation
η	Ratio, particle flow rate to total flow rate, dimensionless
π	Notation, dimensionless group, dimensionless

INTRODUCTION

A fast breeder nuclear reactor employing a mobile fuel system shows real promise of being able to produce electrical energy at a price competitive with conventional fossil fuel power plants. Such a reactor would have several significant advantages to the fixed fuel types of reactors. Use of a mobile fuel system eliminates the need for the complex mechanical components for handling fuel. Fuel cycle costs would be reduced by low fuel fabrication costs and improved irradiation stability. In addition, the mobile fuel systems would be amenable to on-site fabrication and reprocessing as an integrated part of plant operations. Before such a reactor plant could be built, however, the major technological problems associated with achieving a mobile fuel system must be solved.

Several ways of achieving fuel mobility may be considered for fast breeder reactors. In order to achieve a fast neutron spectrum the fuel system cannot utilize a medium with good moderating properties. Also, in order to accommodate the high power densities and to permit attainment of high steam temperatures, it is required that the fuel system utilize a liquid metal medium. Several types of mobile fuel systems employing a liquid metal medium have been considered, eg.,

1. Fuel in molten metal solution.
2. Fuel particle suspension in a molten metal, i.e., Slurry system.

3. Molten fuel.

4. Closely packed fuel particles in a liquid metal carrier, i.e., "Paste System".

Among these approaches, the first one is regarded as infeasible because of limited solubilities of uranium and/or plutonium in liquid metals of interest. The second system, a slurry of solid fuel particles in a molten metal, is unstable and tends to settle into a more dense system and increase the reactivity of the system. Furthermore, the technological problems confronting the slurry fuel system concepts are known to be extremely difficult to solve. The third system, a molten fuel, even though being studied by some investigators, is subject to difficult material problems since the corrosion rates reported are very high. Unless a breakthrough in obtaining highly corrosion-resistant container material under the severe condition is achieved, the system can be regarded as still impractical. The fourth, and the last approach, however, seems most promising. Here, the fuel is in the form of very closely packed particles in a liquid metal carrier -- so closely packed that they are essentially at settled density -- and is moved through the reactor at comparatively low velocity. This type does not present any serious material problems and still gives necessary fuel density needed for the fast reactor core. In some ways, this system can be regarded as a compromise among these possible fuel systems mentioned above.

Once this system -- called "paste system" henceforth -- is taken up seriously, several inevitable questions arise. What is the maximum density at which paste will flow in various possible conduit geometries? What is the magnitude of pressure drop through the various paste flow paths and how is this related to solid and liquid flow rates? In more general terms,

would it be possible to obtain any general quantitative and dependable correlations among the related physical quantities so that one can design and control a fast reactor employing a fuel system of this type?

To obtain some basic understandings of the problem, Atomic Power Development Associates, Inc. in Detroit, Michigan, has sponsored projects at Southern Research Institute in Alabama and the University of Michigan in Michigan. Similar studies have been recently initiated by Los Alamos Scientific Laboratory. The results of the work done at the former institutions include some valuable, but nevertheless preliminary, findings; and the work conducted by the latter has not yet been published.

The flow study for upward paste flow through a hairpin type U tube, on which the main emphasis was placed at the University of Michigan, clarifies the basic characteristics of upward cocurrent flow of solids and of a liquid such as water. The work confirms that Leva's correlation (29, 30), developed originally for a fixed bed system, can be applied to the moving bed under sets of somewhat restricted conditions. On the other hand, the experimental data obtained at Southern Research Institute on downward flow of paste beds is based on actual uranium-sodium and uranium oxide-sodium systems, and are valuable in that sense, but the exit conditions employed in the experiments are not likely to be realized in an actual nuclear fuel system. Thus far no theoretical or empirical correlation had been developed for the SRI data prior to the present work.

It was discovered, however, by the author of this paper in a preparatory stage of the work, that the above data obtained at Southern Research Institute can be interpreted by a typical moving bed correlation, such as Happel's, as far as the excess liquid flow rate of the liquid and

the frictional pressure drop of liquid through the moving bed in a straight tube section are concerned. But it was found that there was no available correlation through which absolute particle flow rate or absolute liquid flow rate can be estimated. In fact, the liquid-sodium, two phase flow through the orifice which restricts the flow at the end of the flow tube, is now found as the most important aspect of the total physical picture, in the sense that it does define the absolute physical quantities of the system. Very few investigations have been found to exist on this subject, while orifice theory as well as working formula for single phase flow have been established fairly well.

Considering the variety of fuel particle -- carrier liquid combinations which could be used in the mobile fuel reactors as shown in Table I, the need of rather general correlations among the associated physical variables should be definitely recognized before any preliminary design is attempted. Therefore, the problems which are vital in the evaluation and control of fluid characteristics of this type of reactor remain to be solved.

TABLE I

EXAMPLE OF POSSIBLE PASTE FUEL SYSTEM

Fuel Particles and Approximate Composition	Carrier Liquid
1. Metal Alloy	1. Sodium
a. 20 w/o Pu; 70 w/o U; 10 w/o Fissium*	2. NaK
b. 90 w/o U; 10 w/o Mo	3. Lithium
2. Metal Alloy with Metal Surface Coating	4. Bismuth
a. 20 w/o Pu; 70 w/o U; 10 w/o Fissium*	
b. 90 w/o U; 10 w/o Mo	
3. Oxide	
a. 50 w/o PuO_2; 50 w/o UO_2	
b. UO_2	
4. Carbide	
a. 33 w/o PuC; 67 w/o UC	
b. UC	

* Remaining fission products in the reprocessed fuel elements.

RELATED LITERATURE SURVEY

A rather extensive literature survey has been carried out in connection with the present work. Since it was found that very few investiations have been carried out on the bed moving through orifices under imposed liquid pressures, except some fragmentary work previously mentioned, the survey had to be mainly on related subjects.

Fixed Bed System With Vertical Flow

Many studies have been carried out on the flow of fluids through fixed beds since as early as 1856. Leva (29, 30) reviews a series of classic works; and among them are such empirical equations as developed by Muskat (35) who obtained the following equation from data on the flow of air through glass beads and sands.

$$\Delta p = K (U\rho)^{3/4}$$

Where ρ = air density

U = air velocity

Δp = pressure drop

K = empirical coefficients

White (29) first recognized the role of Reynolds.number and gave the correlation in the form

$$\frac{\Delta p}{L} = \frac{2f \rho U^2 Fa}{g D_p}$$

Where f = friction factor

g = gravity constant

D_p = particle diameter

L = length of bed

Fa = empirical factor dependent on particle sizes

ρ = fluid density

Fujita and Uchida (29) passed gases through beds of broken limestones and expressed their results as

$$\frac{\Delta p}{\rho L} = A \left(\frac{U^2}{2gD_p}\right)^{l} (Re)^{m} \left(\frac{Dt}{Dp}\right)^{n}$$

Where l and n = function of packing

A and m = function of both packing and Reynolds number

Other notations are conventional as shown in Nomenclature.

Bakhmetett and Feodoroff (29) followed a somewhat different approach and expressed their results in terms of friction factor. Comparatively recently, Happel (23) correlated friction factor versus Reynolds number and obtained the expression

$$f = \frac{\Delta p \, D_p \, g_c \rho}{LG^2 (1-\epsilon)^3}$$

Where $1-\epsilon$ is the solid volume ratio.

Happel reported that, for the laminar range

$$f = 103 / Re$$

and for the turbulent region,

$$f = 207 / (Re)^{0.22}$$

Prior to Happel's work, Brownell and Katz (7) developed the expression for pressure drop by means of a dimensionally homogeneous equation. Max Leva (29) combined Happel's modified friction factor and the Kozeny-Carman type equation to obtain

$$\Delta p = \frac{2f\, G^2\, L\, (1-\epsilon)^{3-n}}{D_p\, \phi_s^{3-n}\, \epsilon^3\, g_c\, \rho_F}$$

For Reynolds number less than ten, the flow is laminar and $n \simeq 1.0$. For Reynolds number greater than one hundred, the flow tends to become turbulent and n approaches 2. The modified friction factor is a function of Reynolds number in a similar fashion. Thus, for the laminar flow range, $f = 100\, (D_p G / \mu)^{-1.0}$. The substitution of this value of f and $n = 1.0$ into the Kozeny-Carman equation yields

$$\Delta p = \frac{200 G \mu L\, (1-\epsilon)^2}{D_p^2\, \phi_s \rho_F\, g_c\, \epsilon^3}$$

It is this correlation that Calvert (12) used in interpreting his upward cocurrent paste flow system.

Moving Bed System With Vertical Flow

Several papers have appeared since 1947, among them the most prominent is Happel's work (23). The work will be specifically discussed in a later chapter.

Solid-Fluid Two-Phase Flow Through Orifices

Almost no work on two phase (i.e.: liquid and solid) flow through an orifice has been taken up seriously until the present time. Several investigations (34), which appeared mostly after World War II are of free fall gravity flow type, where no positive drag force on the solid particles are exerted by a liquid phase. These systems did not employ two phase flow in a true sense, although the fluid phase existed around the solid particles.

Recently, however, Calvert (10, 11) obtained some empirical data on the subject and tried to find the empirical equation which correlates the solid flow rate with orifice pressure drop among other physical variables. The equation is expressed as below.

$$W = \frac{\Delta P_o - Q/\rho_p - C_5}{2.303 \ell a/Do + m D_p + C_4}$$

Where W = solid flow rate

Δp_o = orifice pressure drop

ρ_p = density of particle

D_o = orifice diameter

D_p = particle diameter

Others are constants.

The equation may be useful in giving an estimation of the orifice pressure drop and solid flow rates for a water carrier system even though the position of the pressure tap above the orifice was taken rather arbitrarily in his experiments; and there is no way of coupling the orifice pressure drop with the total pressure drop across the flow tube. In spite of these restricted conditions, this work is noted to be

the first serious attempt to handle the general problem of two phase flow through an orifice.

Solid-Fluid Two-Phase Flow Through Horizontal Tube

Horizontal flow of slurries and a related correlation was introduced by Lowenstein (31) recently, who reviews a work done in Britain. This scheme of system, however, will not bear direct connection with the present problem.

APPLICABILITY OF EXISTING CORRELATIONS TO THE PASTE FUEL REACTOR CONCEPT AND ITS LIMIT

As a preliminary study of the paste system, the existing data for uranium-sodium, uranium oxide-sodium, and uranium oxide-water systems obtained at Southern Research Institute, have been tested along the straight tube section with some of the typical moving bed correlations, such as Happel's (24). As shown in Fig. (1), very few of the data points deviate from Happel's curve by as much as fifty per cent in the modified friction factor, (which cover a range of 3 decades) and the probable deviation seems to be around twenty-five per cent. Considering the fact that Happel developed his correlation with data taken for gas-solid two phase flow, the accuracy obtained for the uranium-sodium as well as uranium oxide-water type systems is certainly surprising. This result strongly indicates the existence of similarities between the systems in the first place. Secondly, this also implies that some of the physical quantities such as buoyancy of particles may not be important in the mechanism of pressure drop. Thus the correlation based on free fall type particle flow such as the one mentioned in the preceding chapter, seems not applicable to this scheme of mass transfer.

Happel's Correlation

Happel established the effect of void fraction on the relationship which governs two phase flow. After a mathematical derivation of the manner in which void fraction affects the correlation, he suggests a modified Reynolds number $N_{Re,mod} = N_{Re}(1-\epsilon)$ and a modified friction factor

$f_{mod.} = f/(1-\epsilon)^3$ where ϵ is the void fraction in the bed. The correlation is then a log-log plot of $N_{Re,\,mod.}$ versus $f_{mod.}$

The basic correlation as well as definitions are as follows:

$$N_{Re} = D_p G / \mu$$

Where

N_{Re} = Reynolds number

D_p = Average particle diameter (cm)

G = Excess fluid flow rate per unit area of total channel (g/sec - cm^2)

μ = fluid viscosity (g/ sec - cm)

$$f = \frac{g \Delta p\, D_p \rho}{2LG^2}$$

Where

f = friction factor (dimensionless)

g = gravity constant (981 cm/sec^2)

$\Delta p/L$ = pressure gradient in bed (g/cm^3)

D_p = average particle diameter (cm)

ρ = fluid density (g/cm^3)

Excess Fluid Flow Rate

The excess fluid flow rate, which is one of the prominent factors in determining the pressure drop across the tube, is the total fluid less that amount associated with the solid. Thus, if total flow = 38.3 cc/min,

solids flow = 15.9 cc/min, and bed density 59 vol % solid, then the flow of settled paste = 15.9/0.59 = 26.9 cc/min. Thus flow of excess liquid = 38.3 - 26.9 = 11.4 cc/min.

TABLE II

EXAMPLE OF S.R.I. DATA

Flow Properties of 100/140 Mesh UO_2- Na Paste
(0.075" tapered orifice at 310°C)

Pt/L	Total Flow		Solid Flow		Paste Composition
"H_2O"	g/sec	cc/min	g/sec	cc/min	Vol % Solids
4.2	2.9	38.3	2.6	15.9	59.0
6.3	3.9	49.1	3.4	20.4	61.7
10.4	5.1	65.4	4.5	26.9	63.5
15.1	6.3	80.9	5.6	32.5	63.5

In the first line of the data presented above,

$$G = \frac{(11.4)\ (0.8815)^*}{(60)\ (0.713)^*} = 0.235 \text{ g/sec cm}^2$$

$^* \rho_{Na} = 0.8815 \text{ g/cm}^3$ at 310°C

* Tube I.D. = 0.375" so cross-sectional area = 0.713 cm^2

$$N_{Re,\ Mod.} = DpG/\mu$$

$$= \frac{0.0126\ (0.235)}{0.00339}$$

$$= 0.873$$

$$N_{Re,\ Mod.} = N_{Re}\ (1 - \epsilon)$$

$$= (0.873)\ (0.59)$$

$$= 0.51$$

Close examination of the original experimental conditions and proper corrections of pressure gradients give P/L = 9" H_2O/" or 9 gr/cm^3 for total flow rate of 38.3 cc/min.

Thus

$$f = \frac{g \Delta P D_p \rho}{2LG^2}$$

$$= \frac{(981)(9)(0.0126)(0.8815)}{2(0.235)^2}$$

$$= 898$$

$$f \text{ Mod.} = f/(1-\epsilon)^3$$

$$= 4400$$

As observed in Fig. 1, the general agreement is excellent for all of the experimental data.

Discussion

As far as the pressure gradient through the straight tube is concerned, the Happel type moving bed correlation was found to be satisfactorily applicable. This implies that excess velocity and the subsequent drag force applied on each particles contribute to the pressure drop across the vertical straight tube section in the uranium-sodium system as Happel assumed in his particle-gas carrier system.

However, in the design of a paste reactor subassembly or in any other practical application of the moving bed, the excess velocity between the fluid and the solid, which is the basis for the correlation, is not known. Rather, the problem will be usually stated as follows. "For a given solid flow rate, what pressure gradient will be experienced under a given set of physical conditions?" Or conversely, "For a given available pressure

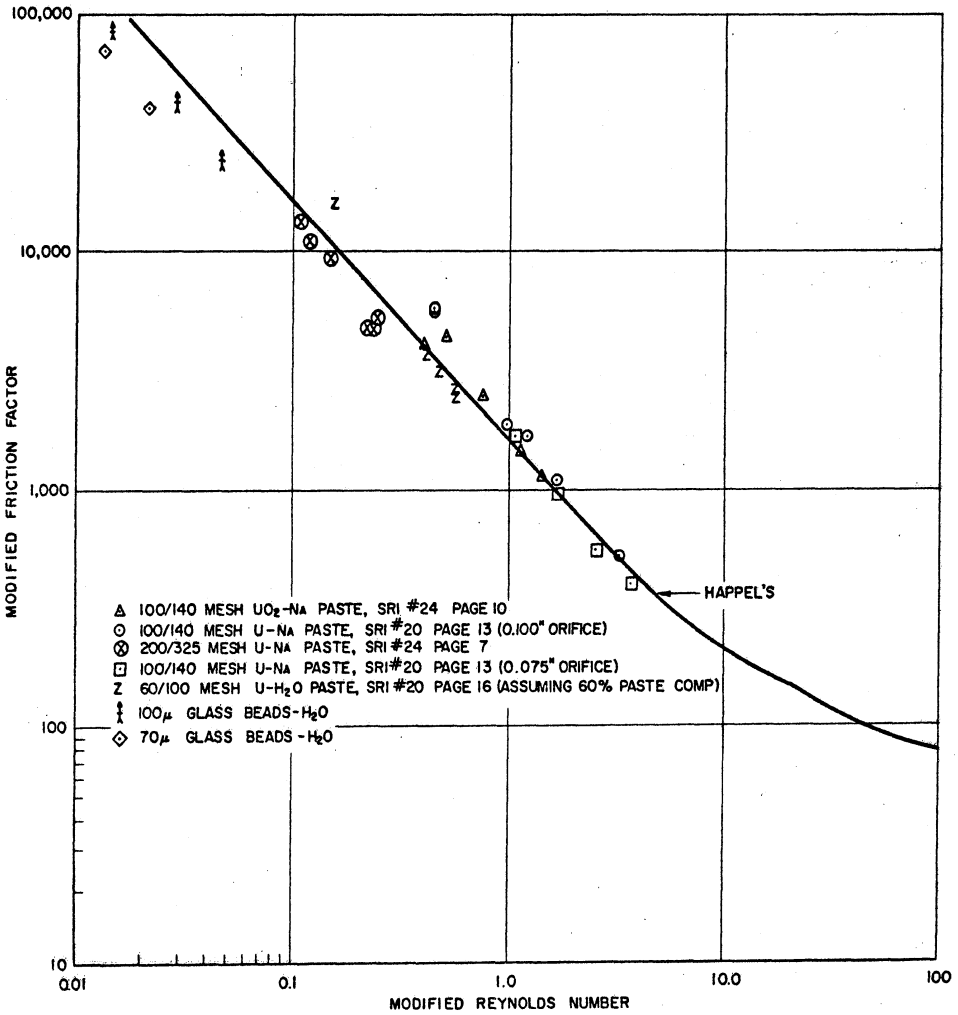

FIG. 1 MODIFIED FRICTION FACTOR AS A FUNCTION OF MODIFIED REYNOLDS NUMBER

gradient as well as other physical conditions, what solid flow rate is possible?" The problem, which cannot be solved by any presently existing two phase correlation, is then to determine the relationships between solid flow rate, and excess liquid flow rate, and the relation appears to be governed particularly by the orifice conditions, particle conditions, and liquid conditions among others.

STATEMENT OF THE PROBLEM TO BE SOLVED

As has been observed, the presently available information on the fluid flow characteristics of the paste-type system is quite restricted. Even though the relation between the excess velocity and other physical variables can be handled quantitatively using the conventional two phase moving bed correlations, it is merely one aspect of the whole physical picture. There has been very little work done to correlate absolute solid flow rate with other variables for two phase flow through a tube ligament with an end orifice. The two phase flow near the orifice may be difficult to analyze and yet a basic understanding and quantitative treatment of the effect combined with the flow in the rest of flow tube, are essential to the solution of the overall two phase fluid flow problem.

Basic Geometry

A schematic diagram of a conceptual paste type reactor core is shown in Fig. 2. Fuel particles are continuously carried into the core by a carrier sodium stream from the top of the reactor and settle on the bed already formed in the core. After descending the flow path, the particles are exhausted through the restricting orifices. It is noted that the orifice is washed by a stream of sodium and the leaner downstream portion is carried away outside the core. If one considers a single flow ligament only, then the basic geometry in which one is interested will become such as the one shown in Fig. 3. It will be seen easily that the flow regimes handled by most of the previous investigators, including Happel, are all concerned with the Region I in the figure. Partially satisfactory correlations are already available for this region. Region II coupled with Region

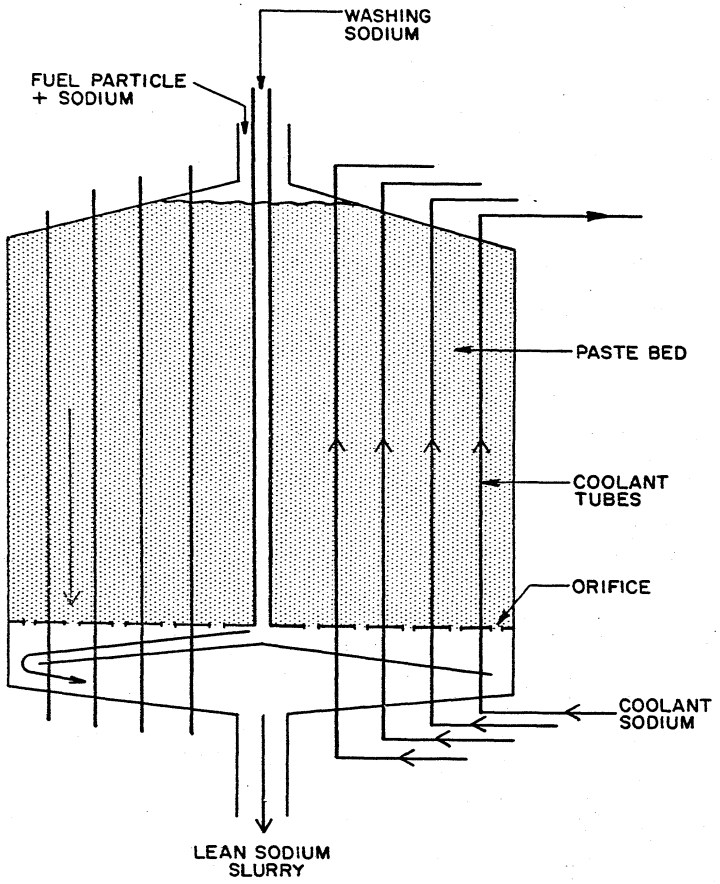

FIG. 2 SIMPLIFIED DIAGRAM OF PASTE-TYPE REACTOR

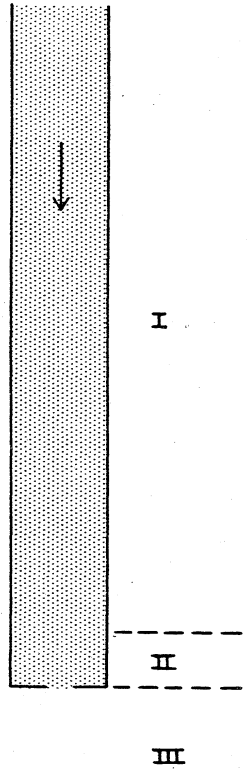

FIG. 3 SINGLE FLOW LIGAMENT

III is now the main portion where a new contribution has been made. It should be mentioned at this point that the orifice will be immersed (washed) in a liquid phase such as sodium, rather than being exposed in a gas phase, in an actual system.

Statement of Problem

Considering the basic geometry and configurations described above, and also reviewing the discussions covered in the preceding chapters, the problem to be solved may be well stated as follows.

Find the general correlations which govern the particle-liquid two phase cocurrent downward flow through a tube with a restricting orifice end, the emphasis always being on the application to a mobile fuel system in a nuclear reactor. The physical variables which are to be investigated should include the following:

1. particle size
2. particle shape
3. particle density
4. liquid density
5. liquid viscosity
6. orifice shape
7. orifice size
8. pressure drop
9. flow rate
10. tube diameter
11. conditions below the orifice

PRELIMINARY EXPERIMENTS FOR NON-WETTED ORIFICE CONDITION (PASTE DISCHARGED INTO A GASEOUS MEDIUM)

Even though the non-wetted orifice conditions are believed to be not applicable to the reactor system, an effort has been made to study this particular physical condition. Such an effort was believed to give at least preliminary information on the moving bed system and will serve further in exploring the general correlations for the more realistic case of wetted orifices (paste discharged into a liquid phase) in the later stages of the work.

This effort also will confirm and supplement the existing data obtained at Southern Research Institute which have been taken under non-wetted condition, and utilize them in obtaining a proper correlation applicable under such a condition.

The Ratio of Particle— To Total Flow Rate and Modified Happel Type Equation

A close observation of the existing data shows that the effluent paste density, i.e. the volume fraction of solids in the effluent paste through an orifice varies widely from below 40% up to 60% as the overall flow conditions were varied. If one defines a quantity η as

$$\eta = \frac{Fs}{F\ total} \qquad (1)$$

Where F = Flow Rates, vol/unit time

Then since G = V excess ρ_ℓ ,

and Vexcess $= \dfrac{F_t}{\pi\left(\frac{D_t}{2}\right)^2} - \dfrac{Fs}{\pi\left(\frac{D_t}{2}\right)^2(1-\epsilon)}$

$= \dfrac{Fs}{\pi\left(\frac{D_t}{2}\right)^2 \eta} - \dfrac{Fs}{\pi\left(\frac{D_t}{2}\right)^2 (1-\epsilon)}$

it is seen that

$$G = \frac{\rho_\ell \, Fs}{\pi\left(\frac{D_t}{2}\right)^2} \left(\frac{1}{\eta} - \frac{1}{1-\epsilon}\right)$$

or

$$G = \frac{\rho_\ell \, Fs}{\pi\left(\frac{D_t}{2}\right)^2} \frac{1-\epsilon-\eta}{\eta(1-\epsilon)}$$

substituting this back into Happel's correlation, one obtains

$$\frac{\Delta p}{L} = \frac{2G^2 f_{mod.}(1-\epsilon)^3}{g D_p \rho_\ell}$$

$$= 2\left[\frac{16 \rho_\ell{}^2 Fs^2 (1-\epsilon-\eta)^2}{\pi^2 D_t{}^4 \eta^2 (1-\epsilon)^2}\right] * \left[\frac{f_{mod.}(1-E)^3}{g D_p}\right]$$

or $$\frac{\Delta p}{L} = \frac{32 f_{mod.}(1-\epsilon)(1-\epsilon-\eta)^2 Fs^2 \rho_\ell}{D_p g_c \eta^2 \pi^2 D_t{}^4} \quad ---(2)$$

This is a modified moving bed correlation, in which an absolute particle flow rate instead of excess liquid flow rate appears together with the η value, the latter being the effluent paste density as previously defined.

Several investigators have studied the paste density of moving bed in a tube (40). Even though the bed density varies slightly as a function of flow rate and the particle shape, it has been found that the variations are minor and that the bed density is always about 60 volume per cent solids. i.e. $\epsilon \simeq 0.4$ for most cases. This means that the system variables are well correlated by the equation (2), once η is found for a set of specific physical conditions.

Physical Variables to be Studied And Their Experimental Dimensions

As discussed in the preceding chapter, important independent variables will be as follows.

1)	particle size	D_p
2)	particle density	ρ_p
3)	orifice diameter	D_o
4)	liquid density	ρ_l
5)	liquid viscosity	μ_l
6)	pressure drop	Δp
7)	flow rate	F
8)	tube diameter	D_t ,

The orifice shape as well as the particle shape is treated separately.

The range of numerical values of these variables to be adopted in the experiment should be selected so that they are in a similar range dynamically to that of a uranium-sodium or akin nuclear systems. If one assumes the order of flow tube diameter being in the vicinity of 0.280" and that of particle size lies between 50 μ and 500 μ average, i.e. between 0.002" and 0.02", then the ratio D_t/Dp ranges from 14 to 140. This suggests that the particle size which is to be used in the experiments should be around one-eightieth of the tube diameter or 0.0125" average for median test tube diameter of 1".

Furthermore, considering the result of previous investigators, the orifice diameter should be at least seven particle diameters to avoid bridging. Hence the orifice diameter should be at least 0.1".

The densities and viscosities of several materials which could be used as possible carrier liquids for paste type nuclear reactors (fast or thermal) are shown below:

TABLE III

DENSITY AND VISCOSITY OF POSSIBLE CARRIER LIQUID FOR PASTE FUEL REACTORS

Substance	^{o}F	ρ_l (gm/cc)	μ_l (cp)	ν_l (cm^2/sec)
Na	932	0.834	0.243	2.90×10^{-3}
NaK (43% wt. K)	932	0.790	0.207	2.62×10^{-3}
Diphenyl	700	0.72	0.157	2.18×10^{-3}
D_2O	482	0.881	0.124	1.41×10^{-3}

As clearly seen from Table III, any correlation which is to be obtained in the present work should be valid over the density

and kinematic viscosity ranges of 0.8 ~ 0.9 gr/cc and 1 x 10^{-3} ~ 3 x 10^{-3} cm^2/sec respectively, to be specifically applicable to these thermal or fast nuclear reactor concepts employing the paste type fuel systems.

Finally, since the fuel particles which can be used in the paste system will include uranium, plutonium as well as oxide and carbide forms of these elements, the final correlation should be applicable to the corresponding density range, namely specific gravity of ten and above, i.e., ρ = 10 ∧ 18. g/cc.

To summarize:

a) In case one is forced to express the correlations through empirical equation or empirical data plot, the actual physical ranges mentioned above should be covered in the experiment. Otherwise, the validity of the correlation to the nuclear system would not be definitely established.

b) Since the reproduction of these physical ranges as described in (a) are rather difficult, utmost efforts should be made to find the controlling dimensionless groups. Correlations using dimensionless groups are more general than empirical equations, and the extension of physical ranges from those used in the experiment to those found in nuclear systems will be more easily justified.

Experimental Apparatus

Experimental apparatus designed and built for the preliminary experiments consist of seven main portions as follows:

1. Water feed and control line.
2. Water ejector and feedback line.
3. Paste reservoir with overflow and pressure control line.
4. Pressure drop test tube with interchangeable orifice end.
5. Paste receiver.
6. Secondary paste reservoir.
7. Manometers.

Detailed descriptions of each portion are given below. The overall layout of the apparatus is shown in Figure 4 and Figure 6.

1. Water feed and control line

These consist of a half-inch tap water line which is extended by nine-feet long, half-inch rubber steam tubing, followed further by a heat exchanger portion of spiral tubing of total length of around ten feet. A half inch globe valve is placed between the tap water line and rubber tubing, which shuts and opens the water supply and at the same time controls coarsely the amount of water flow as well as line pressure. A pressure gauge was provided just before the spiral heat exchanger tubing. The spiral lines, which are wound with a diameter of around seven-inches, are immersed in water and the surrounding water is contained by a plastic jar. The provision of an immersion type heater (Harshaw Scientific Co.) and a laboratory type stirrer (Palo Laboratory Model 7609-B) helped to control the temperature of feedwater through the system in the range of 60°F to 120°F quite easily. An enclosed gas pressure type thermometer was used to monitor the bath temperature.

2. Water ejector and feedback line

A glass ejector which is basically similar to the laboratory type suction eductor was used in the experiment, although an industrial jet eductor of one-half inch size was tried and discarded. A water jet and subsequently developed pressure gradient at the nozzle suck down the particles from the secondary paste reservoir just above it and discharges the particles in the form of lean slurries through the feedback line of one-eighth inch plastic tubing. The tubing rises up to the top of the paste reservoir and discharges the particles at the top of the reservoir.

3. Paste reservoir with overflow and pressure control line

The paste reservoir is a glass cylinder of 6" in diameter which was pressurized by the line pressure and contains a substantial amount of paste. Particles, poured from the feedback line opening, can settle due to the sudden expansion of the flow path in the reservoir.

4. Pressure drop test tube with interchangeable orifice end

The test tube used in the experiment has 3/4-inch I.D. and was made from plexiglass and has a length of 17 inches. Interchangeable orifice plates (see Figure 5) are attached at the end of the tube with the provision of three pressure taps, located at 1-1/8", 7-3/8" and 13-5/8" from the tube end respectively, thus the distances between pressure taps are 6-1/4".

5. Paste receiver

A glass receiver was placed somewhere below the orifice, thus receiving the paste exhausted through the orifice. Usually a glass funnel was placed in the receiver which was found convenient in short-circuiting the paste directly to the secondary reservoir, thus preventing a possible aeration of the system due to bubbling caused by the overflow line stream. Near the top of the receiver, an overflow line of one-inch diameter is provided.

6. Secondary paste reservoir

This connects the paste receiver and jet ejector and serves as a paste reservoir whenever it was needed. The existence of this portion also helped to increase the static pressure head of the suction side of the ejector, improving the function of the ejector.

7. Manometers

Two types of manometers were used, i.e., open straight tube and enclosed differential U-tube, (Meriam Instrument - 30" C.O. - Standard Cleanout Manometer), each measuring the orifice pressure drop and total pressure drop respectively. Manometer liquid of 2.9 density (No. 3 Liquid - Meriam Instrument) was used for the differential tube.

Experimental Procedure

First the orifice is closed and the globe valve is opened. Referring to the pressure reading on the pressure gauge, the valve opening is regulated. As soon as the whole system is filled with water, the

differential tube is filled exhausting the air pocket through the openings at the top. Then the valve is closed. Before this procedure, the open tube manometer is closed to avoid the overflow of water through the top end. The particles desired are put in the receiver from the top. (The particles should be washed thoroughly before use to avoid the aeration of the system.) After the main reservoir and test tube are filled with paste, the orifice is opened. By the adjustment of the pressure drop across the overflow line from the top of the reservoir, obtained by means of a clamp screw, the fine pressure control across the reservoir and test tube is accomplished.

Based on the reading on the differential tube, the total pressure gradients are adjusted and set. By this time the single tube manometer is open to obtain the orifice pressure drop reading. The paste flowing down through the orifice is observed and the quantities measured by means of a graduated cylinder, in most cases of 25 cc capacity. After repeated measurements are done, a new pressure drop (and thus a new flow rate), is chosen and the procedure repeated.

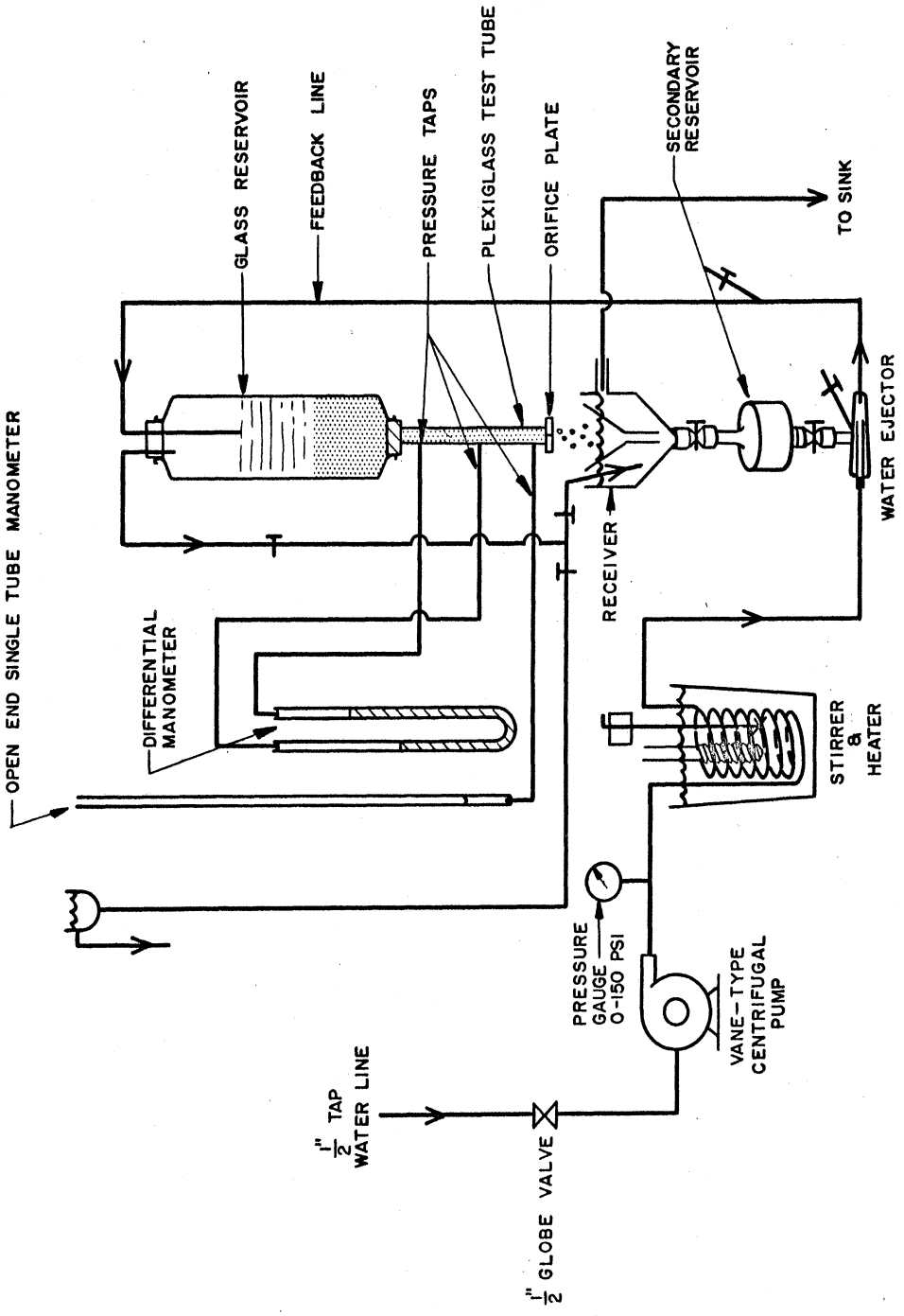

FIG. 4 OVERALL LAYOUT OF APPARATUS FOR PRELIMINARY EXPERIMENT

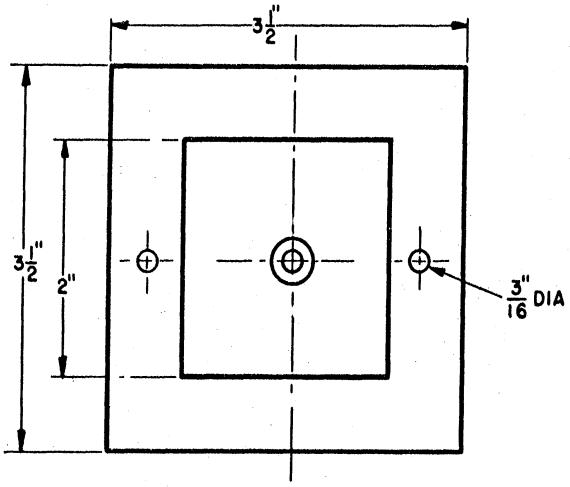

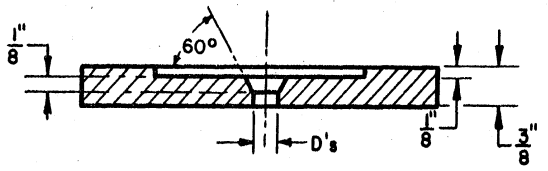

D_1 = 0.100"
D_2 = 0.200"
D_3 = 0.300"

FIG. 5 ORIFICE PLATES

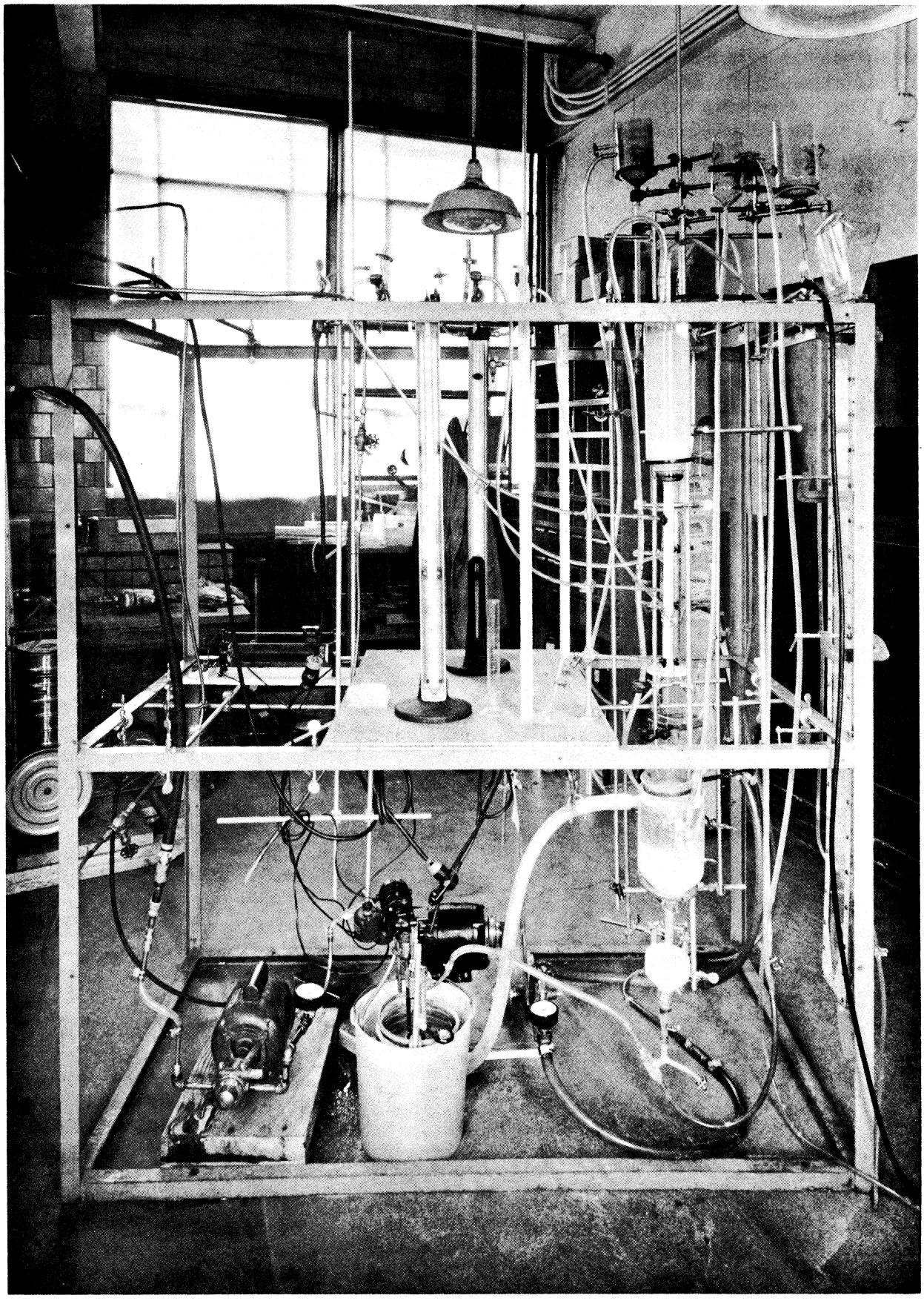

FIG. 6 OVERALL VIEW OF
APPARATUS FOR PRELIMINARY EXPERIMENT

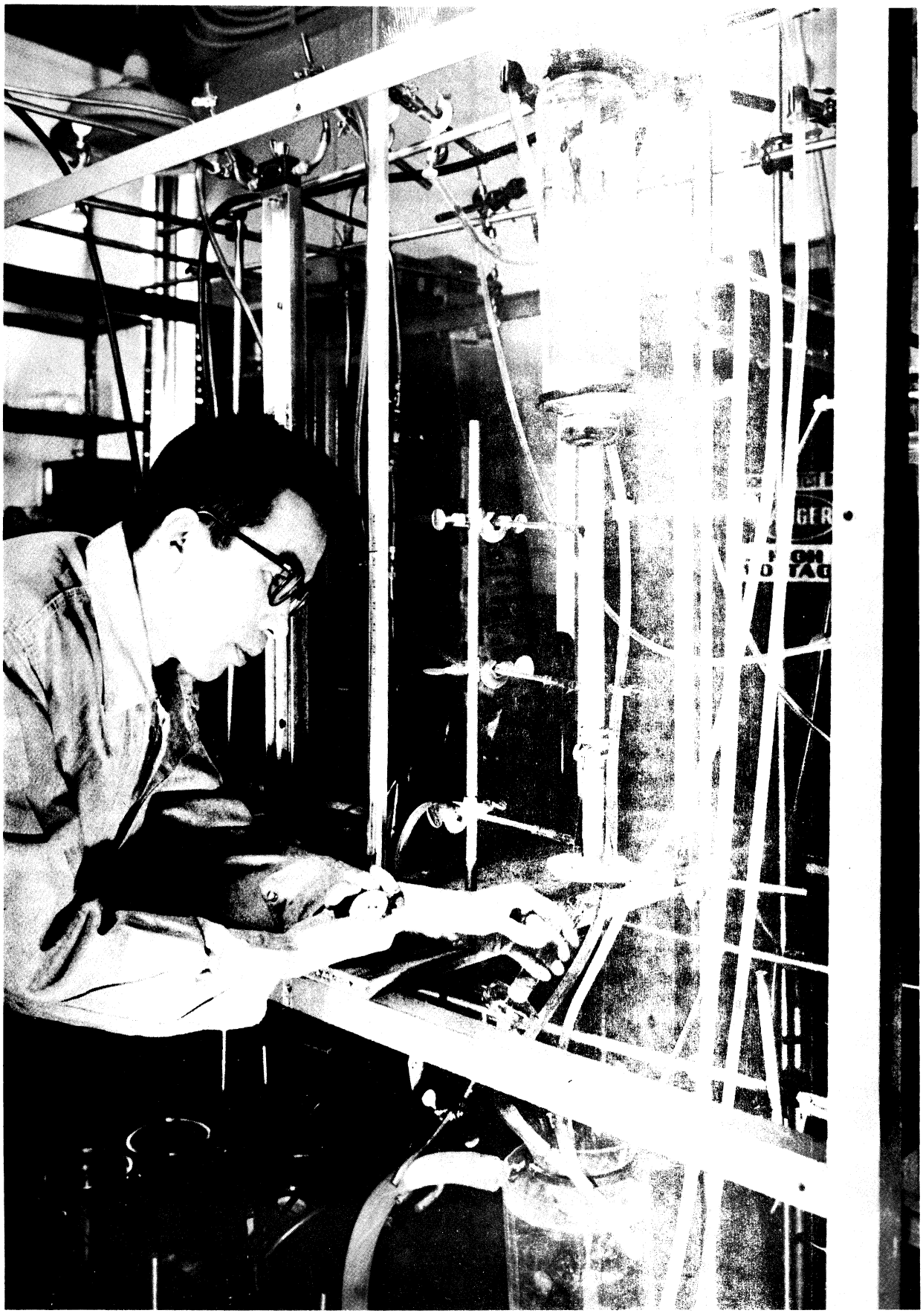

FIG. 7 MEASUREMENT (NONWETTED ORIF[illegible]ONDITION)

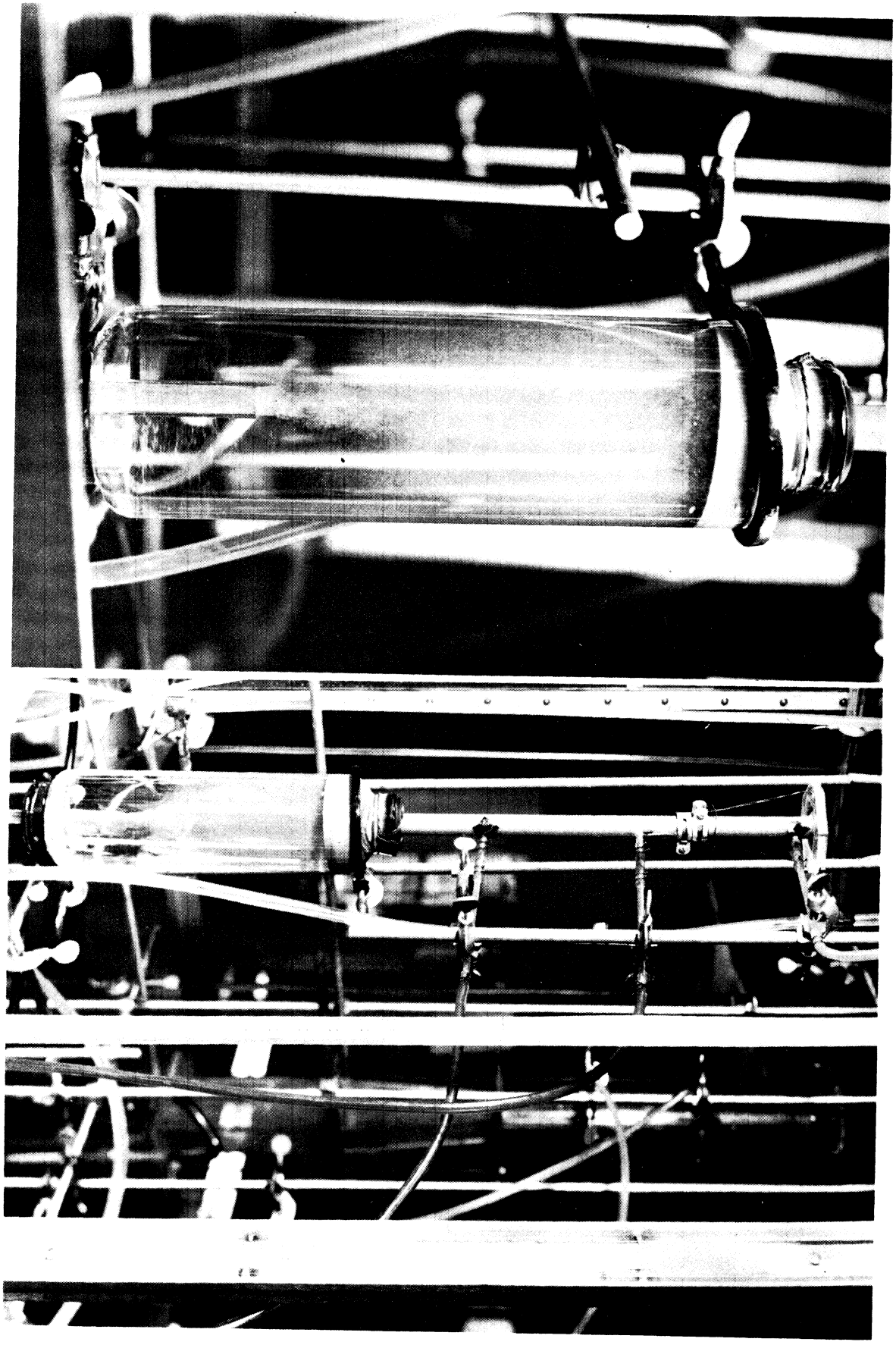

FIG. 8 RESERVOIR AND TEST TUBE

FIG. 9 SETTLING PARTICLES

RESULTS OF PRELIMINARY EXPERIMENTS AND DISCUSSIONS

Since there exists a substantial amount of data, as mentioned previously, on the paste flow through an orifice under non-wetted orifice condition, a rather limited amount of data were collected in this experiment. However, several interesting findings were made with regard to the effects of flow rate, particle density, the sphericity of the particle, and the aeration in the system on η value. Also the magnitude of orifice pressure drop compared to the total pressure drop across a tube were estimated from the data.

Finally, a correlation based on the dimensionless quantity, i.e. η and a newly modified Reynolds number, $\frac{D_p(F_t - F \text{ paste})\rho_l}{D_o^2 \mu_l}$

or $\frac{Dp\ F_{excess}\ \rho_l}{D_o^2\ \mu_l}$ was established.

The Effect of Excess Flow Rate on η Value in General

It was observed during the experimental runs, that there exists different modes of paste flow through the orifice. When the pressure gradient across the test tube is small and thus the excess flow rate of the liquid (water) is low (low flow rate region), the η value is high and close to the value of $1 - \epsilon$, i.e., 0.6 or 60%. However, as the pressure gradient is increased, the η value drops down gradually until some critical point is reached, beyond which the value seems to stay around a constant (plateau region). Thus it seems certain that the physical phenomena and their contribution to the η value in these regions

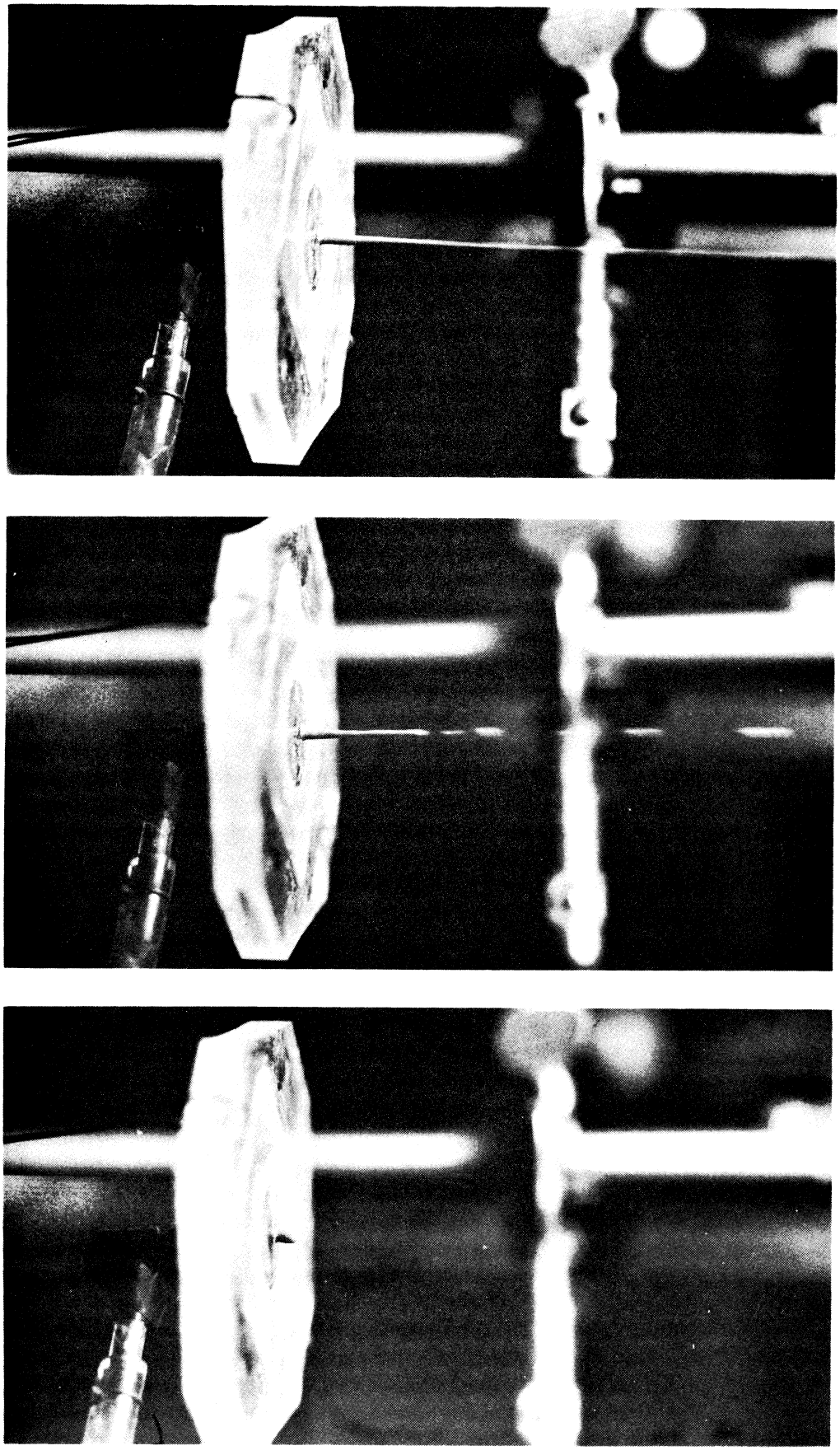

FIG. 10 EFFLUENT PASTE

are different. The trend applies to all the different particles used in the experiments, such as spherical copper particles, glass-beads and non-spherical atomized head particles.

The Effect of Excess Flow Rate and Particle Density on η Value in the Plateau Region

To evaluate the effect of particle density on η value, two sets of experiments were carried out. They are:

a. 100/120 mesh glass beads - H_2O flow through 0.100" tapered orifice.

$$\rho_p = 2.6 \ \frac{gr}{cc}$$

b. 100/120 mesh cu-H_2O flow through 0.100" tapered orifice,

$$\rho_p = 8.92 \ \frac{gr}{cc}$$

The η values obtained are listed below.

ρ_p \ Δp	5.7	6.8	11.4	13.3	15.2	19.0
2.6	2.0	51.3	50.8	50.2	1.4	52.1
8.9	1.6	52.4	51.1	50.5	50.3	51.1

Where Δp is the frictional pressure drop across the bed in terms of H_2O, and hence is dependent on the square of excess flow rate according to the Happel's correlation.

At this point one can analyze the variances (see the Appendix) of the data into between-column (variance due to different Δp, and hence different excess velocity) and between row (variance due to the different particle density) and residual.

After performing a two factor variance analysis for the data (see the Appendix IV) one obtains a table of the analysis of variance as shown below.

Table IV

TABLE OF VARIANCE ANALYSIS

Source of Variance	Summary of Squares	Degrees of Freedom	Mean Squares	Components of Variance
Between Rows	(2) - (4) = 31498.30 - 31498.25	$n_1 - 1 = 1$	0.05	$n_2 \sigma_1^2 + \sigma_o^2$
Between Columns	(3) - (4) = 31501.94 - 31498.25	$n_2 - 1 = 5$	0.73	$n_1 \sigma_2^2 + \sigma_o^2$
Residual	(1) + (4) - (2) - (3) = 1.83	$(n_1 - 1)(n_2 - 1) = 5$	0.36	σ_o^2
Total	(1) - (4) = 5.57	$n_1 n_2 - 1 = 4$		

Applying the ratio test and comparing the each mean squares with the Residual, one can examine the significance of effects of each Δp (and thus excess flow rate) and particle densities on η value.

For Between Rows (particle density effect)

$$F = \frac{0.36}{0.05} = 7.2 \text{ for degrees of freedom } n_1 = 5 \quad n_2 = 1$$

This value is far below F = 230.2 for 5% significance level. In fact the value is even smaller than F=14.0 for 20% significance level.

Hence, assuming that the two sets of figures were drawn from the same population, i.e., the variabilities were the same, we will very likely have the present data. Thus, the effect of particle density effect on η appears highly insignificant in a statistical sense.

For Between Columns (Δp effect):

$F = \frac{0.73}{0.36} = 2$, for $n_1 = 5$, $n_2 = 5$ which is certainly below $F = 5.1$ for 5% significance level or even lower than $F = 2.2$ for 20% significance level and hence the effect of pressure drop is seen as not significant at least in the plateau region and in the range of pressure intervals examined here.

The Effect of Sphericity or Shape Factor on η Value in General

To observe the effect of particle shape on the η value, atomized lead particles of 100/120 mesh were used in the flow study. As clearly seen in Figure 11, the value of η is considerably lower than for the spherical glass and copper particles, value of η being 42 to 43 per cent compared to the η value of 52 per cent for the latter particles in the plateau region. One interesting point is that the tendency of an enhanced η value in the region of low flow rate is quite similar to that for spherical particles even though the enhanced value of η is still lower, i.e., η value being approximately 48 per cent against the η value of 55 per cent for the latter. This implies that the effect which enhances the η value in the low flow rate region is still valid even for non-spherical cases, and the effect which differentiate the values for spherical and non-spherical particles differs apparently from the effect that contributes to the enhanced η value in the low flow rate region, whatever the effects may be.

The Effect of Aeration in the System on the η Value

In most of the runs, particles were thoroughly washed before use. Also, the entire system was carefully checked for any possible leakages especially where negative pressures were present, i.e., the suction side of the water ejector etc. By doing so, possible chances of introducing air bubbles into the system were eliminated.

However, by either charging fresh (unwashed) particles such as copper, or forcing bubbles which were formed at the end of overflow line into the water ejector suction line through the secondary paste reservoir, it was possible to introduce air bubbles and thus aerate the system. One such run was made to compare the flow characteristics (Figure 12). Even though it appears that the values are very closely gathered in the low flow rate region for aerated and deaerated Cu - H_2O systems, the η value drops significantly in the plateau region as the pressure gradient across the test tube is increased. It was also observed, as seen in the data (Appendix), that the overall flow rate is considerably slower than that for the deaerated system for the same pressure gradients across the tube, implying that there exists much internal friction in the moving bed.

The Magnitude of Orifice Pressure Drop

For some of the initial runs, orifice pressure drops were measured. As was expected initially, the pressure drop is not of a significant magnitude. This was mentioned previously for already existing sodium system data. The present check is merely a reconfirmation of this fact.

Some of such orifice pressure data are plotted against the corresponding total pressure gradient in Figure 13. It is merely intended by this graphical plot to show that the magnitude of the "orifice pressure gradient" is of the same order as that of total pressure gradient, and not to prove identity between them. It should be noted here that the magnitude of orifice pressure drop itself will be negligible when it is compared to the total pressure drop across the tube whenever tube length is substantially long, and minor degree of variations in orifice pressure drop does not contribute to the overall physical picture.

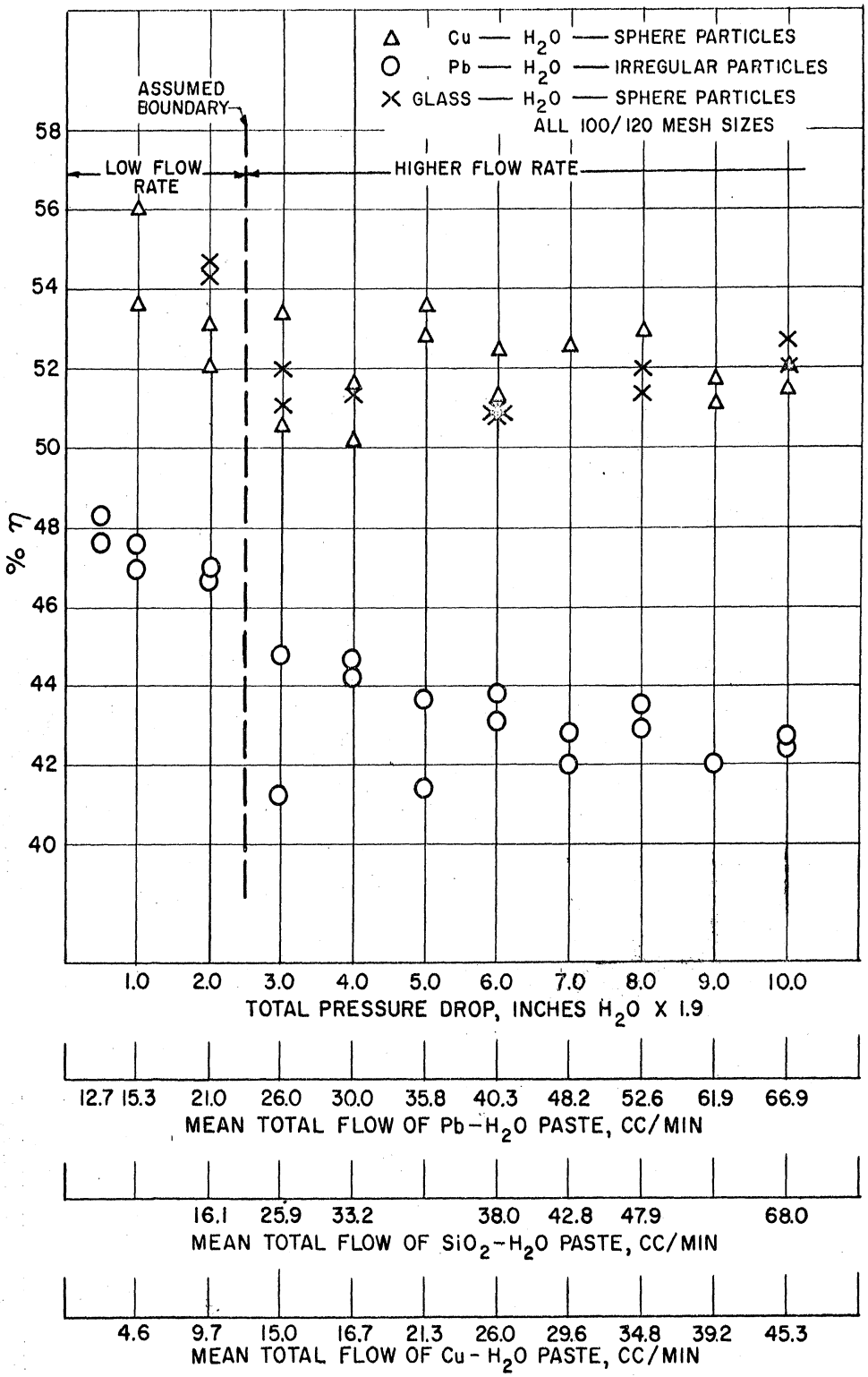

FIG. 11 THE EFFECT OF VARIOUS PARTICLES ON η

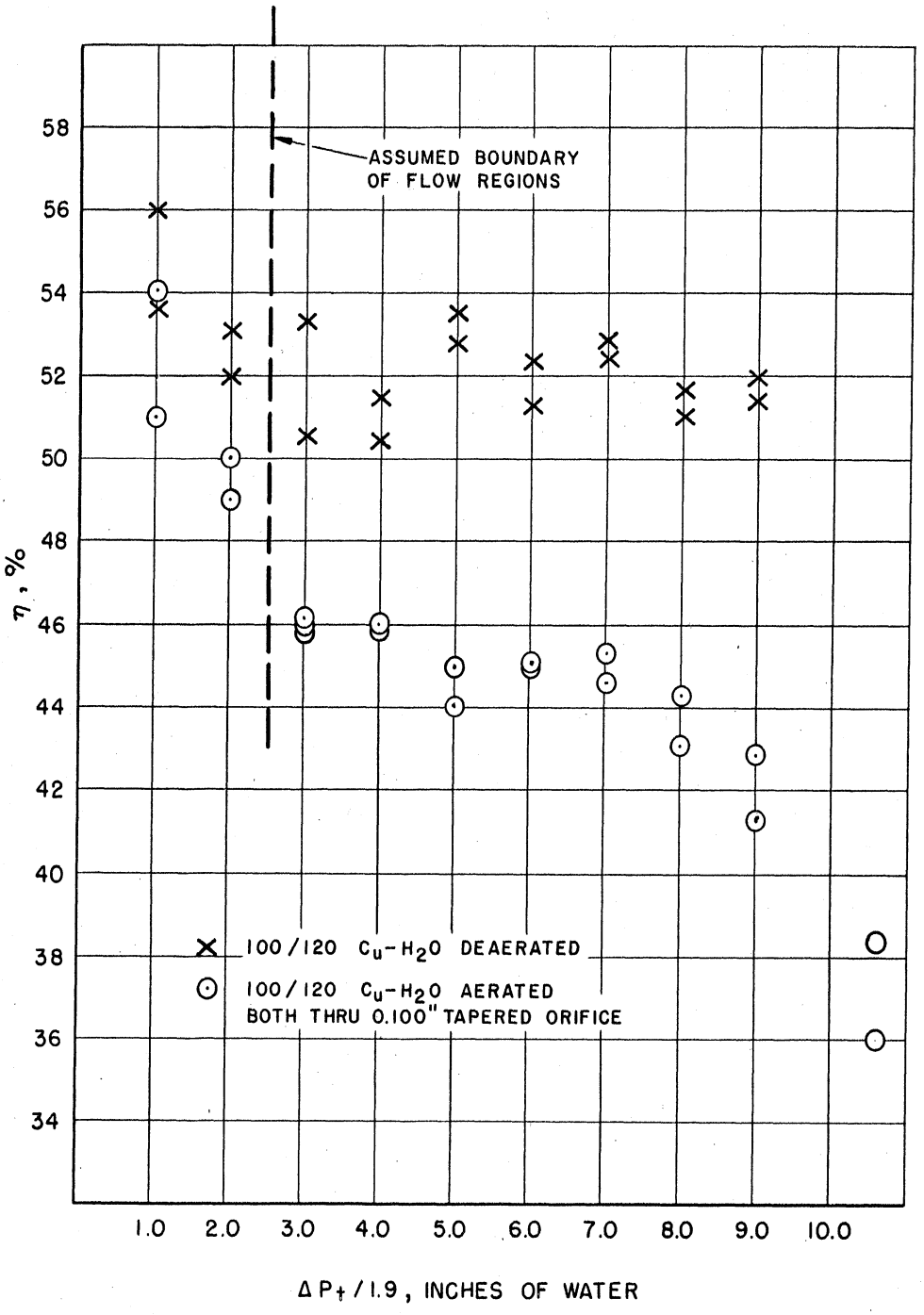

FIG. 12 EFFECT OF AERATION ON η

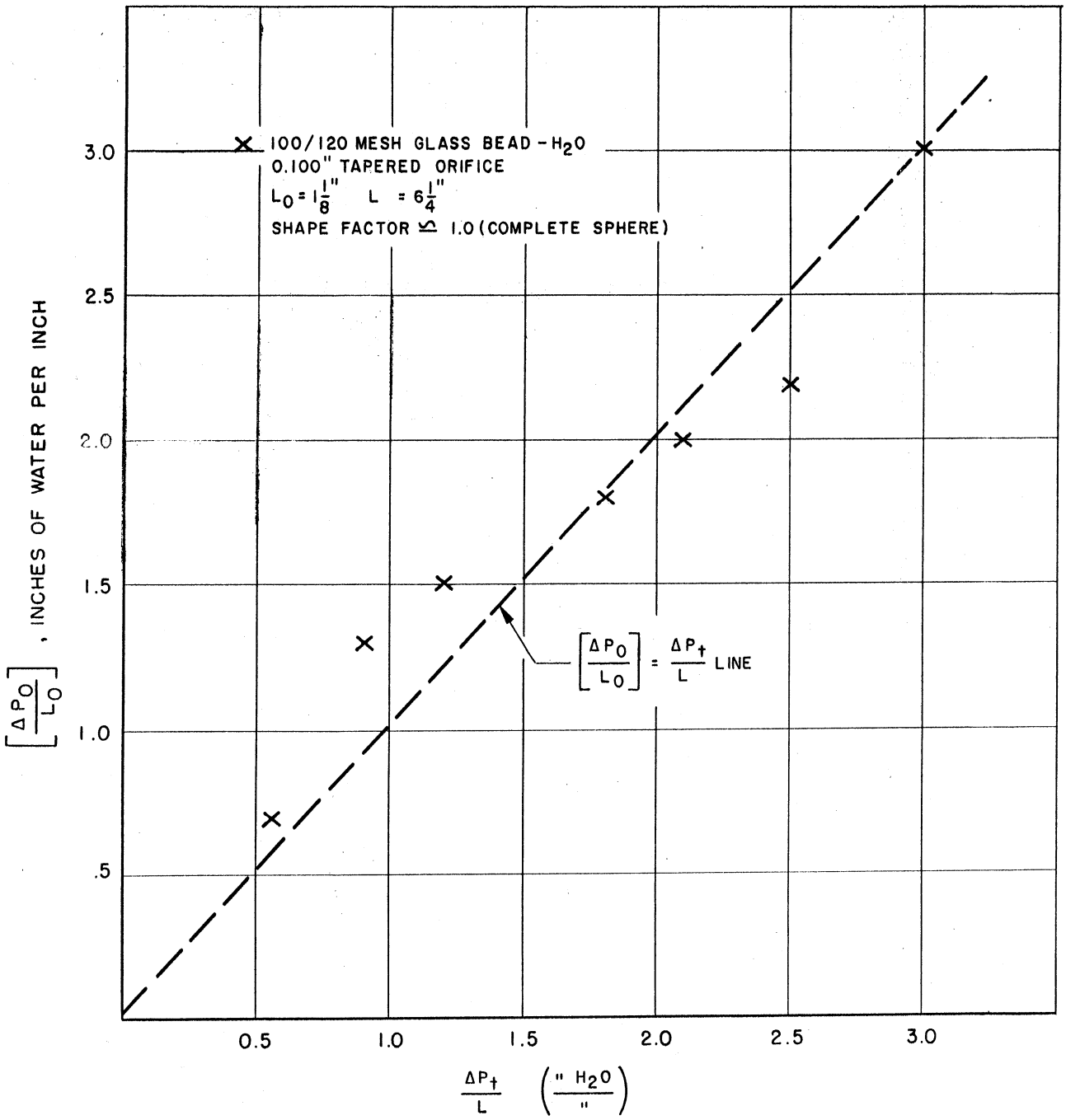

FIG. 13 MAGNITUDE OF ORIFICE PRESSURE DROP

CORRELATION BASED ON DIMENSIONLESS GROUPS FOR NON-WETTED CONDITION

Actual observation of the flow pattern, and the statistical findings obtained and described in the preceding chapter enables one to choose physical quantities which are regarded to be important in understanding the basic flow behavior. From such an effort, correlations using dimensionless groups have been developed. The existing Southern Research Institute data as well as the data obtained in the preliminary experiments were both used for the work. Modified Reynolds number in the orifice, which could be more properly called "In-orifice" modified Reynolds number, and the effluent paste density, i.e., the ratio of solid-to-total flow rate, are the dimensionless groups finally chosen to give a satisfactory interpretation of the result. The correlation obtained is to be coupled with the Happel type moving bed correlation and should give the relations among the physical quantities associated with the present problem including the absolute particle flow rate, provided the orifice end is not wetted.

The latter condition, i.e., non-wetted orifice condition, restricts the applicability of the correlation obtained here, though it was later discovered that the correlation obtained for wetted orifice condition is of similar type to the present one and thus the present study should be well regarded as a preliminary part of the overall work.

Dimensional Analysis and Correlation

Quantities related to the problem and which may hence define the system were tentatively assumed as follows:

QUANTITY	SYMBOL	DIMENSIONS
Gravity	g	LT^{-2}
Excess Velocity of Liquid	V_ℓ	LT^{-1}
Particle Density	ρ_p	ML^{-3}
Liquid Density	ρ_ℓ	ML^{-3}
Ratio, Particle to Liquid Flow Rate	η	Dimensionless
Particle Diameter	D_p	L
Fluid Viscosity	μ	$ML^{-1}T^{-1}$
Pressure Drop	p	$ML^{-1}T^{-2}$
Ratio, Orifice diameter to particle diameter	$R = \frac{D\ \text{orifice}}{D\ \text{part}}$	Dimensionless
Void Fraction	ϵ	Dimensionless

A functional relationship $F(g, V_\ell, \rho_p, \rho_\ell, \epsilon, \eta, D_p, R, \mu, p)$ which can interpret the experimental data is now to be found in terms of dimensionless parameters. As three dimensions (L, T, and M) are involved, three quantities are first selected, i.e., V_ℓ, ρ_ℓ, and D_p.

According to Buckingham's π theorem, one may write,

$$\pi_1 = \epsilon, \qquad \pi_2 = R$$

$$\pi_3 = V_\ell^{x_1} \rho_\ell^{y_1} D_p^{z_1} \cdot g \qquad \text{-------(a)}$$

$$\pi_4 = V_\ell^{x_2} \cdot \rho_\ell^{y_2} \cdot D_p^{z_2} \cdot \rho_\ell \qquad \text{-------(b)}$$

$$\pi_5 = V_\ell^{x_3} \cdot \rho_\ell^{y_3} \cdot D_p^{z_3} \mu \qquad \text{-------(c)}$$

$$\pi_6 = \eta \qquad \text{-------(d)}$$

From (a), comparing the exponents of resultant dimensions, one obtains $\pi_3 = \frac{D_p g}{V\ell^2}$

Similarly from (b), (c), and (d),

$$\pi_4 = \frac{\rho_p}{\rho_\ell} \qquad \pi_5 = \frac{\mu}{V\ell \cdot \rho\ell \, D_p} \qquad \text{and} \qquad \pi_6 = \frac{p}{V\ell^2 \rho\ell}$$

After examining each group, one recognizes,

π_3 = $\frac{\text{gravity force}}{\text{inertia force}}$ (Froude number)$^{-1}$

π_5 = $\frac{\text{Viscous force}}{\text{inertia force}}$ (Reynolds number)$^{-1}$

π_6 = $\frac{\text{pressure force}}{\text{inertia force}}$ Euler number

As observed previously, the effect of bouyancy force in the system seems negligible. The fact that the Happel type correlation which was originally derived from the data obtained for solid particle - gas system is satisfactorily applied to the solid-uranium data across the flow tube, indicates that the group π_4 should not be important. This point is further stressed especially when the effect of particle density is not important as found statistically in the preceding chapter.

As to the group π_3, it will be readily conceived that the gravity flow is not likely an important factor unless extremely low excess flow rate is realized in the system. Thus, the effect would not appear significantly in most of the flow region. The group π_6, on the other hand, was already handled as a constituent of Happel type correlation and is to be coupled with the correlation for η which is presently being sought.

The remaining dimensionless groups which could be correlated with η are then π_1, π_2, and π_5. The value of ϵ has been found by many investigators to fall in the vicinity of 0.4 or 40% for round particles, with only minor variations around this value for various sets of conditions. If one intends to obtain a final correlation with the accuracy similar to that associated with the variation of ϵ, the term may not be worthwhile to consider as a variable. Thus, π_1 term may be well dropped. After the series of these screening processes it may be written now as,

$$\eta = \eta\left(\frac{D\ \text{orifice}}{D\ \text{particle}},\ \frac{V\ell\ \rho\ell\ D_p}{\mu}\right)$$

The modified Reynolds number, $\frac{V\ell\ \rho\ell\ D_p}{\mu}$ can be evaluated at any arbitrary points in the system, however the value at or in the vicinity of the orifice would be more proper to use considering the fact that the dependent variable η is associated with the local phenomena in or just above the orifice section. Employing the excess liquid flow rate, F excess of F total-F paste instead of linear excess velocity $V\ell$, one obtains for "In-orifice" Modified Reynolds number,

$$\text{Re, mod, o} = \frac{Dp\ (Ft - Fpaste)\rho\ell}{Do^2\mu}$$

$$= \frac{Dp\ Fexcess\ \rho\ell}{Do^2\mu}$$

$$= \left(\frac{Dp}{Do}\right)\left(\frac{Fexcess - \rho\ell}{Do\ \mu}\right)$$

The η values were successfully plotted versus the Re, mod. o or simply Re_o as shown in Figure 14. The plateau region which was discussed in the preceding chapter is virtually flat. The effect of Re appears practically non-existant between $Re_o = 0.2$ and $Re_o =$ 4 to 5 in the semi-log plots. However, above and below these critical Reynolds numbers, the value is definitely dependent on In-orifice modified Reynolds number. The data scatter a little around the local medium values by about 2 to 3 per cent throughout the whole flow rate regions, but the accuracy observed here is considered consistent with the one associated with those obtained by fixing $1-\epsilon = 0.6$.

Discussions

The understanding of the foregoing results requires essentially a review of the basic mechanism of drag on a submerged particle in liquid. Assuming a single spherical particle placed in an ideal fluid as shown in Figure 15 (c), the conversion between the kinetic energy term of total energy, and pressure force term p in the flow should be symmetric in front of and behind the particle. In a viscous fluid, however, the friction effect exists and when the fluid passes from point I to point II, dissipation of kinetic energy will be experienced. This energy dissipation implies that the energy conversion, i.e., the recovery of pressure from kinetic energy behind the particle is not as complete as in an ideal liquid, and hence, the change of flow pattern is inevitable, causing a discontinuous layer behind the spherical particle. Reversed flow develops in the discontinuous layer, and a vortex forms. As the Reynolds number is

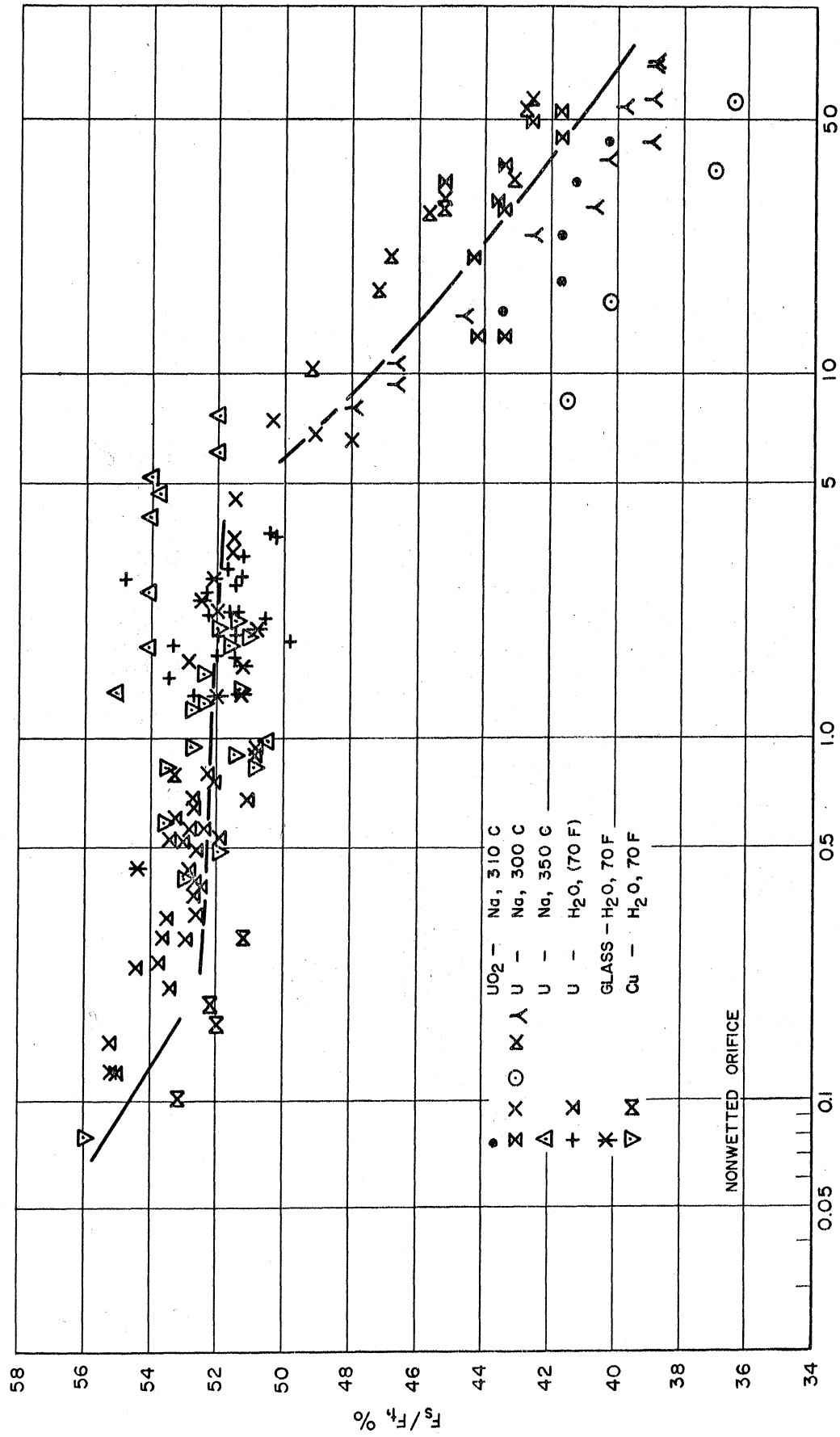

FIG. 14 IN-ORIFICE MODIFIED REYNOLDS NUMBER AS A FUNCTION OF η

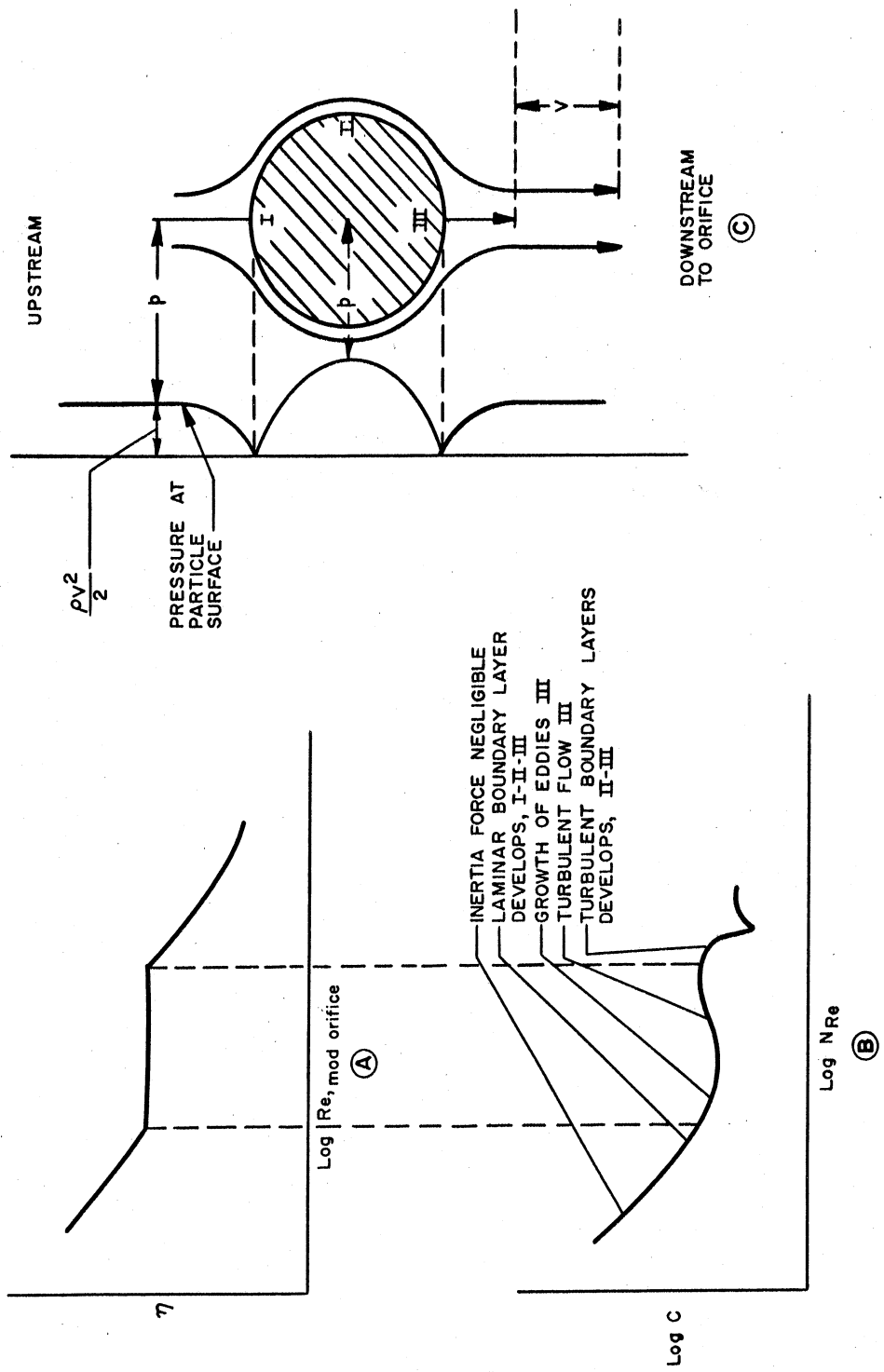

FIG. 15 THEORY OF DRAG COEFFICIENT AND OBSERVED η CURVE

gradually increased, such vortex formation is further enhanced, and the eddy will dominate the region behind the particle. Since the pressure in the eddied wake is low, and the impact pressure on the front surface of the particle high, great pressure drag results, which in turn adds up to the tangential shear drag of the particle and increases the total drag force as shown in Figure 15 (b). However, as the eddies develop fully behind the particle, the boundary layer changes to that of turbulent flow, and decreases the low pressure eddy portion of the contact surface behind the particle. The result will then lessen the total drag effect, causing decreased drag coefficient C.

Quite surprisingly, the trend of η value obtained as the result of the experiment is seen very similar to the curve for the drag coefficient described above. This suggests that the mechanisms which control both phenomena may be the same, which makes one able to propose the following possible explanation.

Consider two particles placed in the stream. When the flow between the particles which are placed near the orifice is laminar, the streamlines between the two spheres are spaced further apart than those outside, involving much higher pressure in this region, which then leads to a repelling, as shown schematically in Figure 16 (A). This will tend to make the interparticle spacing large in the orifice as the flow rate is increased and thus will contribute to the decrease in the η value. However, as soon as the eddies start to develop in the wake, the pressure in the wake decreases as observed for single sphere cases and the repelling action which is experienced in the case of laminar flow is cut down, hence, showing a stabilized inter-

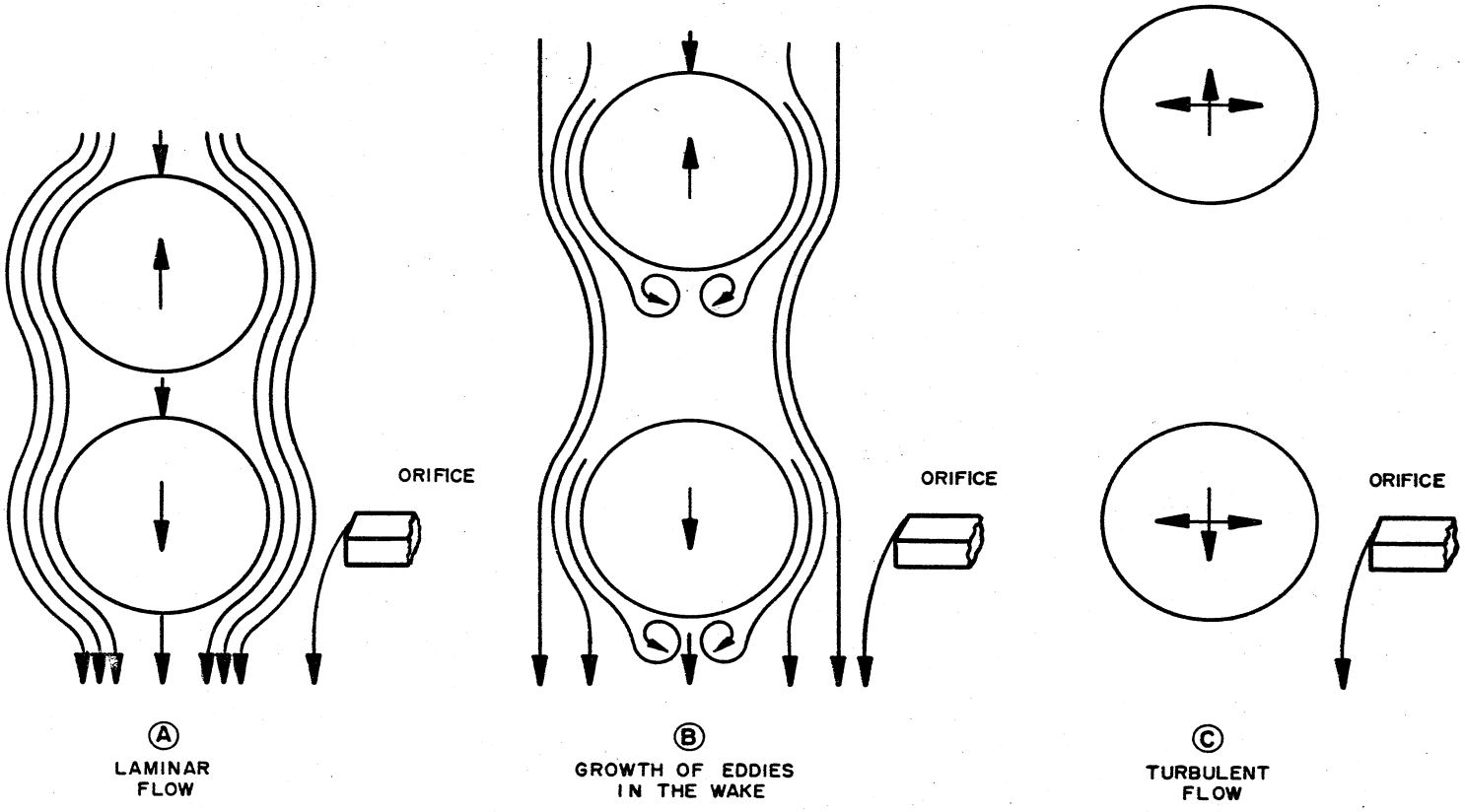

FIG. 16 TWO-BODY MODEL

particle distances in the orifice, which characterizes the plateau region of η values in the correlation. However, due to the porous nature of the overall system, it is extremely easy to have a turbulent boundary layer developed on the surface of particles which is flowing in the downstream portion of the system, i.e., in the orifice section. Thus, even at very low modified Reynolds number such as Re_o values of $4 \longrightarrow 5$. Now as the Reynolds number is further increased, the turbulent boundary layers develop quickly on the particle surfaces and hence in overall downstreams. By this time, the bed has expanded to such an extent that the individual particles have been disengaged from each other sufficiently to permit random motion of the particle with the aid of ambient turbulence. This condition will be very similar to the fluidization and so called "maximum fluid density" will be attained at this point.

Additional Notes on the Proposed Flow Mechanism in the Orifice

The transient and consecutive developments of laminar boundary layer, eddies, and finally turbulent boundary layers on a particle surface and their effects on the adjacent particles, as explained for most simple case of two body system, were considered to be the main contributing factors which affect the flow in the orifice. However, it is conceivable that some other effects may be also playing some roles. Several additional thoughts can be made as follows:

1) Collision of particles: Momentum and energy change. Since there exists certain angle of slide in the flow and thus the particles are converging into the orifice portion, the possibility of interparticle collision and subsequent interchange of energy as well as momentum change certainly may exist, however this phenomena does not explain the region of plateau in the correlation satisfactorily, and thus is weak to support the experimental observation.

2) Observed low η values for non-spherical particles: For non-spherical particles, the evolution of eddies in the effective wake as well as subsequent development of turbulence is much easier to achieve than when the particles are spherical. The proposed mechanism thus explains the observed low η values for these particles satisfactorily, which is believed

to be another evidence that the explanation based on the drag effect and development of consecutive boundary layers on particle surfaces as proposed above would be more satisfactory and logical.

CORRELATION EXPERIMENTS FOR WETTED ORIFICE CONDITION

In the actual nuclear system, it is most likely that the orifices through which the paste passes are immersed in the carrier liquid itself. This condition, i.e., the wetted orifice condition may affect the physical behavior originally experienced with non-wetted orifices. Hence, data should be obtained under this condition.

Efforts to obtain a correlation for η under wetted orifice condition have been made. Experimental designs, apparatus, as well as experimental procedures adopted in the study are described in the present chapter.

Experimental Design

Experiments were divided into two parts, i.e., reference experiments and additional experiments. The reference experiment consists of essentially the main correlation experiment where the physical variables related to the in-orifice Reynolds number and η are examined following the findings in the preliminary experiments. On the other hand, one is not quite sure that some of the effects which were assumed negligible under both non-wetted condition and wetted condition are really non-significant, and hence a separate examination is required. The additional experiments were so designed that these checks can be made most effectively with the minimum amount of experimental data.

1. Design for the reference experiment:

   Prior to the experimental design, a series of experimental runs were made to preview the general trend of η value variations and to decide the experimental dimensions as

well. Copper particles of 100/125 U. S. mesh sizes and orifice diameters of 0.046", 0.073", 0.101", 0.120", 0.149" and 0.199" were chosen and experimental runs were made for these combinations. After a series of preliminary runs, the following design basis was finally established:

a) Particles to be used

Copper particle

$\rho = 8.9$

Spherity $\simeq$ 1.0 as checked under the microscope.

b) Particle Sizes

60/80 U. S. mesh

100/125 U. S. mesh

230/325 U. S. mesh

c) Orifice

Tapered orifice (60^{o})

0.101", 0.120" and 0.149"

(plus 0.073" and 0.199" as supplementary)

d) Carrier liquid

Water at room temperature and ethylene glycol at different degrees of dilutions.

e) 3 factor full factorial experiment.

f) Combination of

Two duplicate three levels
and
Two duplicate nine levels.

The Table IV shows the overall experimental design.

Table V

REFERENCE EXPERIMENTAL DESIGN

D_o / D_p	(0.073")	0.101"	0.120"	0.149"	(0.199")
60/80 mesh	(9 levels) (2 dupl.)	$\frac{Do}{Dp}$ max. 9 levels 2 dupl.	3 levels 2 dupl.	9 levels 2 dupl.	
100/125		3 levels 2 dupl.	9 levels 2 dupl.	3 levels 2 dupl.	(9 levels) (2 dupl.)
230/325		9 levels 2 dupl.	3 levels 2 dupl.	$\frac{Do}{Dp}$ Min. 9 levels 2 dupl.	

( ) : Supplementary Experiments

2. Designs for the additional experiments.

These were determined after the reference experiment was done and hence will be described in separate chapters.

Experimental Apparatus

The apparatus consists of the following portions:

a) Test tube turret: Three test tubes six inches long with inside diameters of half inch each, having different size orifices at their ends, were bundled in a No. 12 rubber stopper, which in turn plugs the lower end of the reservoir previously described.

b) Paste reservoir:

The reservoir is a 34 inch long acrylic tube with inside diameter of 2-1/4 inches and wall thickness of 1/4 inch. Overflow points were located at every 3" of tube walls, the lowest of which being at 6-1/2" above the lower tube end. (See Fig. 17 and 18.)

c) Miscellaneous:

Three inch glass funnel connected with twenty-five inch long tygon tubing was inserted into the top opening of the reservoir, which facilitated the charging of paste. Tap water line was introduced in the reservoir also through the top opening of the reservoir.

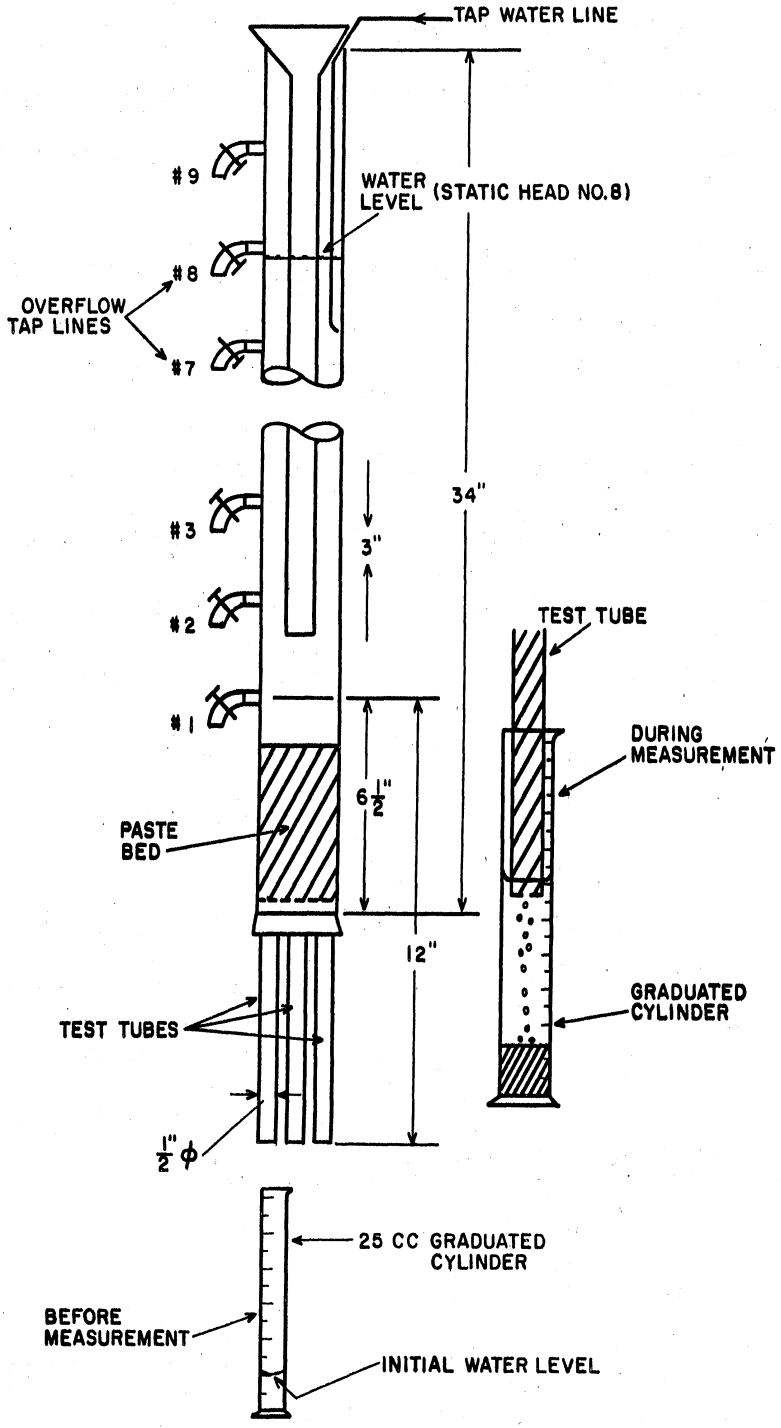

FIG. 17 LAYOUT OF APARATUS

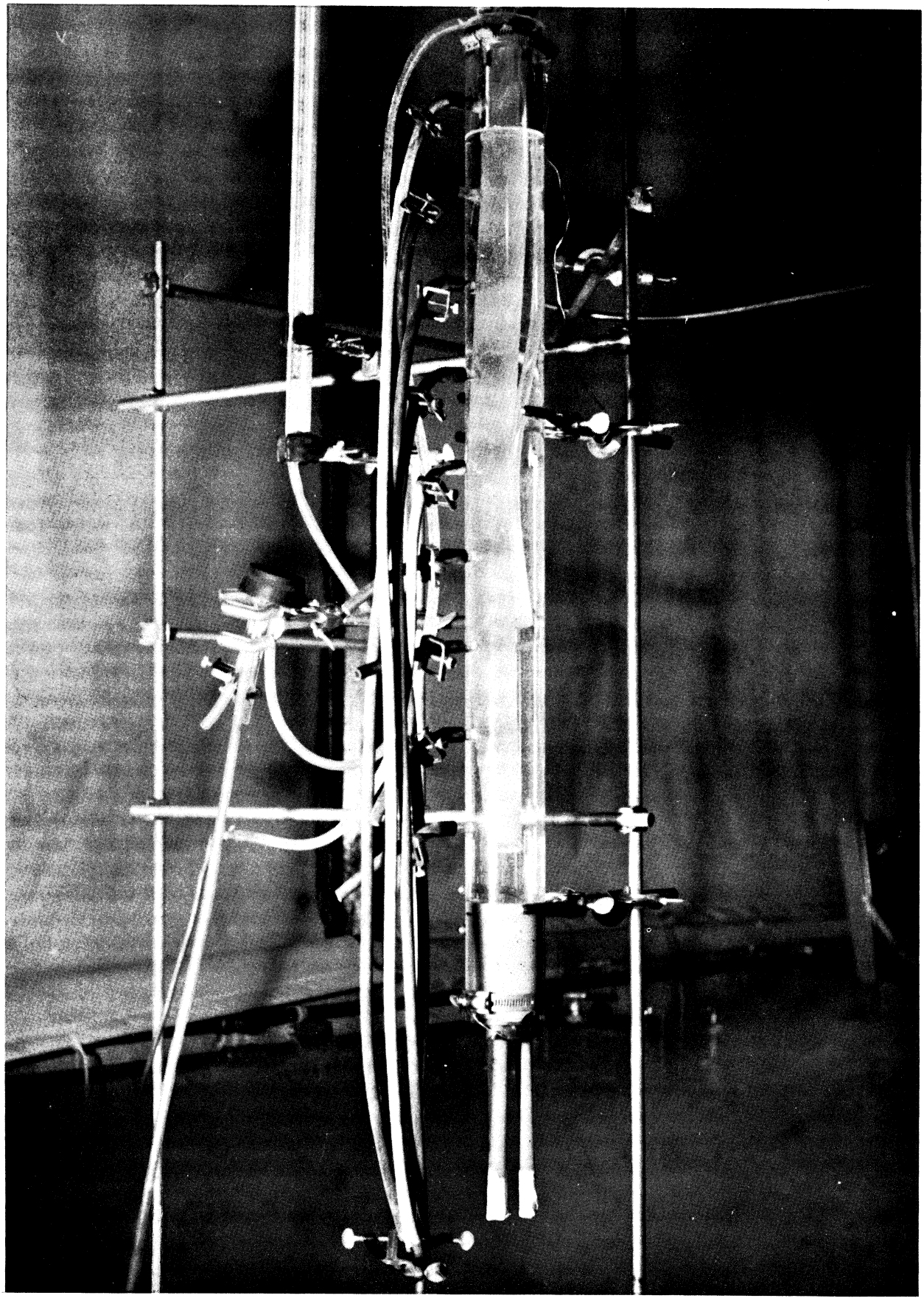

FIG. 18 APPARATUS FOR CORRELATION EXPERIMENTS

Experimental Procedure

Utmost care had to be taken to avoid the aeration of the paste system whenever a new charge of paste was made. First, the orifices were closed by means of Masking tape. Water was filled up to the half way of the reservoir. Thoroughly washed copper paste was then charged from the top. During the charge, the whole system had to be tapped lightly to liberate the air bubbles introduced at the surface of the gradually accumulating paste bed. In every run the bed height was kept slightly more than six inches in the reservoir. The total bed was thus twelve inches high, counting six inches for bed height in the test tube. After the bed was formed, water was added and its level was adjusted using the overflow line. Masking tape was then removed from the orifice end and paste started to flow. At this point, the orifice was immersed into water filled in a small beaker. For a while the paste was allowed to flow. Then the beaker was removed, and a 25 cc graduated cylinder filled with a known amount of water was brought under the orifice, the latter being then immersed in water. Time was recorded until the cylinder was finally removed. Due to the substantial amount of particles and liquid in the reservoir, the change in bed height and water level during each measurement was negligible. The cylinder was tapped until paste bed settled and did not show further decrease in the bed volume. The increase in water volume as well as bed height was measured and η values were calculated.

Prior to the experiments, the settled paste densities for different particle species as well as sizes were measured for a standardized degree of tapping condition. In all cases, the paste beds were formed at the bottom of 25 cc graduated cylinder, amount of excess liquid being added

above it. Both total volume and the paste volume were measured for a standardized tapping condition, and the excess liquid was discarded. The cylinder was placed in a dryer overnight, and the weight of particles was then determined. From these data, the paste densities were calculated.

RESULT OF CORRELATION EXPERIMENTS

The result of the experiments for wetted orifice conditions showed that the general tendency observed under the condition is quite similar to the one observed under the non-wetted orifice conditions. The critical values of in-orifice modified Reynolds number as well as the constant plateau value differ only slightly. The surface tension effect which differentiates the one case from the other is believed responsible for these slight differences.

General Tendency of Flow Data as the In-Orifice Modified Reynolds Number Increases

Whenever the particle diameter becomes small, the value of Reo tends to stay small and laminar orifice flow is easily realized. A set of such flows is shown in Fig. 19. The η value decreases gradually as the flow rate is increased until a critical flow rate is reached, beyond that point the η values tend to stay constant for quite a wide flow rate region. As defined previously for a non-wetted orifice, the plateau region is thus attained. As particle sizes as well as flow rates are further increased, the flow goes through the plateau region (Fig. 20) until a second critical in-orifice modified Reynolds number is reached. From that point on, the η value drops as the Re_o is further increased. (Fig. 21). The lowest η value attained in the experiment was around 0.41 or 41 per cent corresponding to Re_o of about 15, but it is believed that η would decrease still further if more pressure were applied across the bed.

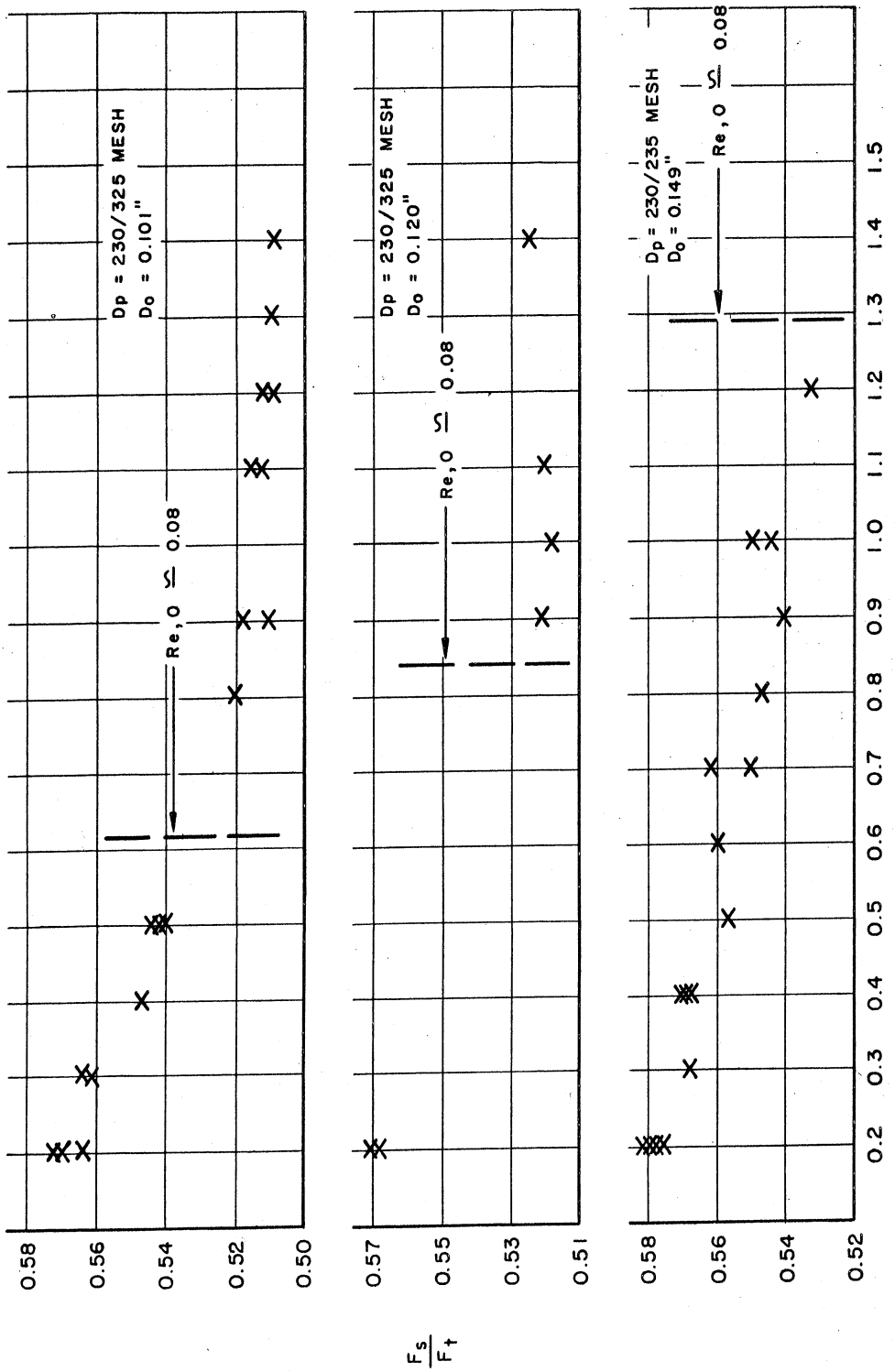

FIG. 19 EXCESS FLOW RATE AND η

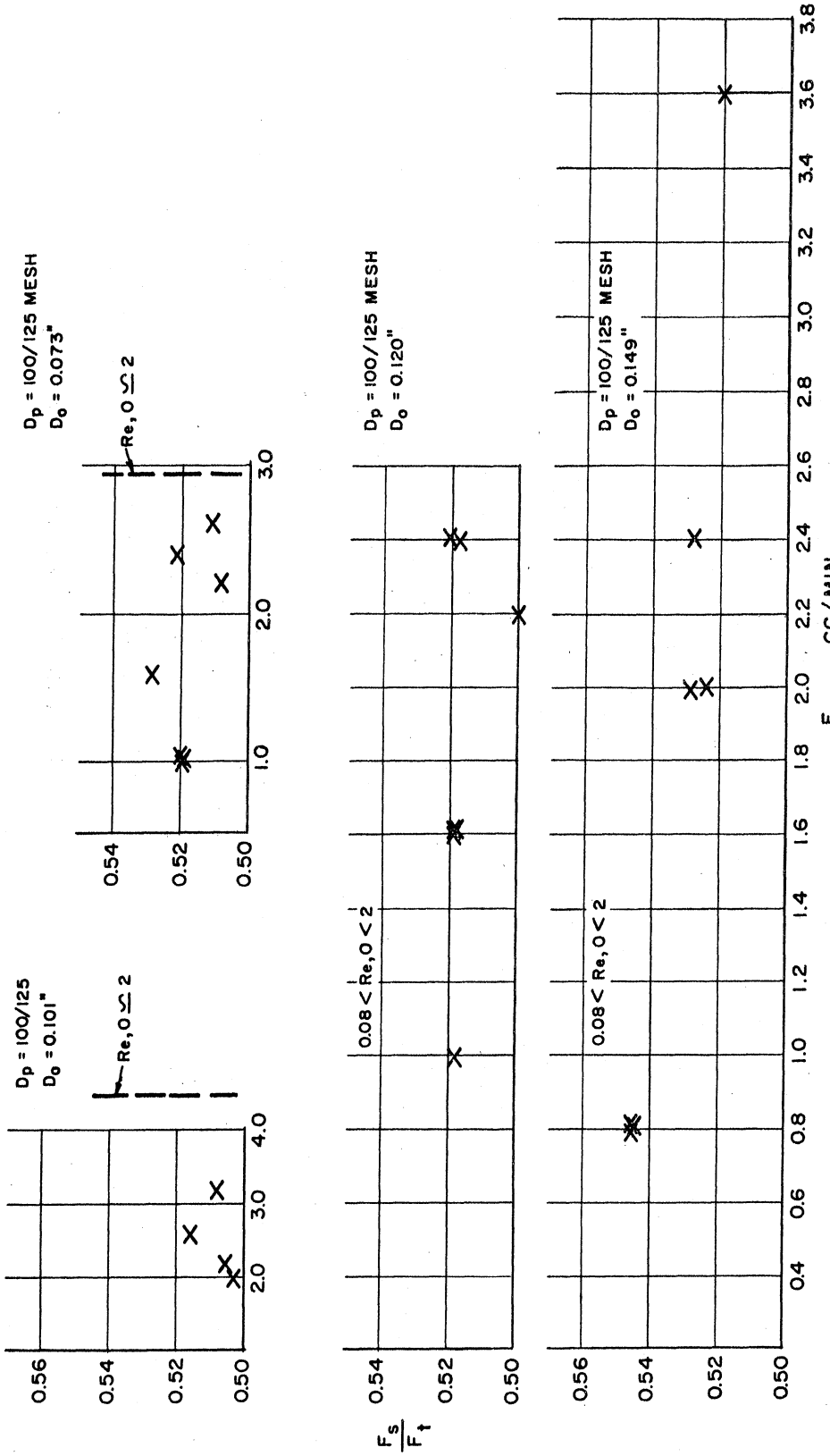

FIG. 20 EXCESS FLOW RATE AND η

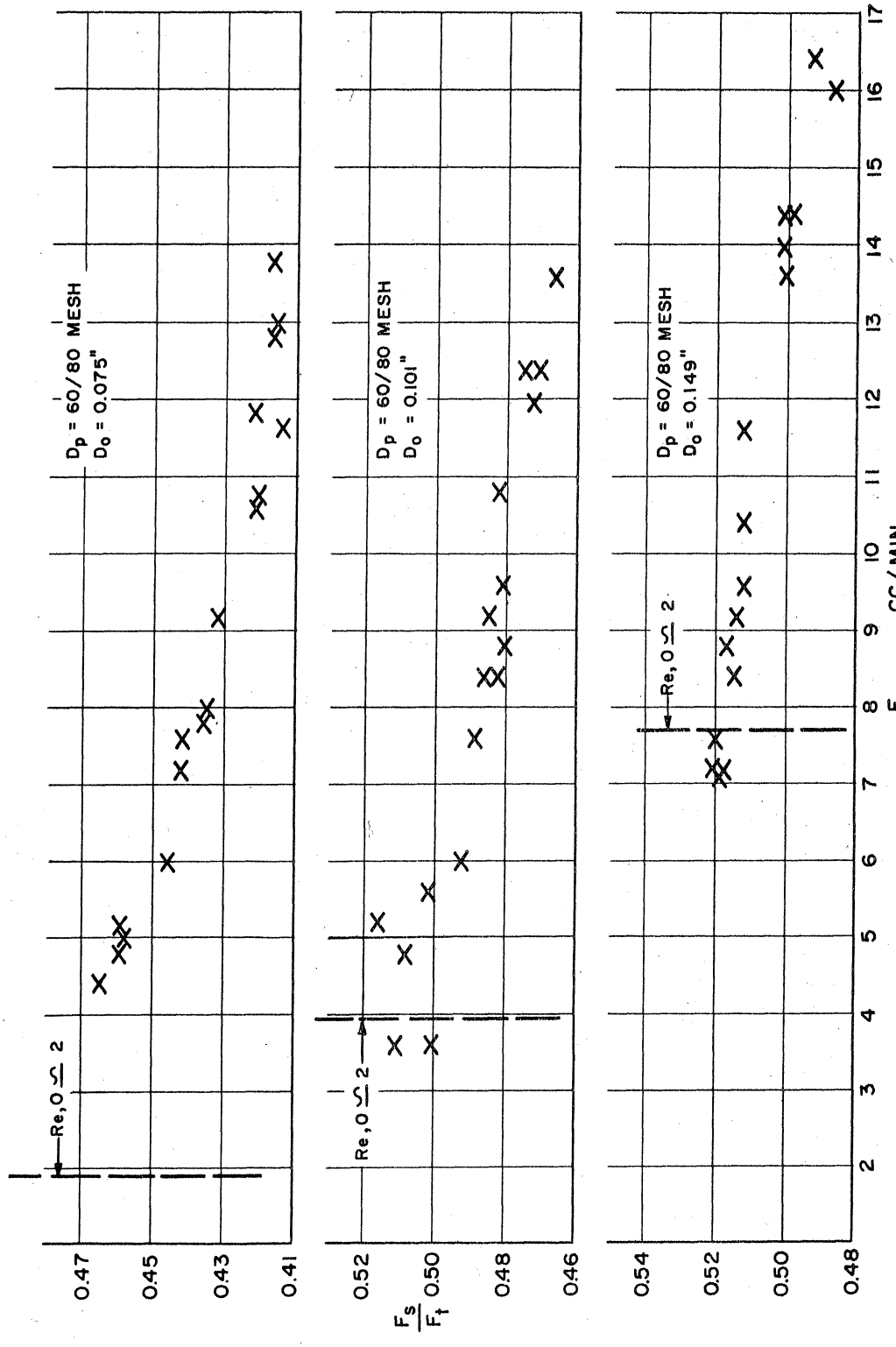

FIG. 21 EXCESS FLOW RATE AND η

Correlation for Wetted Orifice Condition

A similar correlation to the one previously obtained for the non-wetted orifice condition was established using the same dimensionless groups as before. As mentioned above, there exists two critical Reynolds numbers which divide the overall flow regions into three portions: i.e., the laminar region, plateau region, and turbulent regions as shown in Fig. 22. The η value starts from near settled paste density of 0.6 when the flow rate is extremely low, down to 51.5 per cent, the typical value for the plateau region where the first critical in-orifice modified Reynolds number, $Re_o \simeq 0.08$ is reached.

The second critical in-orifice modified Reynolds number which terminates the plateau region and brings the system into turbulence appears to be $Re_o = 2 \sim 3$. The general trend is seen very similar to the one for the non-wetted case. The mechanism responsible for these overall trends may be considered the same as the one proposed previously for the non-wetted orifice condition.

Comparison of Wetted and Non-Wetted Correlations

The correlations between η and Re_o obtained for wetted and non-wetted cases are not substantially different. Only the average plateau value of η and the critical in-orifice modified Reynolds numbers appear slightly different. This indicates that the surface tension effect imposed on the effluent paste flow does affect the η value only slightly.

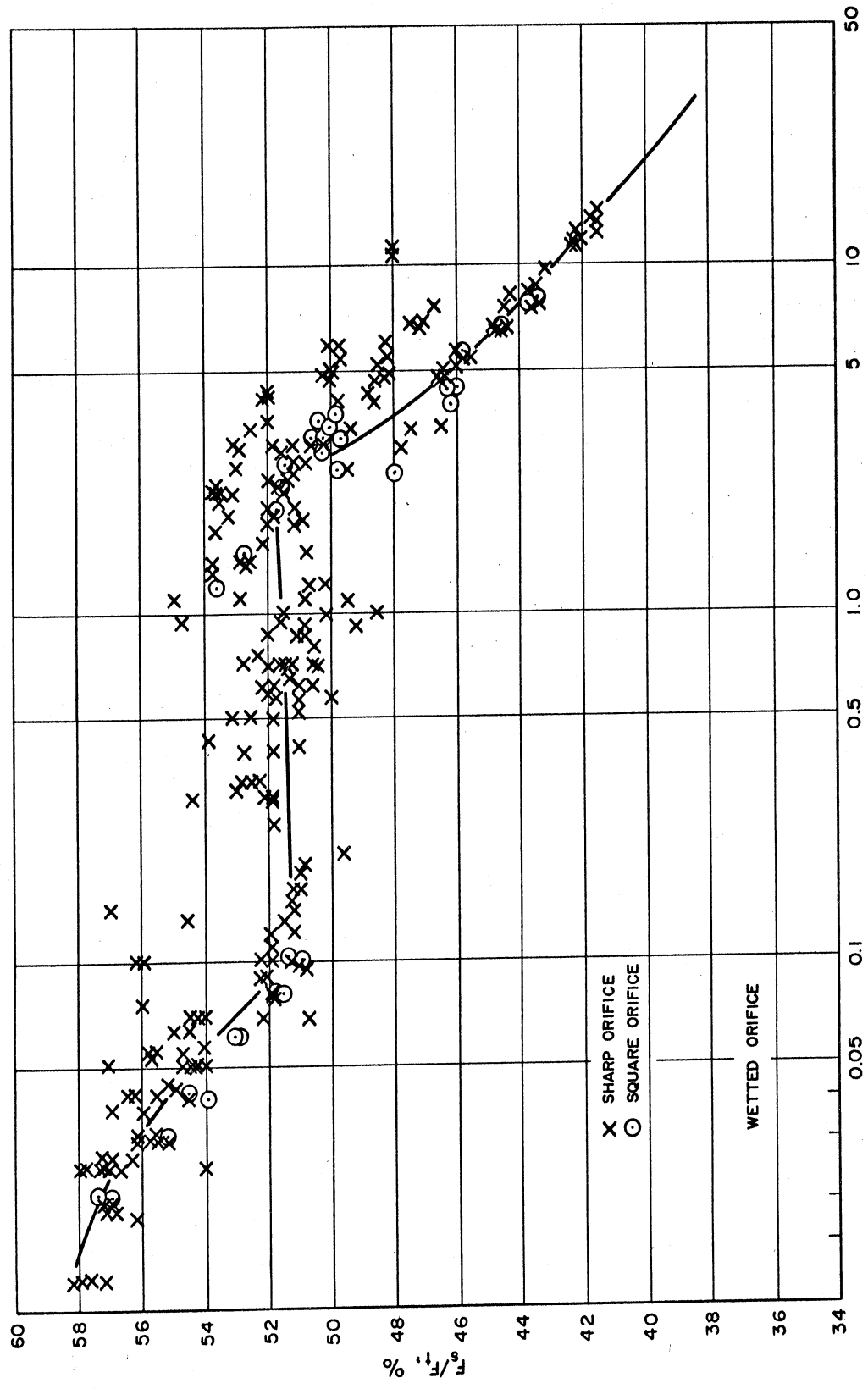

FIG. 22 IN-ORIFICE MODIFIED REYNOLD NUMBER AND η

Terminal Flow Rate for Cocurrent Downward Flow and Validity of the Correlation

Since the correlation was obtained under cocurrent downward flow conditions where positive excess liquid velocity is always realized, the correlation bears these conditions whenever it is applied. The moving bed correlation such as Happel's is applicable to both downward and upward flow. It is also applicable to both cocurrent and counter-current. However, this is not the case for the present correlation. Since the flow through the orifice is an irreversible phenomenon, the result obtained for cocurrent downward flow where positive excess fluid velocity always exists, should be applied to such a system only.

In the final correlation experiments, the solid flow rate was controlled by the static water level above the paste bed. As the level was lowered, the particle flow rate decreased and approached some terminal value. The points on the envelopes in Figure 23 represent such minimum terminal flow rates and the corresponding η values under the conditions specified thereupon.

It appears from the figure that there exists a minimum threshold solid flow rate which can be attained under cocurrent downward (and hence cogravity) flow conditions, implying that only the other flow scheme, i.e., the counter-current flow, will permit the flow rates below the threshold value. One should not, then, apply the correlation presently obtained and presented in this chapter to the flow where flow rate is less than the approximate threshold values as shown in Fig. 23.

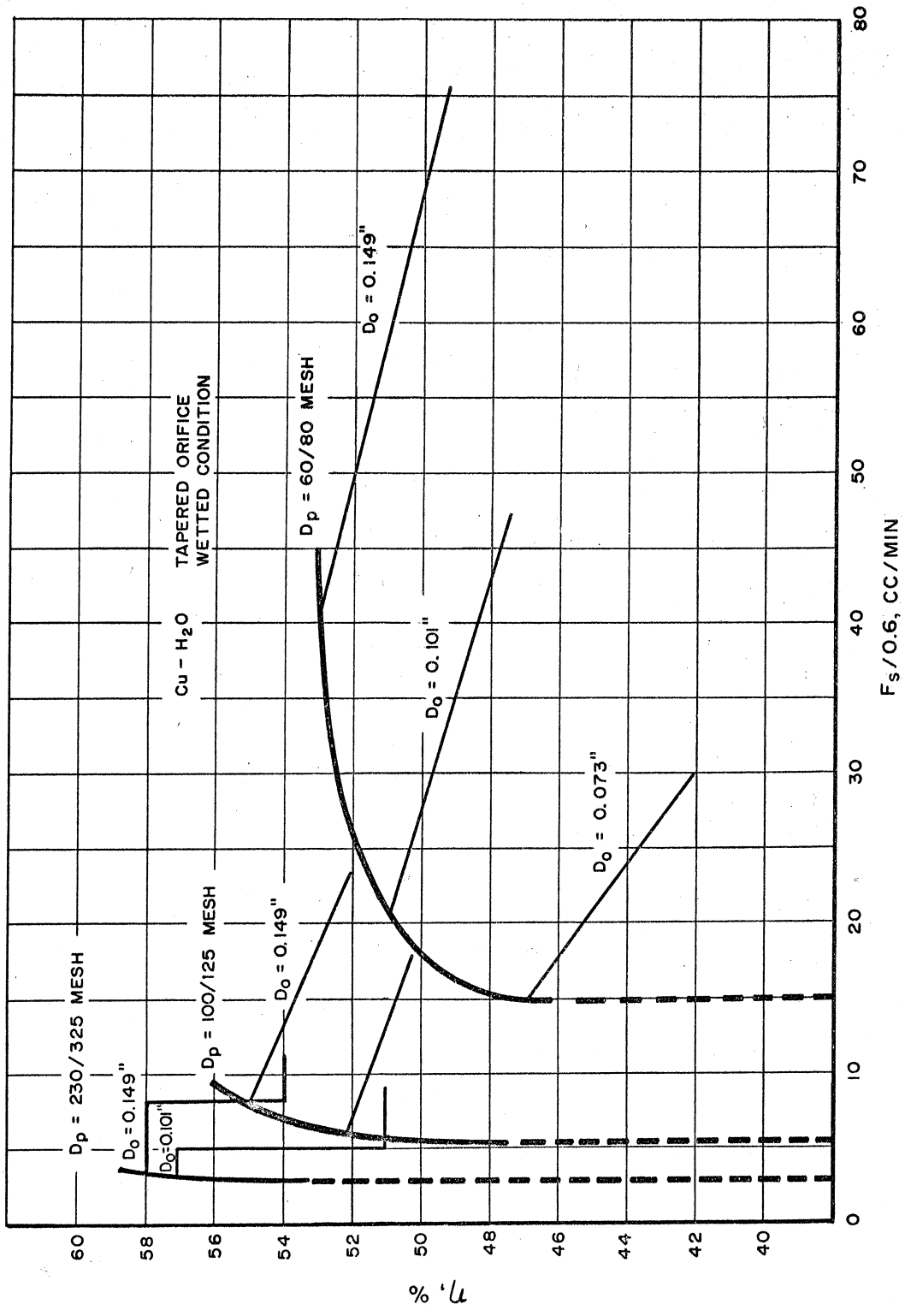

FIG. 23 LIMITS OF SOLID FLOW RATES

Even though only the values for the Cu-H_2O system were shown in Figure 23, it was discovered that the evaluation of the approximate magnitude of threshold flow rates for other systems is possible by simply comparing the free fall terminal velocity for any system to that of the Cu-H_2O system using Stokes' law. The absolute free fall terminal velocity is not helpful due to the wall effects which are inherent in the system, but the relative magnitude of the velocity compared to the reference Cu-H_2O system is important.

In the Stokes' law as expressed by

$$V = \frac{g Dp^2 (\rho_s - \rho_\ell)}{18 \mu}$$

where V: Terminal Settling Velocity,

there can be several cases which make the comparison simple.

a) Different particle size

Since ρ_s, ρ_ℓ, μ are the same, the ratio will be

$$r = \frac{V_1}{V_2} = \frac{Dp_1^2}{Dp_2^2}$$

One such a check using existing data, is given in Table VI.

TABLE VI

COMPARISON OF RATIO OF FREE SETTLING VELOCITY

AND THRESHOLD FLOW RATE RATIO (I)

(0.101" tapered orifice, Cu-H_2O system)

Particle Sizes	Average Diameter"	$\frac{D1^2}{D2^2}$	Observed Threshold Flow Rate $\frac{cc}{min}$	Ratio
60/80	0.0084 D_1	8.4	14.2	7.9
230/325	0.0029 D_2		1.8	

b) Different carrier liquid

Since Dp is the same,

$$r = \frac{V_1}{V_2} = \frac{(\rho_s - \rho_{l1}) \cdot \mu_2}{(\rho_s - \rho_{l2}) \cdot \mu_1}$$

A set of experimental data for Cu-Ethylene Elycol system was used to show the fair agreement between the calculated and actual data, as shown in Table VII.

TABLE VII

COMPARISON OF FREE SETTLING VELOCITY RATIO

AND MINIMUM FLOW RATE RATIO (II)

(0.149" tapered orifice, Cu - H2O system)

Particle Meshes	Carrier Liquid	$\frac{(\rho_s - \rho_{l_1})\mu_2}{(\rho_s - \rho_{l_2})\mu_1}$	Observed Minimum Flow Rate $\frac{(cc)}{(min)}$	Ratio
60/80	#2 Ethylene Glycol $\rho_1 = 1.11 \frac{gr}{cc}$ $\mu_1 = 15.9$ c.p.	3.0	1.7	2.8
60/80	#3 Ethylene Glycol $\rho_2 = 1.08 \frac{gr}{cc}$ $\mu_2 = 5.3$ c.p.		4.8	

Particularly for the nuclear system, one such a use of Stokes' law in determining the applicability of the cocurrent downward flow correlation, was demonstrated in the sample calculation in the following chapter.

Finally, in case of an actual nuclear reactor, an additional effect will be experienced in the system. The fission gas will be formed inside the fuel particles and diffuse toward the particle surface. Hence gas bubbles will drift through the system. The estimated amount of such a gasification, however, is rather small. Hammitt (22) observed such a condition, and discussed the possible effects.

REGRESSION ANALYSIS

AND

SAMPLE CALCULATION FOR WETTED ORIFICE CONDITIONS

A simple regression analysis was performed to check the possible linearity of the portions of the correlation curve. The portions chosen for the analysis are the laminar region and transient plateau region. The coupling of Happel correlation and the regression equation obtained in this work were examined closely and presented in the form of simultaneous equations. A typical sample calculation was presented to indicate the application of the correlations to the evaluation of reactor systems.

Regression Analysis of Laminar Flow Region

Since the higher limit of in-orifice modified Reynolds number lies around 0.08 in the laminar region, the data to be used for the analysis were chosen from this region. Data which were picked in a random manner, stand as follows:

η	56.2	54.1	54.0	55.6	54.5	54.7	54.1	
Re_o	0.030	0.050	0.050	0.030	0.062	0.050	0.056	
η	53.3	54.0	56.0	57.1	58.1	57.8		
Re_o	0.075	0.025	0.037	0.025	0.012	0.012		
η	56.8	57.1	55.0	57.2	54.8	56.4	54.2	---
Re_o	0.019	0.019	0.043	0.027	0.054	0.027	0.068	---

Replacing $\eta = y$ and $Re_o \; x$,

the following calculations are made.*

$$\Sigma (x - \bar{x})^2 = \Sigma (X^2) - \frac{(\Sigma x)^2}{n} = 0.0067$$

$$\Sigma (y - \bar{y})^2 = \Sigma (y^2) - \frac{(\Sigma y)^2}{n} = 40$$

$$\Sigma (x - \bar{x})(y - \bar{y}) = \Sigma (xy) - \frac{\Sigma (x) \Sigma (y)}{n} = -0.44$$

the correlation coefficient, r, defined as

$$r = \frac{\Sigma (x - \bar{x})(y - \bar{y})}{\sqrt{\Sigma (x - \bar{x})^2 (y - \bar{y})^2}}$$ is calculated next.

$$r = -0.86$$

From the table of r values, the probability of getting such a value for r in the absence of any linear correlation is far less than 0.001 or 0.1%. Thus the assumed linearity is seen more than reasonable.

Assuming the well-promised linearity, the slope coefficient b is calculated.

$$b = \frac{\Sigma (y - \bar{y})(x - \bar{x})}{\Sigma (x - \bar{x})^2} = -66.7$$

Also

$$a = \frac{\Sigma y}{n} = \bar{y} = 55.1$$

$$\bar{x} = 0.0385$$

* Following a standard statistical method as shown in Goulden, C.H. Methods of Statistical Analysis Chapter 7, or Brownlee, M.A. Industrial Experimentation Chapter 9, among others.

The regression of y upon x is then

$$y = a + b\,(x - \bar{x})$$

$$= 55.1 - 66.7\,(x - 0.0385)$$

$$y = 57.8 - 66.7x \quad \text{or}$$

$$\eta(\%) = 57.8 - 66.7\,(Re_o) \quad \text{for } Re_o = 0 \sim 0.08$$

Regression Analysis of Plateau Flow Region

As observed in the graphical representation of the correlation, the region bound by $Re_o = 0.08$ and $Re_o = 2$ appears to be horizontal in which the η value seems not to vary too much. Regression analysis of this region is hence very interesting.

Data stands as follows:

Re_o	1.6	0.69	0.93	0.41	0.56	0.59	2.0
η	52.1	52.0	51.6	51.9	50.0	52.0	52.0
Re_o	2.0	0.46	0.46	0.24	1.9	0.41	1.8
η	51.1	50.8	50.8	52.0	53.2	51.0	52.0
Re_o	1.5	1.9	2.0	1.8	0.93	1.0	----
η	52.9	51.9	51.1	51.5	50.6	51.6	----

Replacing $\eta = y$ and $Re_o = x$.

the following calculations are made:

$$\Sigma (x - \bar{x})^2 = 8.33$$

$$\Sigma (y - \bar{y})^2 = 11.2$$

$$\Sigma (x - \bar{x})(y - \bar{y}) = 3.508$$

The correlation coefficient r is then,

$$r = \frac{\Sigma (x - \bar{x})(y - \bar{y})}{\sqrt{\Sigma (x - \bar{x})^2 (y - \bar{y})^2}} = 3.65$$

This is between the significance levels of 0.01 and 0.001. Hence the assumption of linearity in this region is very sound.

Regression coefficients are calculated as follows:

$$b = 0.42$$

$$a = \frac{\Sigma y}{n} = 51.6$$

$$\bar{x} = 1.16$$

The regression of y upon x is then

$$y = a + b (x - \bar{x})$$

$$= 51.6 + 0.42 (x - 1.16)$$

$$\therefore y = 51.2 + 0.42x$$

or

$$\eta (\%) = 51.2 + 0.42 (Re_o) \quad !$$

for $Re_o = 0.08 \rightarrow 2$

The second term is negligible compared to the first term, and the value in the region is practically constant (plateau).

Coupling of the Regression Equations with Moving Bed Correlation

As developed in a previous chapter, the typical moving bed correlation can be modified slightly and represented in the following form:

$$\frac{\Delta p}{L} = \frac{32\, f_{mod}\, (1-\epsilon)\, (1-\epsilon-\eta)^2\, F_s^2\, \rho\ell}{D_p\, g_c\, \eta^2\, \pi^2\, D_t^4}$$

where

$$f_{mod} = f/(1-\epsilon)^3$$

On the other hand,

$$N_{Re,mod} = N_{Re}\,(1-\epsilon)$$

$$= \frac{DpG}{\mu}\,(1-\epsilon)$$

Rewriting this, $N_{Re,mod} = \frac{Dp\ Vexcess\ \rho\ell}{\mu}\,(1-\epsilon) = \frac{4D_p\ Fexcess\ \rho\ell\,(1-\epsilon)}{\pi\, D_t^2\, \mu}$

On the other hand, our regression analysis shows that

a) For $Re_o = 0 \backsim 0.08$

$100\eta = 57.8 - 66.7\ (Re_o)$

b) For $Re_o = 00.8 \backsim 2$

$100\eta = 51.2 + 0.42\ (Re_o)$

Remembering

$Fexcess = Ftotal - \frac{F_s}{1-\epsilon}$ one obtains

$$F_s = \frac{Fexcess\ \eta\,(1-\epsilon)}{1-\epsilon-\eta}$$

Combining these relations, one has now the following simultaneous equations:

$$\frac{\Delta p}{L} = \frac{32\, f_{mod}\, (1-\epsilon)\, (1-\epsilon-\eta)^2\, F_s^2 \rho_\ell}{D_p\, g_c\, \eta^2\, \pi^2\, D_t^4} \quad \text{--(1)}$$

$$100\eta = 57.8 - 66.7 \left(\frac{D_p\, F_{excess}\, \rho_\ell}{D_o^2\, \mu} \right) \text{--(2)} \quad \text{for } Re_o = 0 \sim 0.08$$

$$100\eta = 51.2 + 0.42 \left(\frac{D_p\, F_{excess}\, \rho_\ell}{D_o^2\, \mu} \right) \text{--(3)} \quad \text{for } Re_o = 0.08 \sim 2$$

$$F_s = \frac{F_{excess}\, \eta\, (1-\epsilon)}{1-\epsilon-\eta} \text{----------(4)}$$

Sample Calculation

To demonstrate the application of the coupled correlations to the evaluation of the nuclear problems, a sample calculation is made on the following basis:

Basis:

System	=	UO_2 - Na	
Temperature	=	400°C	
Flow tube	=	Length 40" (101.6 cm)	
		i.d. 0.280" (0.711 cm)	
Orifice	(immersed in sodium)		
	Shape 60° tapered orifice		
	Diameter 0.075" (0.190 cm)		
Particle	flow rate	=	20 cc/min
Particle	shape	=	Spherical
	size	=	100/125 mesh

Calculation:

First the particle flow rate requirement is examined to determine whether cocurrent downward flow scheme can give such a flow rate. The ratio of terminal settling velocities for UO_2-Na system and Cu-H_2O system is calculated first.

$$\frac{V_{uo2}}{V_{cu}} \simeq \frac{F_{uo2}}{F_{cu}} = \frac{(\rho UO_2 - \rho Na).\ \mu H_2O}{(\rho cu - \rho H_2O).\ \mu Na}$$

$$= \frac{(10.3 - 0.854)(1.0)}{(8.9 - 1.0)(0.269)} \quad *$$

$$\simeq 4.47$$

From Figure 23, one can observe that the approximate threshold flow rate for 100/125 mesh particles, and 0.075" size orifice is around 3 cc/min. Hence the threshold flow rate for UO_2-Na system is around

$$3 \times 4.47 \simeq 14 \text{ cc/min.}$$

---

* For 400°C,

$\mu \ell$ = 0.269 c.p. $\qquad \rho UO_2 = 10.3$

$\rho \ell$ = 0.854 g/cc

Hence, the present solid flow rate requirement of 20 cc/min will certainly be attained in the cocurrent downward flow.

The in-orifice modified Reynolds number is formulated next.

Since $D_p = 0.0135$ cm,

$$Re_o = \frac{(0.0135)\ (Fexcess)\ (0.854)\ (100)}{(0.190)^2\ \ (0.269)\ \ (60)}$$

$$Reo = 1.98\ \ Fexcess \quad - - - - - - - - - (a)$$

But $Fs = 20$ cc/min

Hence, from equation (4),

$$20 = \frac{Fexcess\ \ \eta\ \ (0.6)}{0.6 - \eta}$$

assuming $\epsilon \lesssim 0.40$

$$\therefore\ 0.6\ \eta\ \ Fexcess = 12 - 15\ \eta \quad - - - - - (b)$$

Substituting the Fexcess term in (b) into (a), one obtains

$$Re_o = \frac{23.8 - 39.6\ \eta}{0.6\ \eta}$$

or

$$\eta = \frac{23.8}{0.6\ Re_o + 39.6}$$

At this point, one can proceed as follows:

(a) Use regression equations:

Since one has no idea about the final Re_o value, two sets of simultaneous equations can be tentatively set for laminar and transition

flow regions. They are:

$$\begin{cases} \eta = \dfrac{23.8}{0.6\ Re_o + 39.6} \\ 100\,\eta = 57.8 - 66.7\ Re_o \end{cases}$$

and

$$\begin{cases} \eta = \dfrac{23.8}{0.6\ Re_o + 39.6} \\ 100\,\eta = 51.2 + 0.42\ Re_o \end{cases}$$

Solving these equations, one learns that the first set of equations give negative Re_o value. On the other hand, the second set gives $Re_o \simeq 7.1$, which is beyond the applicable range of this set of equations.

(b) Knowing now that the in-orifice flow is in the turbulent region, one uses try-and-error method and find the set of values for Re_o and η which falls on the curve in the turbulent region.

After several trials, one finds these values to be

$$Re_o = 35 \quad *$$
$$\eta = 39.8\%$$

and hence

$$F_{excess} = 25.5 \text{ cc/min.}$$

---

* It is interesting to observe that S.R.I. data gives
$F_s = 20.4$ cc/min and $\eta = 41.7$
for 100/140 UO_2-Na and 0.075" tapered orifice under 310°C.
(Appendix I)

Now substituting these values into (2),

$$N_{Re,\ mod.} = \frac{4\ (0.0135)\ (25.5)\ (0.854)\ (0.6)\ (100)}{60\ \pi\ (0.190)^2\ (0.269)}$$

$$\simeq 3.85$$

From Happel's plot, it is found that

$$f_{mod} \simeq 105$$

Hence, from equation (1),

$$\frac{\Delta p}{L} = \frac{(32)\ (105)\ (0.6)\ (0.202)^2\ (20)^2\ (0.854)}{(60)^2\ (0.0135)\ (981)\ (0.398)^2\ \pi^2\ (0.711)^4}$$

$$= 1.46 \quad \frac{g}{cm^3}$$

Since $L = 101.6$ cm,

$$\Delta p = (1.46)\ (101.6)\ \frac{g}{cm^2}$$

$$\therefore \Delta p = 1.48 \times 10^2\ \frac{g}{cm^2}\ !$$

THE EFFECT OF TUBE DIAMETER ON η VALUE UNDER WETTED AND NON-WETTED CONDITIONS

In the foregoing discussions, the effect of tube diameter on η value was tentatively assumed negligible for the range of ratios of tube diameter to orifice diameter which were used in the experiments. In order to confirm the assumption, or rather to observe the general trend of the effect, experiments were carried out. Copper and alumina particles of 100/125 mesh sizes in water were used. The ratio of tube to particle diameter is generally very large in the system in which one is interested, and hence particle sizes are believed not important in this aspect. It was found that the critical value of the ratio lies between 2 and 2.5 for the physical regions investigated.

Apparatus and Experimental Procedure

The apparatus consists of two parts. The first is an acrylic cylinder of 2-1/4 inch i.d. and 12 inches long (Figure 24). The second component is a bundle of test tubes of 6" length which is attached to the end of the cylinder. Each test tube has tapered orifices of 0.300" diameter at the lower end. Tube diameters ranging from 3/8" to 1" were used, thus varying the ratio of tube to orifice diameters from 1.25 up to 3.33. Two levels of above-bed static heads were chosen, one 2" above the upper end of the particle bed, and the other being 4" above the upper bed end. First, the paste is charged from the open top of the cylinder and the level of liquid properly adjusted. Before the charge, the orifices at each end of the test tubes were plugged by cork stoppers. The orifice to be used was opened. Using a 25cc capacity graduated cylinder, the

non-wetted as well as wetted effluent flow rates were measured. For wetted cases, a known amount of water is kept in the cylinder beforehand and the orifice end is immersed in it during the collection of the effluent paste.

Results

As observed in Figure 25 and 26, the effect of tube wall is eminent when the ratio of tube to orifice diameter is less than 2. In the vicinity of the ratio of 2.5, the effect is still slightly felt, above which value the effect seems negligible. This result then suggests that for the half inch test tube diameter used in the correlation experiment, the data obtained for the orifices of 0.073", 0.101", 0.120", and 0.149" will be free of the tube wall effect. On the other hand, the data obtained for 0.199" orifice probably should not be used in the correlation work. It actually was observed that these data for 0.199" orifice are slightly in the higher side and falls a little above the best fitted line of plateau region.

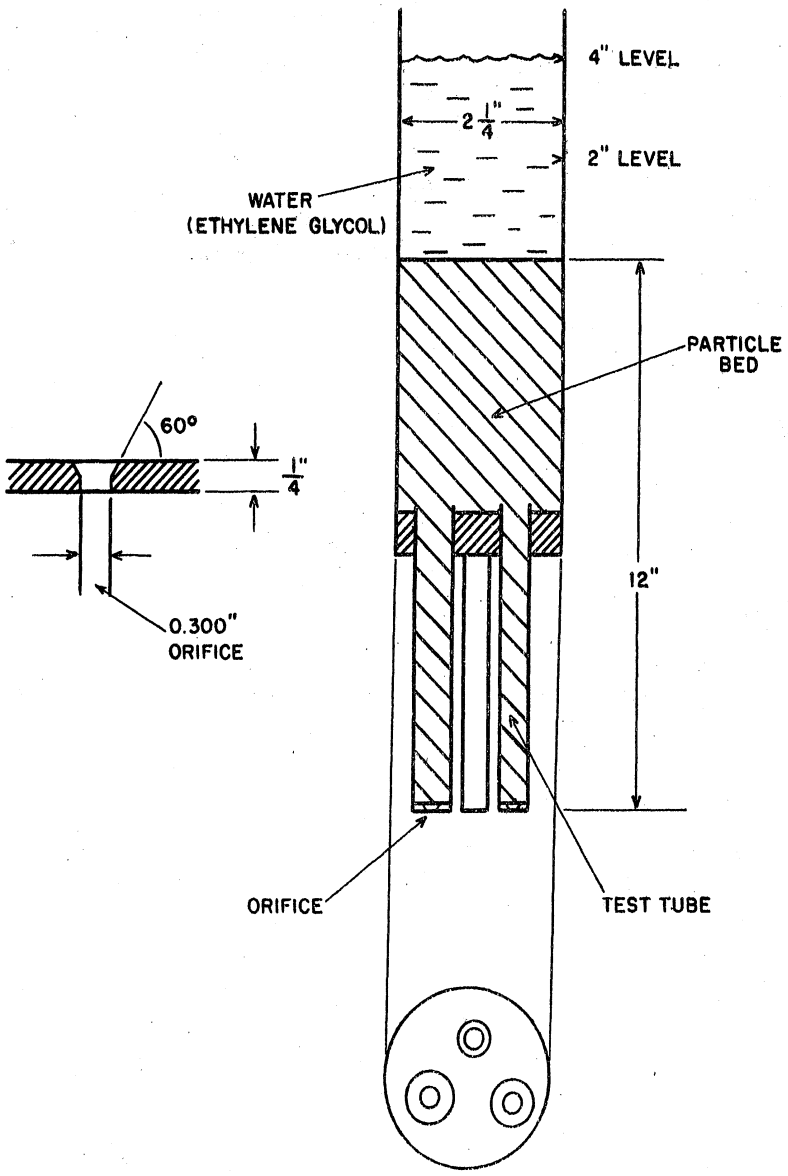

FIG. 24 APPARATUS USED FOR
THE STUDY OF WALL EFFECTS

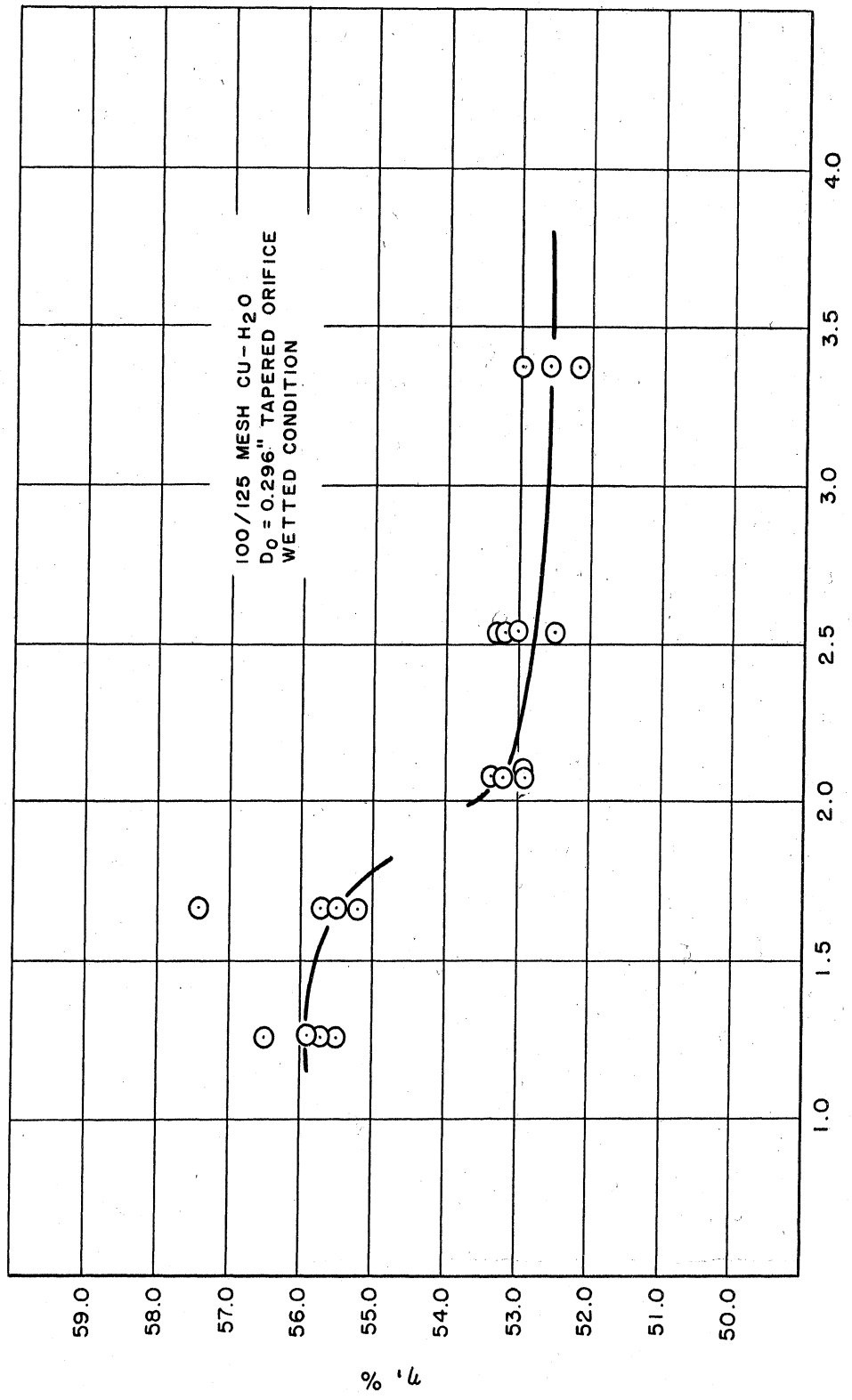

FIG. 25 EFFECT OF TUBE DIAMETER

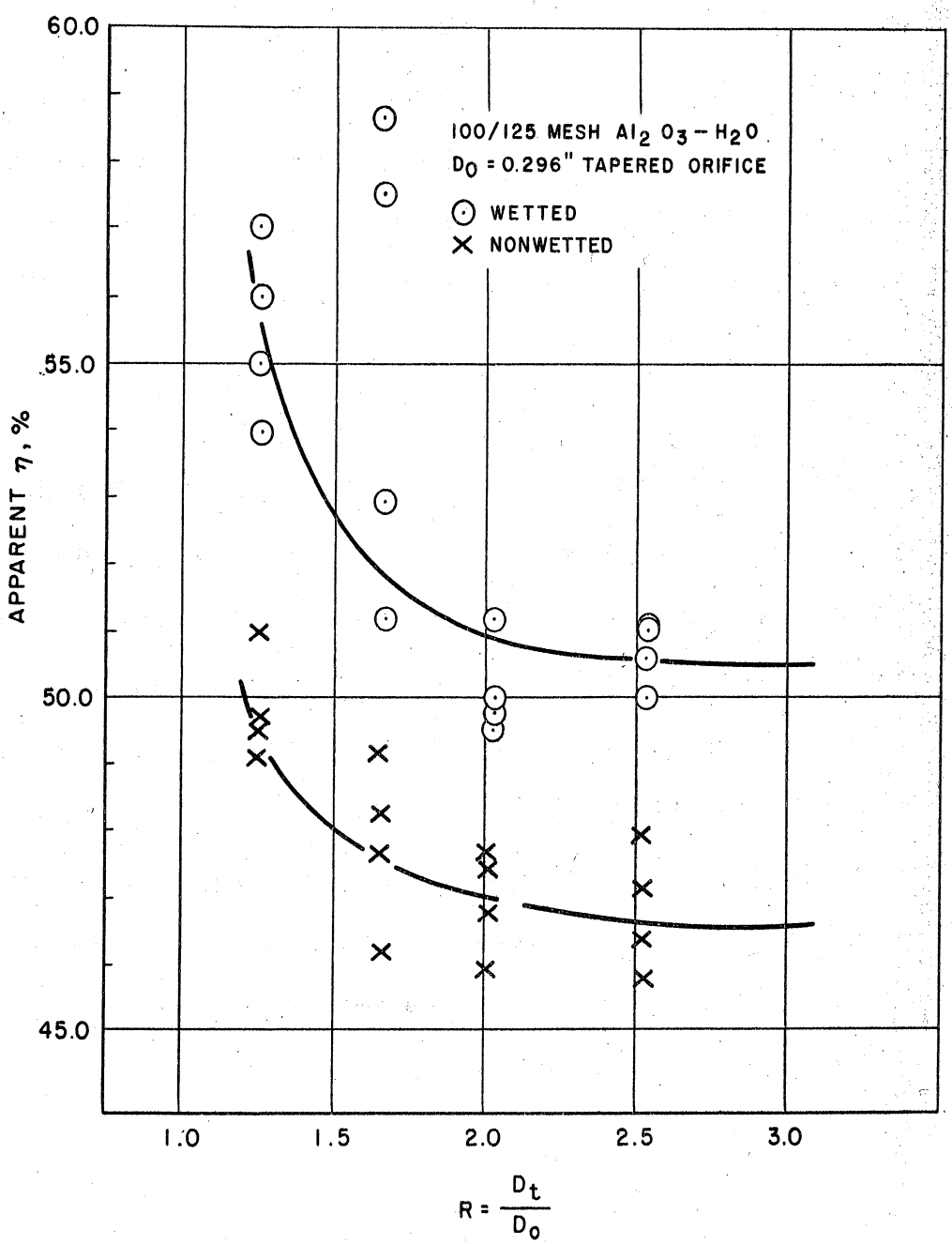

FIG. 26 EFFECT OF TUBE DIAMETER

OBSERVATION OF FLOW PROFILE

The flow profile of a two phase moving bed in a straight tube with an orifice end was observed using a thin slab flow channel which simulates the "nearly two dimensional" condition of the flow. The profile observed in a laminar region of liquid flow rate is very steep, and the angle of slide lies near 80 degrees. Experimental approaches, the description of the profile, and implications of such a profile in the nuclear applications, are described here very briefly.

Apparatus

The apparatus as shown in Fig. 27 is constructed from Plexiglas G grade sheets with a clear transparency. Since the flow channel provided between two sandwich sheets is very thin having the dimension of 3-1/2" x 1/8" x 50", and the particles used for this study have average diameter of around 0.015", one can observe practically two-dimensional flow profile of downstream moving bed through the front sheet. A typical sharp orifice was placed near the bottom end, and the provision of orifice washing stream inlet and outlet was done just below the orifice. The orifice opening is 1/2" diameter. Atop the flow channel is a reservoir portion. Tap water is led through a line to the reservoir and supplied to the reservoir through a glass distributor.

In this particular experiment, copper particles were used. Fresh copper particles can be easily distinguished from surface treated green copper particles of the same size, and are quite convenient for the observation of the boundary between original and new particles during the flow.

Experimental Dimensions and Dynamic Similarity

Since the set-up has scaled-up dimensions compared to the actual reference system, considerations were made in such a way that the relative dimensions of physical variables involved in this experiment hold the dynamic similarity to the reference system. The ratio of orifice size to particle, i.e., D_o/D_p is around 33.3, and the ratio of tube diameter to orifice diameter, i.e., D_t/D_o is 7, both being in accord with the relative dimensions of the reference system. The flow rate employed in this observation is in the laminar region.

Procedure and Result

First, the exit of the channel is closed, the whole flow channel being filled with water thereafter. The orifice washing line is opened and the air pockets in the inlet as well as outlet water lines are removed by the overflow of the water stream through the channel. After a while both portions of the washing lines are closed. Fresh copper particles are charged slowly from the top through the reservoir until they fill most of the flow channel just below the reservoir. The apparatus is tapped and the upper boundary is made flat and even. Carefully, the surface-treated green copper particles are charged onto the fresh portion of copper bed until about half of the reservoir is packed completely. Water is added until it fills the reservoir and the system is ready for the experiment. Both inlet and outlet of the orifice washing line are opened and water is passed through. The exit is then opened. Sequence pictures of the flow pattern are taken at appropriate intervals.

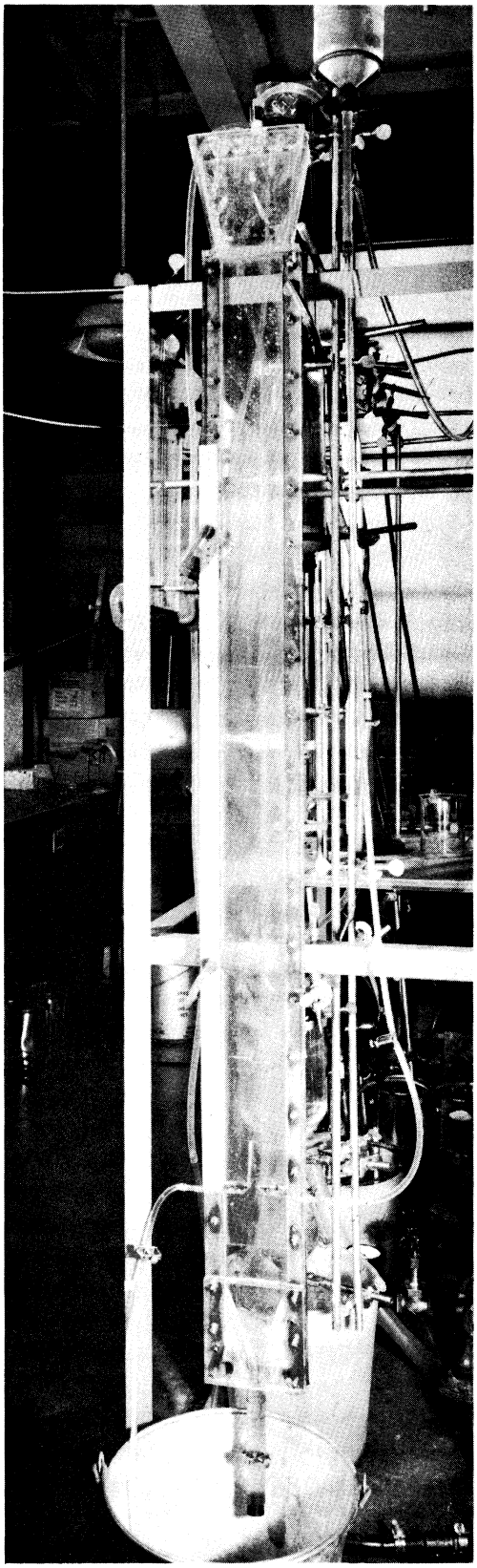

FIG. 27 FLOW PROFILE APPARATUS

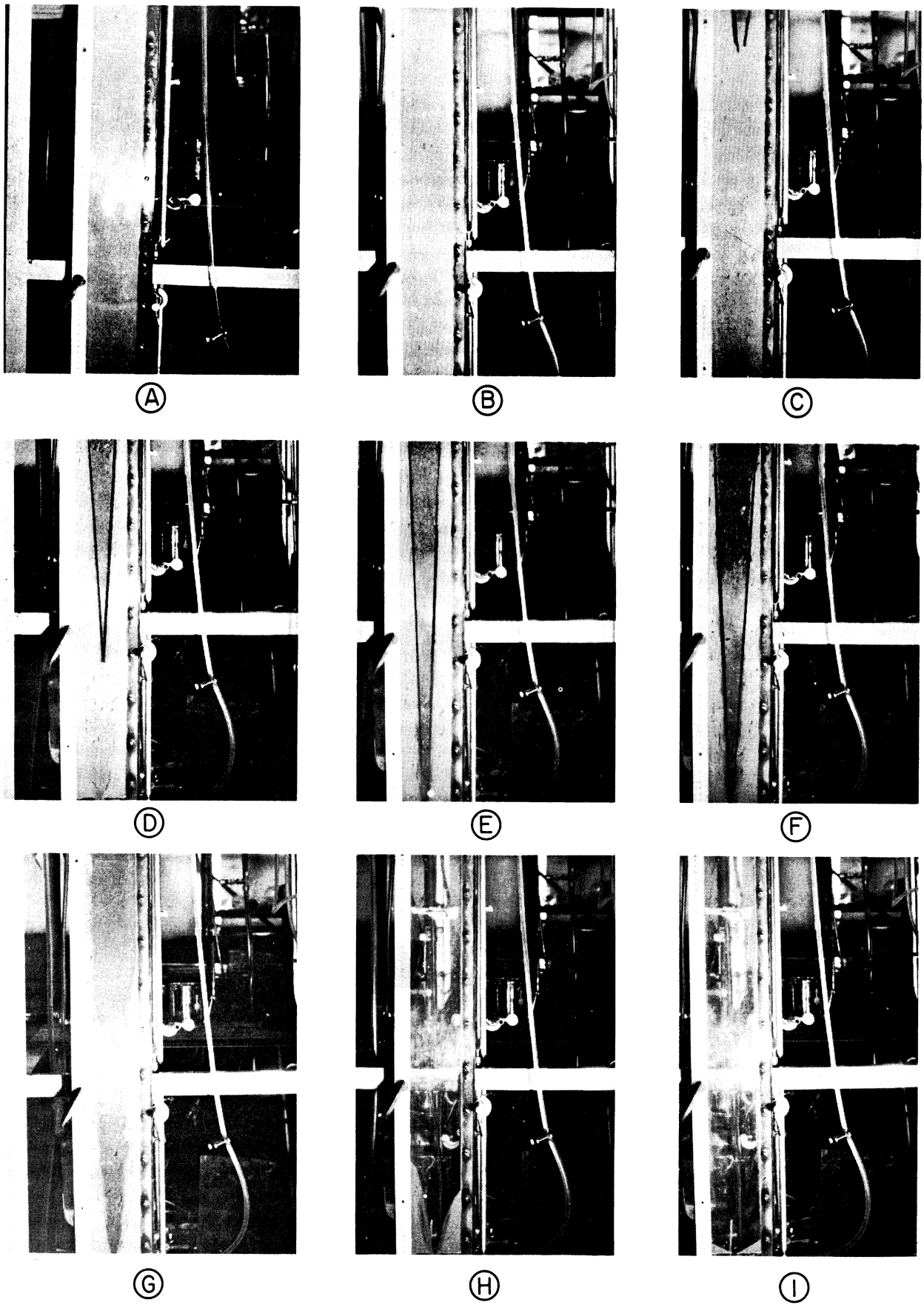

FIG. 28 FLOW PROFILES

The result of such an observation is shown in Fig. 28. The profile of the flow is quite steep as seen, and the angle of slide lies between 78° and 80°.

The Effect of Orifice Shape

The orifices used in this study are 60 degrees tapered orifices and square orifices as mentioned before. As shown in Fig. 22, the η values attained for each orifices both fall on the same correlation line, and the effect of orifice shape seems not as significant as expected prior to the experiment. A possible explanation for this unexpected result may be given by considering the angle of slide as observed in the present experiment. As just concluded, the angle of slide is very steep even at the low flow rate employed in this experiment. This implies that the tapered portion of the orifice is not affecting the flow profile at any significant degree since the narrowest portions of orifice are "looking" always all range of oncoming flow profiles, as long as the tapered angle is smaller than the angle of slide. Thus it would be concluded that the shape of orifice does not affect the correlation already established, but the narrowest opening of the orifice, i.e., the nominal orifice diameter is in fact the dominating factor.

SOME RECOMMENDATIONS FOR FURTHER INVESTIGATIONS

Even though basic schemes of cocurrent downward two phase fluid flow through a round tube with a restricting orifice end have been generally covered in this study, there still remain some related problems which have to be solved in connection with any generalized flow cross section of similar type, even though one strong indication here is such that the tube diameter used in this study may be safely replaced by a general hydraulic diameter. Some suggested further studies are listed as below.

1) Study using various shapes of flow tube cross sections, using the similar experimental approaches taken in this study. Among these, triangular cross sections as well as quadratic ones can be tried.

2) Flow study through a gradually converging tube instead of suddenly contracting orifice geometry. This way, a more practical restricting exit condition may be most possibly realized, especially when one is interested in avoiding fuel particles sintering at the exit.

3) Replication of all experiments using actual sodium-uranium system. The frequently quoted Southern Research Institute experiments are close to this, but the dry orifice condition employed in their work is not adequate, and should be replaced by wetted orifice condition.

4) Theoretical study of the orifice pressure drop for two phase flow.

5) Theoretical comparison of pumping power requirements between cocurrent downward flow and cocurrent upward flow. Since basic data for the latter case have been available, this comparison is now possible and important in comparing the economic aspects of both approaches.

CONCLUSIONS

As has been observed, the mobile-fuel nuclear system based on solid-liquid two-phase downward-flow through a straight tube with a restricting orifice at the bottom can be handled quantitatively using the correlations obtained in this study. Since the correlation was established in a general form using dimensionless groups, the result can also be extended and applied to any generally similar systems. In such a correlation, the concept of "in-orifice" modified Reynolds number is most important. The number determines the effluent paste density through an orifice and in turn defines the absolute physical quantities of the system with the aid of conventional moving bed correlations. The effects of miscellaneous physical variables associated with the present system, and possible explanations regarding their mechanisms, were explored in addition to the main correlation work, and the direction of further investigations to perfect the understanding of the system were suggested.

APPENDIX I

EXPERIMENTAL DATA I

(Southern Research Institute)

100/140 UO_2 - Na

0.075" Tapered Orifice, 310 C

Δ Po "H_2O	Δ Po/Lo "H_2O/"	Δ Pt/L "H_2O/"	Total g/sec	Flow cc/min	Solid g/sec	Flow cc/min	Composition Effluent vol %	Paste vol %	Re,o	Remarks
0	0	4.2	2.9	38.3	2.6	15.9	41.7	59.0	16.7	S.R.I. 24
4.4	5.63	6.3	3.6	49.1	3.4	20.4	41.7	61.7	23.6	P. 10
8.0	10.2	10.4	5.1	65.4	4.5	26.9	41.3	63.5	33.6	L = 6 1/4"
12.2	15.6	15.1	6.3	80.9	5.6	32.5	40.3	63.5	43.0	Lo = 25/32"
0	0	4.2	2.8	34.0	2.5	14.8	43.5	62.1	14.7	

200/325 U - Na
0.075" Tapered Orifice 300 C

-3.0	-3.84	1.0			2.9	9.4				S.R.I., 24
-0.6	-0.76	3.8	4.4	25.9	4.2	13.5	52.0		2.2	p. 7
-3.0	-3.84	1.0			3.1	9.8				L = 6 1/4"
2.5	3.2	7.1	5.7	33.8	5.5	17.5	51.6	61.7	3.5	Lo = 25/32"
5.8	7.4	10.7	7.4	46.6	7.0	22.4	48.0	61.1	6.5	
10.3	13.2	14.2	8.3	51.5	7.9	25.3	49.1	61.7	6.8	
15.5	19.7	19.2	10.2	61.6	9.7	31.1	50.4	61.6	7.4	
2.5	3.2	7.1	5.3	31.0	5.0	16.0	51.6	61.4	3.2	
5.8	7.4	10.7	7.1	42.3	6.8	21.8	51.6	61.5	4.5	
-3.0	-3.84	1.0	3.0	17.6	2.9	9.3	52.8	61.4	1.6	

100/140 U - Na
0.075" Tapered Orifice 300°C

8.0	10.2	9.12	8.58	68.9	8.0	25.3	37.0	56.8	35.7	L = 6 1/4"
1.1	1.41	3.20	5.44	40.5	5.1	16.1	40.2	54.2	15.7	Lo= 25/32 "
-1.1	-1.41	1.10	4.56	33.1	4.3	13.6	41.5	50.1	8.4	
18.3	23.4	15.8	13.1	106	12.2	38.6	36.5	57.2	55.6	
33.2	42.5	24.2	15.9	138	14.6	46.1	33.7	57.6	85.0	
47.9	61.4	36.8	22.2	193	20.5	64.8	33.7	58.2	120	

100/140 U - Na
0.100" Tapered Orifice, 300 C

p_o	$\Delta p_o/L_o$	Δp_t	$\Delta p_t/L$	Total Flow		Solid Flow		Composition Effluent	Paste	$Re_{,o}$	Remarks
2^0	"H_2/"	"H_2O	"H_2/"	g/sec	cc/min	g/sec	cc/min	Vol %	Vol %		
.6	-4.6	57.8	9.3	8.28	48.4	7.9	25.2	52.0	>64		S.R.I. 20
.7	16.3	156.9	25.1	18.8	124	17.7	56.2	45.3	62.7	28.0	p 13
.8	40.7	293.3	47.0	29.7	211	27.7	88.0	41.8	62.1		L = 6 1/4"
.6	-4.6	57.8	9.3	9.23	56.8	88	27.9	49.2	62.9	10.2	Lo= 25/32"
.7	16.3	156.9	25.1	18.2	120	17.2	54.8	45.8	63.2	27.2	
.8	40.7	293.3	47.0	31.6	220	29.2	93.7	42.7	62.0	56.7	
.7	16.3	156.9	25.1	20.3	140	19.0	60.3	43.1	61.0	33.8	
.6	-4.6	57.8	9.3	6.04	33.3	5.8	18.4	55.2	>64		
.8	40.7	293.3	47.0	29.2	202	27.3	86.9	43.1	62.8	52.8	
.9	11.4	49.0	7.8	5.18	28.4	5.0	16.1	56.8	>64		
.6	-4.6	56.2	9.0	6.88	37.9	6.6	21.2	55.8	>64		
.6	-0.77	75.2	12.0	9.75	55.2	9.3	29.9	54.2	>64		
.2	2.8	94.2	15.1	12.8	82.9	12.2	39.2	47.2	62.7	16.7	
.0	6.4	112.5	18.0	14.3	91.0	13.6	43.7	48.0	63.8	18.9	
.9	11.4	135.0	21.6	16.4	104	15.5	49.8	46.8	63.4	20.9	
.5	16.0	157.7	25.2	19.9	133	18.7	60.0	45.2	62.2	30.0	

200/325 U - Na
0.100" Tapered Orifice 350 C

.8	13.8	Not Measured		16.4	97.0	15.6	49.3	52.0		5.90	S.R.I. 20
.9	5.0			11.0	63.0	9.5	30.1	54.0		5.08	p 15
.9	-2.4			6.4	36.5	6.1	19.3	54.0		1.71	
.9	-2.4			6.6	37.0	6.4	20.2	55.0		1.30	
.9	5.0			10.5	60.0	10.1	32.2	54.0		2.48	
.8	13.8			15.6	89.0	15.0	47.4	54.0		3.98	
.0	23.0			21.2	125.0	20.2	63.8	52.0		7.55	
.0	23.0			21.1	125.0	20.2	63.8	52.0		7.55	
.5	32.7			25.6	245.0	24.6	77.5	53.8		4.60	
.5	32.7			25.5	244.0	24.4	76.9	53.8		4.60	

140/200 U - H_2O
0.100" Tapered Orifice

ΔPo "H_2O	ΔPo/Lo "H_2O/"	ΔPt "H_2O	ΔPt/L "H_2O/"	Total g/sec	Flow cc/min	Solid g/sec	Flow cc/min	Effluent Composition Vol %	Re,o	Remarks
1.14	1.46	35.3	5.65	5.58	32.0	5.34	16.9	52.8	1.28	S.R.I. 20
0.98	1.25	37.5	6.00	5.74	33.6	5.48	17.3	51.5	1.62	p 19
1.10	1.41	38.0	6.08	5.54	32.5	5.13	16.2	49.8	1.81	
1.57	2.01	43.9	7.02	6.42	37.3	6.13	19.4	52.0	1.69	
1.89	2.42	45.0	7.20	6.71	39.9	6.40	20.2	50.6	2.10	
2.87	3.67	49.8	7.97	6.79	38.2	6.47	20.4	53.4	1.42	
2.32	2.97	49.3	7.89	7.41	45.0	7.07	22.3	54.8	2.64	
2.95	3.77	51.4	8.22	7.14	40.7	6.76	21.3	47.3	1.73	
3.35	4.28	54.1	8.66	6.90	40.4	6.58	20.8	51.5	1.89	
3.31	4.23	56.2	9.00	7.17	41.9	6.91	21.8	52.0	1.89	
3.66	4.68	59.0	9.45	7.65	44.5	7.28	23.0	51.7	2.13	
4.72	6.03	66.0	10.6	8.38	47.5	8.02	25.3	53.3	1.77	
4.61	5.90	66.9	10.7	7.80	45.8	7.46	23.6	51.5	2.17	
4.92	6.29	71.7	11.5	8.52	49.4	8.15	25.8	52.2	2.17	
5.74	7.33	75.5	12.1	8.90	52.1	8.50	26.8	52.3	2.48	
6.65	8.50	86.2	13.8	9.40	55.5	8.98	28.4	51.2	2.76	
6.85	8.75	88.7	14.2	9.41	55.0	8.97	28.3	51.5	2.60	
7.55	9.65	90.5	14.5	10.21	61.4	10.01	31.7	51.6	2.88	
7.48	9.56	92.6	14.8	10.05	58.9	9.58	30.3	51.4	2.84	
8.03	10.3	98.0	15.7	10.24	61.5	9.98	31.5	51.2	3.03	
7.87	10.1	101.7	16.3	10.15	60.0	9.71	30.7	51.2	3.00	
8.43	10.8	103.3	16.5	10.71	63.8	10.17	32.1	50.3	3.47	
8.70	11.1	104.9	16.8	10.94	65.4	10.41	32.9	50.3	3.58	
8.98	11.5	107.6	17.2	10.79	64.0	10.38	32.8	51.3	3.15	
9.33	12.0	113.5	18.1	11.21	67.0	10.68	33.7	50.3	3.66	

100/140 U - Na
0.075" Tapered Orifice, 300 C

ΔPo "H_2O	ΔPo/Lo "H_2O/"	ΔPt "H_2O	ΔPt/L "H_2O/"	Total g/sec	Flow cc/min	Solid g/sec	Effluent Flow cc/min	Effluent Composition Vol %	Re,o	Remarks
6.1	7.8	58.9	9.42	8.2	60.2	7.6	24.4	40.8	28.5	S.R.I. 21
0.1	0.13	20.5	3.28	5.3	35.6	5.0	16.1	44.7	14.2	p 14
-1.4	-1.8	5.5	0.88	4.4	28.4	4.1	13.2	46.7	9.30	
14.1	18.0	99.3	15.9	10.9	83.7	10.1	32.5	39.0	43.0	
25.2	32.2	143.6	23.0	14.3	109.7	13.3	42.6	39.0	56.1	
39.3	50.3	187.6	30.0	17.8	137.2	16.5	52.8	38.7	71.4	
6.1	7.8	58.9	9.42	7.9	55.7	7.4	23.6	42.6	23.9	
-0.7	-8.9	16.1	2.58	5.0	32.6	4.7	15.2	46.7	10.6	
-1.4	-1.8	5.5	0.88	4.2	26.8	4.0	12.8	47.9	8.0	
14.9	24.3	99.9	16.0	10.8	80.5	10.1	32.4	40.3	38.6	
25.2	32.2	151.9	24.3	14.1	106.7	13.1	42.1	39.7	53.5	
36.5	46.7	184.8	29.6	17.6	134.5	16.3	52.2	39.0	69.3	

140/200 U-Na
0.075" Tapered Orifice 300 C

7.2	9.2	57.6	9.23	7.6	50.9	7.2	23.0	45.2	32.9	S.R.I. 21
15.5	19.8	100.4	16.1	10.6	73.0	9.9	31.9	43.8	29.0	p 15
27.7	35.5	139.7	22.3	13.1	90.9	12.3	39.5	43.5	36.4	
39.6	50.7	199.2	31.9	16.0	113.2	15.0	48.2	42.7	48.0	
0.6	0.76	24.4	3.90	4.8	30.9	4.5	14.5	47.2		
-1.1	-1.4	9.1	1.5	3.2	21.3	3.0	9.6	45.2		
39.6	50.6	-	-	16.3	122.7	15.1	48.4	39.7		
27.7	35.4	147.2	23.6	13.6	97.4	12.7	40.6	41.8	43.3	
15.5	19.8	99.9	16.0	10.2	70.9	9.6	30.8	43.5	28.5	
7.2	9.2	57.0	9.1	7.8	53.0	7.3	23.4	44.3	20.4	
0.6	0.76	27.7	4.4	4.5	31.1	4.2	13.5	43.5	12.5	
39.6	50.7	-	-	16.3	117.2	15.2	48.9	41.8	51.9	
0.6	0.76	-	-	4.7	32.1	4.4	14.1	44.3	12.5	

200/325 U - H_2O
0.100" Tapered Orifice

ΔP_o "H_2O	$\Delta po/L$ "H_2O/"	Δpt "H_2O	$\Delta pt/L$ "H_2O/"	Total g/sec	Flow cc/min	Solid g/sec	Flow cc/min	Effluent Composition Vol %	Re,o	Remarks
1.38	1.77	44.4	7.10	3.49	20.2	3.35	10.6	52.5	0.378	S.R.I. 20
1.57	2.01	46.6	7.46	3.70	21.3	3.54	11.2	52.6	0.394	p 21
2.13	2.72	53.5	8.56	4.10	23.5	3.93	12.4	52.8	0.434	
2.68	3.43	56.2	9.00	4.08	23.3	3.90	12.3	52.8	0.434	
2.91	3.72	58.9	9.41	4.30	25.0	4.12	13.0	52.0	0.512	
3.43	4.38	65.3	10.5	4.59	26.4	4.41	13.9	52.7	0.473	
4.09	5.24	73.9	11.8	5.12	29.4	4.87	15.4	52.4	0.550	
4.49	5.75	77.6	12.4	5.34	30.5	5.11	16.1	52.8	0.550	
7.60	9.74	109.8	17.4	6.62	38.3	6.17	19.5	50.9	0.867	
7.80	10.0	111.9	17.9	6.72	38.9	6.43	20.3	52.2	0.787	
7.05	9.03	104.4	16.7	6.45	37.4	6.17	19.5	52.1	0.750	
6.77	8.68	102.3	16.4	6.06	34.7	5.80	18.3	52.7	0.630	
6.54	8.38	98.0	15.7	6.18	35.3	5.94	18.8	53.3	0.590	
6.02	7.71	87.8	14.0	6.18	35.5	5.92	18.7	52.7	0.670	
5.59	7.16	78.7	12.6	5.60	31.8	5.37	17.0	53.5	0.512	
5.31	6.80	82.5	13.2	5.31	30.9	4.99	15.8	51.1	0.670	
0.98	1.25	37.5	6.0	3.49	19.8	3.35	10.6	53.5	0.319	
0.27	0.346	29.4	4.70	2.86	16.0	2.76	8.7	54.4	0.228	
-1.06	-13.6	12.3	1.97	2.11	11.6	2.03	6.4	55.2	0.145	
-1.89	-2.42	4.3	0.69	1.69	9.2	1.62	5.1	55.4		

200/325 U - H_2O

0.100" Square Orifice

Δpo H_2O	Δpo/Lo "H_2O/"	Δpt "H_2O	ΔPt/L "H_2O/"	Total g/sec	Flow cc/min	Solid g/sec	Flow cc/min	Effluent Composition Vol %	Re_o	Remarks
.40	6.69	70.9	11.3	4.47	25.9	4.27	13.5	52.1	0.512	S.R.I. 20
.72	7.17	84.6	13.5	4.58	27.6			52.5		p. 22
.67	8.61	93.7	15.0							
.31	8.06	91.6	14.7	4.61	26.7	4.41	13.9	52.1	0.515	
.91	8.98	99.1	15.9	4.91	30.6	4.67	14.8	48.4	0.905	
.54	13.0	124.2	19.9	6.61	39.1	6.30	19.9	50.9	0.905	
.98	6.05	66.9	10.7	4.21	23.9	4.03	12.7	53.1	0.512	
.78	5.75	65.9	10.4	4.09	23.7	3.91	12.4	52.3	0.473	
.87	4.36	50.9	8.14	3.48	20.1	3.45	10.9	54.2	0.276	
.91	4.41	56.2	9.00	3.84	22.5	3.69	11.7	52.0	0.473	
.44	3.71	48.2	7.70	3.49	20.1	3.34	10.6	52.7	0.433	
.09	3.17	43.4	6.94	3.36	19.4	3.22	10.2	52.6	0.354	
.57	2.38	40.2	6.44	3.19	18.4	3.06	9.7	52.7	0.315	
.18	1.79	32.7	5.23	2.89	16.4	2.77	8.8	53.7	0.276	
.87	1.32	29.4	4.70	2.88	16.6	2.77	8.8	53.0	0.276	
.47	0.71	23.0	3.68	2.54	14.3	2.45	7.7	53.8	0.236	
.00	0.00	16.1	2.56	2.29	12.9	2.20	7.0	53.4	0.197	
.51	-0.78	5.4	0.86	1.64	9.1	1.57	5.0	54.9	0.118	
.14	-1.73	3.2	0.51	1.58	8.8	1.52	4.8	54.5	0.118	

APPENDIX II

EXPERIMENTAL DATA II

(Preliminary Experiment)

Run 1

100/125 Glass Bead - H_2O
0.100" Tapered Orifice

Δ Po "H_2O	Δ Po/Lo "H_2O/"	Δ Pt/1.9 "H_2O	Δ Pt/L "H_2O/"	Ft cc/min	F paste cc/min	η %	Re.o	Remarks
7/8	0.7	2.0	0.61	16.0	14.8	54.3	0.43	Oct. 13, '59
7/8	0.7	2.0	0.61	16.2	15.0	54.7	0.43	70°F
1½	1.3	3.0	0.91	29.6	26.2	52.0	1.26	Sphere glass bead
1½	1.3	3.0	0.91	26.2	22.6	51.1	1.30	L = 6¼"
1 3/4	1.5	4.0	1.2	33.2	29.0	51.3	1.54	Lo= 1 1/8"
1 3/4	1.5	4.0	1.2	33.2	29.0	51.3	1.54	= 2.6
		5.0	1.5					
		5.0	1.5					
2 1/8	1.8	6.0	1.8	38.4	33.0	50.8	1.97	
2 1/8	1.8	6.0	1.8	37.6	32.4	50.8	1.89	
2¼	2.0	7.0	2.1	42.8	38.6	50.2	1.54	
		7.0	2.1					
2½	2.2	8.0	2.5	46.4	40.8	52.0	2.05	
2½	2.2	8.0	2.5	49.4	43.1	51.4	2.32	
		9.0	2.7					
		9.0	2.7					
3 3/8	3.0	10.0	3.0	60.0	53.6	52.7	2.32	
3 3/8	3.0	10.0	3.0	60.0	58.6	52.1	2.72	

Run 2 — 100/125 — Atomized p_b - H_2O
0.100" — Tapered Orifice

ΔP_o "H_2O	$\Delta P_o/L_o$ "H_2O/"	$\Delta P_t/1.9$ "H_2O	$\Delta P_t/L$ "H_2O/"	F paste cc/min	F Total cc/min	η %	Remarks
-3/4	-0.67	0.5	0.15	11.5	13.0	47.7	Settled paste
-3/4	-0.67	0.5	0.15	11.2	12.5	48.4	Density = 0.54
-5/8	-0.55	1.0	0.30	13.2	15.0	47.6	Atomized p_b non-
-5/8	-0.55	1.0	0.30	13.6	15.6	47.0	spherical
-5/8	-0.55	2.0	0.61	19.0	22.0	46.7	
-5/8	-0.55	2.0	0.61	17.4	20.0	47.0	p = 11.3
-3/8	-0.33	3.0	0.91	21.2	25.6	44.8	L = 6¼"
-3/8	-0.33	3.0	0.91	20.2	26.4	41.3	Lo= 1 1/8"
-1/8	-0.11	4.0	1.2	24.0	29.4	44.3	
-1/8	-0.11	4.0	1.2	25.4	30.6	44.7	
1/16	0.05	5.0	1.5	28.8	35.6	41.4	
1/16	0.05	5.0	1.5	29.2	36.0	43.7	
3/8	0.33	6.0	1.8	31.6	39.0	43.8	
3/8	0.33	6.0	1.8	33.2	46.6	43.1	
5/8	0.55	7.0	2.1	39.4	49.6	42.8	
5/8	0.55	7.0	2.1	36.4	46.8	42.0	
1	0.80	8.0	2.5	42.4	53.2	42.9	
1	0.80	8.0	2.5	42.0	52.0	43.5	
1¼	1.1	9.0	2.7	48.4	62.0	42.0	
1¼	1.1	9.0	2.7	48.0	61.9	42.0	
1½	1.3	10.0	3.0	52.8	66.8	42.7	
1½	1.3	10.0	3.0	52.9	67.0	42.4	

Run 3 — 100/125 — Cu - H_2O — 0.100" — Tapered Orifice

$P_t/1.9$ H_2O	$\Delta P_t/L$ "H_2O/"	F paste cc/min	F total cc/min	F excess cc/min	η %	Re, o	Remarks
1.0	0.30	10.6	12.2	1.6	52.1	0.59	% F
1.0	0.30	10.6	12.2	1.6	52.1	0.59	L = $6\frac{1}{2}$"
2.0	0.61	8.9	10.0	1.1	53.5	0.40	Lo= 1 1/8"
2.0	0.61	9.3	10.4	1.1	53.6	0.40	
3.0	0.91	14.2	16.0	1.8	53.3	0.66	
3.0	0.91	13.6	15.8	2.2	51.6	0.81	
4.0	1.2	16.4	18.6	2.2	52.8	0.81	
4.0	1.2	14.0	16.0	3.4	52.4	1.3	
5.0	1.5	21.2	24.6	3.4	51.6	1.3	
5.0	1.5	21.0	24.8	3.8	50.7	1.4	
6.0	1.8	24.0	29.0	5.0	49.6	1.8	
6.0	1.8	26.4	31.0	4.6	51.1	1.7	
7.0	2.1	28.2	34.0	5.8	49.8	2.1	
7.0	2.1	26.6	31.6	5.0	50.5	1.8	
8.0	2.5	31.6	37.6	6.0	50.3	2.2	
8.0	2.5	31.6	38.0	6.4	49.9	2.3	
9.0	2.7	34.0	40.0	6.0	51.0	2.2	
9.0	2.7	34.1	40.6	6.5	50.3	2.4	
10.0	3.0	38.0	44.6	6.6	51.1	2.4	
10.0	3.0	39.0	46.0	7.0	51.0	2.6	

Run 4 — 100/125 Cu - H_2O; 0.100" Tapered Orifice

$\Delta p_t/1.9$ "H_2O	$\Delta p_t/L$ "H_2O/"	F paste cc/min	F total cc/min	F excess cc/min	η %	Re,o	Remarks
9.0	2.7	33.6	38.8	5.2	52.0	1.9	70% F
9.0	2.7	34.0	39.6	5.6	51.5	2.1	
8.0	2.5	30.0	35.2	5.2	51.1	1.9	
8.0	2.5	29.6	34.4	4.8	51.7	1.8	
7.0	2.1	24.0	27.2	3.2	52.9	1.2	
7.0	2.1	28.0	32.0	4.0	52.5	1.5	
6.0	1.8	21.4	25.0	3.6	51.3	1.3	
6.0	1.8	23.6	27.0	3.4	52.4	1.3	
5.0	1.5	19.4	22.0	2.6	52.9	0.95	
5.0	1.5	18.4	20.6	2.2	53.6	0.81	
4.0	1.2	14.6	17.0	2.4	51.5	0.88	
4.0	1.2	13.8	16.4	2.6	50.5	0.95	
3.0	0.91	13.0	15.4	2.4	50.6	0.88	
3.0	0.91	13.0	14.6	1.6	53.4	0.59	
2.0	0.61	8.5	9.8	1.3	52.0	0.47	
2.0	0.61	8.5	9.6	1.1	53.1	0.40	
1.0	0.30	4.2	4.5	0.3	56.0	0.079	
1.0	0.30	4.2	4.7	0.5	53.6		

Run 5 100/125 Cu - H_2O
0.100" Tapered Orifice

ΔP_o "H_2O	$\Delta P_o/L_o$ "H_2O/"	$\Delta p_t/1.9$ "H_2O	$\Delta P_t/L$ "H_2O/"	F paste cc/min	F total cc/min	η %	$Re_{,o}$	Remarks
1/16	0.05	1.0	0.30	3.7	4.3	51		Aerated System 70°F
1/16	0.05	1.0	0.30	3.6	4.0	54		
1/8	0.11	2.0	0.61	5.5	6.5	50		
1/8	0.11	2.0	0.61	4.2	5.1	49		
1/4	0.22	3.0	0.91	5.0	6.5	46		
1/4	0.22	3.0	0.91	4.6	5.9	46		
1/4	0.22	3.0	0.91	4.6	6.0	46		
5/8	0.55	4.0	1.2	6.8	8.8	46		
5/8	0.55	4.0	1.2	6.8	8.8	46		
3/4	0.67	5.0	1.5	7.8	10.6	44		
3/4	0.67	5.0	1.5	8.2	10.8	45		
1	0.80	6.0	1.8	9.5	12.5	45		
1	0.80	6.0	1.8	9.9	13.0	45		
1 1/4	1.1	7.0	2.1	10.5	13.9	45.3		
1 1/4	1.1	7.0	2.1	10.5	14.1	44.6		
1 5/8	1.4	8.0	2.5	12.4	16.8	44.3		
1 5/8	1.4	8.0	2.5	11.5	16.0	43.1		
2	1.6	9.0	2.7	11.5	16.7	41.3		
2	1.6	9.0	2.7	12.0	16.8	42.9		
2 1/4	2.0	10.6	3.2	11.2	17.5	38.4		
2 1/4	2.0	10.6	3.2	9.3	15.2	36		
3	2.4	12.4	3.7	11.2	18.9	35.5		
-	-	13.0	3.9	13.7	21.2	38.8		

APPENDIX III

EXPERIMENTAL DATA III

(Correlation Experiment)

Run 6 100/125 Cu-H_2O
0.101" Tapered Orifice

Static Level #	Initial Reading cc	Apparent Total cc	Ft cc/min	F paste cc/min	F excess cc/min	η o/o	Re,o	Remarks
1			11.6	10.0	1.6	5.17	0.57	
1			12.2	10.4	1.8	5.12	0.64	
1			10.4	9.0	1.4	5.19	0.50	
2			12.8	10.8	2.0	5.07	0.71	
2			13.6	11.6	2.0	5.12	0.71	
3			16.0	13.6	2.4	5.10	0.86	
3			15.6	13.2	2.4	5.09	0.86	
4			17.2	14.4	2.8	5.01	1.00	
4			14.4	12.4	2.0	5.16	0.71	
5			16.8	14.2	2.6	50.8	0.93	
5			15.6	13.6	2.0	52.2	0.76	
		Run 7	100/125 Cu-H_2O					
			0.073" Tapered Orifice					
9	7.7	16.5	17.6	15.0	2.6	51.1	1.8	
9	11.7	21.2	19.0	16.6	2.4	52.1	1.6	
5	10.1	17.3	14.4	12.2	2.2	50.8	1.5	
5	8.4	15.2	13.6	12.0	1.6	52.9	1.1	
1	8.5	12.1	7.2	6.2	1.0	52	0.69	
1	8.4	12.1	7.4	6.4	1.0	52	0.69	
		Run 8	100/125 Cu-H_2O					
			0.101" Tapered Orifice					
9	10.7	20.0	18.6	16.0	2.6	51.6	0.93	
9	10.9	21.3	20.8	17.6	3.2	50.8	1.1	
5	11.9	18.8	13.8	11.6	2.2	50.5	0.79	
5	10.3	16.5	12.4	10.4	2.0	50.3	0.72	
1	11.7	15.8	8.2					
1	15.8	20.1	8.8					
		Run 9	100/125 Cu-H_2O					
			0.120" Tapered Orifice					
9	11.8	20.6	17.6	15.2	2.4	51.8	0.61	Wetted agent
9	10.8	20.1	18.6	16.2	2.4	52.1	0.61	added to the
5	12.2	18.2	12.0	10.4	1.6	51.9	0.41	system.
5	11.5	17.7	13.0	10.8	2.2	50.0	0.56	
5	10.2	16.2	12.0	10.4	1.6	51.9	0.41	
1	10.0	13.5	7.0	6.6	0.4	56.2	0.10	
1	13.5	17.2	7.4	6.4	1.0	51.8	0.25	

Run 10 100/125 Cu-H_2O
0.140" Tapered Orifice

Static Level #	Initial Reading cc	Apparent Total cc	F_t cc/min	F paste cc/min	F excess cc/min	η o/o	Re,o	Remarks
9	9.5	19.3	19.6	17.2	2.4	52.8	0.40	
9	10.3	23.7	26.8	23.2	3.6	52.0	0.59	
5	9.5	17.5	16.0	14.0	2.0	52.4	0.33	
5	9.1	17.4	16.8	14.8	2.0	52.9	0.33	
1	7.7	12.1	8.8	8.0	0.8	54.5	0.13	
1	8.8	13.2	8.8	8.0	0.8	54.5	0.13	

Run 11 100/125 Cu-H_2O
0.120" Tapered Orifice

9	22.0	18.0	4.0	49.1	1.0		
9	22.6	18.4	4.2	48.9	1.1		
8	20.4	16.8	3.6	49.3	0.91		
8	20.6	17.2	3.4	50.0	0.86		
7	21.0	17.0	4.0	48.5	1.0		
7	19.6	16.2	3.4	49.6	0.86		
6	17.2	14.4	2.8	50.1	0.71		
6	18.0	15.0	3.0	50.0	0.76		
5	16.0	13.0	3.0	48.8	0.76		
5	14.0	13.0	1.0	50.0	0.25		
4	15.2	12.8	2.4	50.5	0.61		
4	14.6	12.4	2.2	51.0	0.56		
3	13.6	11.6	2.0	51.1	0.51		
3	13.8	12.0	1.8	52.1	0.46		
2	13.0	11.0	2.0	50.8	0.51		
2	11.4	9.6	1.8	50.5	0.46		
1	8.6	7.8	0.8	54.2	0.20		
1	9.0	8.0	1.0	53.2	0.25		

Run 12 100/125 Cu-H_2O
0.199" Tapered Orifice

Static Level #	Initial Reading cc	Apparent Total cc	Ft cc/min	F paste cc/min	F excess cc/min	η o/o	Re,o	Remarks
1	12.2	20.4	16.4	15.2	1.2	55.4	0.11	
1	8.2	14.7	13.0	12.4	0.6	57.0	0.055	
5	6.5	16.9	20.8	19.0	1.8	54.9	0.17	
5	9.9	20.9	22.0	19.6	2.4	53.5	0.22	
9	6.5	21.7	30.4	26.6	3.8	52.7	0.35	
9	6.4	22.0	31.2	27.2	4.0	52.4	0.37	
3	8.8	17.8	18.0	18.6	0.6	55.1	0.55	
3	7.6	16.2	17.2	15.8	1.4	55.2	0.13	
7	9.0	22.0	26.0	23.4	2.6	54.0	0.24	
7	6.2	19.9	27.4	24.0	3.4	52.6	0.31	
8	5.6	19.7	28.2	25.0	3.2	53.1	0.29	
8	--	21.3	--	24.6		--		
6	7.1	19.1	24.0	21.2	2.8	53.0	0.26	
6	9.0	20.1	22.2	20.0	2.2	54.0	0.20	
6			32.0	27.4	4.6	51.2	0.28	
6			31.2	26.6	4.6	51.1	0.28	
3			23.0	20.0	3.0	52.1	0.18	
3			19.2	16.6	2.6	52.0	0.16	
1			14.2	12.6	1.6	53.1	0.10	
1			14.4	13.0	1.4	54.0	0.08	

Run 13 60/80 Cu-H_2O
0.120" Tapered Orifice

9	7.5	25.8	73.2	61.2	12.0	50.1	4.8
9	3.8	21.7	71.6	59.6	12.0	50.0	4.8
5	3.6	17.3	54.8	46.0	8.8	50.2	3.5
5	5.9	19.8	55.6	48.0	7.6	51.8	3.0
1	10.7	18.9	32.8	30.0	2.8	55.0	1.1
1	13.3	21.3	32.0	29.6	2.4	55.0	0.95

Run 14 60/80 Cu-H_2O
0.101" Tapered Orifice

Static Level #	Initial Reading cc	Apparent Total cc	F_t cc/min	F paste cc/min	F excess cc/min	η o/o	Re,o	Remarks
9	7.8	23.2	61.6	48.0	13.6	46.7	7.6	
9	8.7	23.6	59.6	47.2	12.4	47.5	6.9	
8	6.6	20.9	57.2	44.8	12.4	47.1	6.9	
8	8.3	22.5	56.8	44.8	12.0	47.3	6.7	
7	8.7	22.0	53.2	38.4	14.8	43.5	8.3	
7	7.5	21.2	54.8	44.0	10.8	48.2	6.0	
6	5.8	17.7	47.6	38.4	9.2	48.5	5.2	
6	5.2	16.3	44.4	36.0	8.4	48.6	4.7	
5	5.5	17.7	48.8	39.2	9.6	48.1	5.4	
5	5.2	16.4	44.8	36.0	8.8	48.1	4.9	
4	8.3	19.0	42.8	34.4	8.4	48.3	4.7	
4	5.2	15.5	41.2	33.6	7.6	48.9	4.3	
3	7.9	16.6	34.8	29.2	5.6	50.2	3.1	
3	6.0	15.3	37.2	32.0	5.2	51.6	2.9	
2	6.2	14.0	31.2	26.4	4.8	50.8	2.7	
2	5.3	13.8	34.0	28.0	6.0	49.3	3.4	
1	7.0	13.8	27.2	23.6	3.6	52.0	2.0	
1	7.8	14.0	24.8	21.2	3.6	51.1	2.0	

Run 15 60/80 Cu-H_2O
0.149" Tapered Orifice

9	--	--	92.4	76.0	16.4	49.3	4.2	
9	--	--	85.2	69.2	16.0	48.7	4.1	
8	3.5	24.9	85.6	71.2	14.4	49.9	3.7	
8	2.7	24.7	88.0	73.6	14.4	50.1	3.7	
7	3.5	24.2	82.8	69.2	13.6	50.1	3.5	
7	5.6	26.7	84.4	70.4	14.0	50.1	3.6	
6	4.4	23.0	74.4	62.8	11.6	50.6	3.0	
6	4.2	25.0	83.2	69.6	13.6	50.1	3.5	
5	4.9	22.9	72.0	61.6	10.4	51.2	2.7	
5	4.8	25.1	81.2	69.6	11.6	51.2	3.0	Overtime
4	4.2	20.7	66.0	56.4	9.6	51.2	2.5	
4	6.0	20.9	59.6	51.2	8.4	51.5	2.2	
3	3.0	19.2	64.8	55.6	9.2	51.4	2.4	
3	4.2	20.0	63.2	54.4	8.8	51.7	2.3	
2	7.6	22.0	57.6	50.0	7.6	52.0	2.0	
2	4.7	18.1	53.6	46.4	7.2	51.9	1.9	
1	4.6	16.3	46.8	41.2	5.6	52.8	1.4	
1	6.8	18.5	46.8	41.2	5.6	52.8	1.4	

Run 16 230/325 Cu-H_2O
0.101" Tapered Orifice

Static Level #	Initial Reading cc	Apparent Total cc	F_t cc/min	F paste cc/min	F excess cc/min	η o/o	Re,o	Remarks
9	2.0	8.3	6.3	5.4	0.9	51.2	0.12	
9	11.5	19.8	8.3	7.1	1.2	51.2	0.16	
8	8.8	15.1	6.3	5.4	0.9	51.2	0.12	
8	8.6	16.3	7.7	6.6	1.1	51.3	0.15	
7	7.3	15.0	7.7	6.6	1.1	51.3	0.15	
7	6.0	14.3	8.3	7.1	1.2	51.2	0.16	
6	6.5	14.6	8.1	6.9	1.2	51.1	0.16	
6	6.3	14.9	8.6	7.1	1.5	49.6	0.20	
5	7.2	14.0	6.8	5.9	0.9	52.0	0.12	
5	5.6	12.5	6.9	5.9	1.0	51.2	0.14	
4	5.6	11.6	6.0	5.2	0.8	52.0	0.11	
4	9.8	15.1	5.3	4.6	0.7	52.0	0.09	
3	6.5	10.6	4.1	3.7	0.4	54.1	0.05	
3	12.0	16.9	4.9	4.5	0.4	54.0	0.05	
2	5.4	9.8	4.4	4.0	0.4	54.6	0.05	
2	10.5	14.8	4.3	3.9	0.4	54.5	0.05	
1	7.3	10.5	3.2	3.0	0.2	55.6	0.03	
1	7.5	10.9	3.4	3.2	0.2	56.2	0.03	

Run 17 60/80 Cu-H_2O
0.149" Square Orifice

Static Level #	Original Reading cc	Apparent Total cc	F_t cc/min	F paste cc/min	F excess cc/min	η o/o	Re,o	Remarks
9	4.2	21.5	69.2	57.2	12.0	49.6	3.1	
9	4.2	25.5	85.2	70.8	14.4	49.8	3.7	
8	2.8	23.2	81.6	68.0	13.6	50.1	3.5	
8	3.7	24.1	81.6	68.0	13.6	50.1	3.5	
7	3.8	23.3	78.0	64.8	13.2	49.7	3.4	
7	3.8	22.6	75.2	62.8	12.4	50.1	3.2	
6	3.9	22.7	75.2	62.8	12.4	50.1	3.2	
6	3.2	20.6	69.6	58.4	11.2	50.3	2.9	
5	4.8	22.0	68.8	58.0	10.8	50.6	2.8	
5	2.7	22.5	79.2	66.8	12.4	50.6	3.2	
4	4.2	19.8	62.4	54.0	8.4	52.0	2.2	
4	3.3	19.5	64.8	56.0	8.8	51.9	2.3	
3	2.6	16.6	56.0	48.4	7.6	51.5	2.0	
3	3.6	22.2	74.4	64.0	10.4	51.6	2.7	
2	2.8	16.6	55.2	47.6	7.6	51.8	2.0	
2	3.1	16.3	52.8	46.8	6.0	53.1	1.5	
1	5.0	17.6	50.4	44.4	6.0	52.9	1.5	
1	6.5	18.5	48.0	43.2	4.8	54.0	1.2	

Run 18 60/80 Cu-H_2O
0.101" Square Orifice

Static Level #	Initial Reading cc	Apparent Total cc	Ft cc/min	F paste cc/min	F excess cc/min	η o/o	Re,o	Remarks
9	3.3	15.7	49.6	36.0	13.6	43.7	7.6	
9	3.5	16.2	50.8	36.8	14.0	43.5	7.8	
8	3.5	15.2	46.8	34.8	12.0	44.6	6.7	
8	3.6	14.8	44.8	33.2	11.6	44.5	6.5	
7	5.0	24.4	38.8	29.0	9.8	44.8	5.5	
7	3.0	14.3	45.2	33.6	11.6	44.7	6.5	
6	2.8	13.3	42.0	32.0	10.0	45.7	5.6	
6	4.5	14.0	38.0	28.4	9.6	49.7	5.4	
5	5.1	14.8	38.8	30.0	8.8	46.4	4.9	
5	4.8	14.5	38.8	29.6	9.2	45.7	5.2	
4	3.7	21.2	35.0	27.0	8.0	46.3	4.5	
4	5.2	22.5	34.6	26.6	8.0	46.0	4.5	
3	4.6	20.3	31.4	24.2	7.2	46.2	4.0	
3	4.2	18.6	28.8	22.8	6.0	47.4	3.4	
2	4.4	17.8	26.8	20.8	6.0	46.5	3.4	
2	3.9	17.3	26.8	21.4	5.4	47.8	3.0	
1	4.8	16.0	22.4	18.0	4.4	48.0	2.5	
1	4.3	16.2	23.8	19.2	4.6	49.5	2.6	

Run 19 230/325 Cu-H_2O
0.149" Square Orifice

9	6.2	13.4	7.2	6.1	1.1	50.8	0.068
9	4.6	14.3	9.7	8.2	1.5	50.8	0.093
8	6.9	18.0	11.1	9.5	1.6	51.2	0.099
8	5.8	16.5	10.7	9.1	1.6	51.0	0.099
7	3.9	13.8	9.9	8.6	1.3	51.6	0.080
7	6.1	16.0	9.9	8.6	1.3	51.9	0.080
6	5.0	13.9	8.9	7.7	1.2	51.9	0.074
6	3.8	12.7	8.9	7.7	1.2	51.9	0.074
5	3.6	12.2	8.6	7.5	1.1	52.2	0.068
5	3.8	12.0	8.2	7.2	1.0	52.6	0.06
4	4.9	12.3	7.4	6.5	0.9	52.7	0.06
4	6.2	13.7	7.5	6.6	0.9	52.7	0.06
3	8.0	15.0	7.0	6.5	0.5	55.6	0.03
3	7.3	14.2	6.9	6.2	0.7	53.9	0.04
2	7.3	13.7	6.4	5.9	0.5	55.2	0.03
2	5.2	11.8	6.6	6.0	0.6	54.6	0.04
1	4.3	10.6	6.3	6.0	0.3	57.1	0.02
1	7.1	13.1	6.0	5.7	0.3	57.0	0.02

Run 20 230/325 Cu-H_2O
0.149" Tapered Orifice

Static Level #	Original Reading cc	Apparent Total cc	F_t cc/min	F paste cc/min	F excess cc/min	η o/o	Re,o	Remarks
9	5.8	11.2	10.8	9.8	1.0	54.5	0.062	
9	4.9	11.0	12.2	11.2	1.0	55.0	0.062	
8	7.5	12.0	9.0	8.2	0.8	54.7	0.050	
8	5.7	15.8	10.1	9.2	0.9	54.1	0.056	
7	6.6	12.0	10.8	9.6	1.2	53.3	0.075	
7	7.3	11.5	8.4	8.0	0.4	54.0	0.025	
6	8.6	13.2	9.2	8.6	0.6	56.0	0.037	
6	7.1	10.9	7.6	7.2	0.4	56.9	0.025	
5	8.3	12.7	8.8	8.4	0.4	57.1	0.025	
5	8.8	12.4	7.2	7.0	0.2	58.1	0.012	
4	8.1	16.1	8.0	7.5	0.5	56.2	0.031	
4	7.2	15.6	8.4	7.7	0.7	55.0	0.043	
3	9.6	17.0	7.4	7.0	0.4	56.8	0.025	
3	7.7	14.4	6.7	6.2	0.5	55.6	0.031	
2	8.3	14.6	6.3	6.1	0.2	58.0	0.012	
2	13.4	18.9	5.5	5.2	0.3	56.8	0.019	
1	8.0	12.9	4.9	4.7	0.2	57.6	0.012	
1	7.1	12.6	5.5	5.3	0.2	57.8	0.012	

Run 21 230/325 Cu-H_2O
0.120" Tapered Orifice

9	5.5	13.9	8.4	7.3	1.1	52.1	0.10
9	5.5	15.3	9.8	8.4	1.4	51.5	0.13
5	10.1	17.4	7.3	6.3	1.0	51.9	0.10
5	9.5	16.7	7.2	6.3	0.9	52.2	0.09
1	6.8	10.7	3.9	3.7	0.2	56.9	0.019
1	8.5	12.8	4.3	4.1	0.2	57.1	0.019

Run 22 230/325 Cu-H_2O
0.101" Tapered Orifice

Static Level #	Original Reading cc	Apparent Total cc	F_t cc/min	F paste cc/min	F excess cc/min	η o/o	Re,o	Remarks
9	7.7	16.4	8.7	7.4	1.3	51.0	0.18	
9	8.0	17.2	9.2	7.8	1.4	50.9	0.19	
8	6.5	14.7	8.2	7.0	1.2	51.0	0.16	
8	8.0	15.6	7.6	6.5	1.1	51.3	0.15	
7	7.0	14.9	7.9	6.8	1.1	51.6	0.15	
7	11.4	19.6	8.2	7.0	1.2	51.2	0.16	
6	6.9	13.5	6.6	5.7	0.9	51.8	0.12	
6	8.8	15.0	6.2	5.3	0.9	51.1	0.12	
5	6.4	12.4	6.0	5.2	0.8	52.0	0.11	
5	6.5	11.5	5.0	4.7	0.3	56.4	0.041	
4	9.4	14.5	5.1	4.6	0.5	54.1	0.068	
4	7.5	12.7	5.2	4.7	0.5	54.2	0.068	
3	9.3	14.0	4.7	4.3	0.4	54.8	0.054	
3	8.9	14.3	5.4	4.9	0.5	54.4	0.068	
2	8.1	12.5	4.4	4.2	0.2	57.2	0.027	
2	10.7	15.0	4.3	4.0	0.3	56.2	0.041	
1	9.0	13.1	4.1	3.9	0.2	57.0	0.027	
1	6.3	9.7	3.4	3.2	0.2	56.4	0.027	

Run 23 60/80 Cu-H_2O
0.075" Tapered Orifice

9	3.0	22.9	39.8	28.0	11.8	42.2	12.6
9	1.6	23.4	43.6	30.2	13.4	41.7	14.3
8	2.9	24.0	42.2	29.4	12.8	41.7	13.7
8	3.3	24.5	42.4	29.4	13.0	41.6	13.9
7	3.6	22.8	38.4	26.8	11.6	41.4	12.4
7	3.3	21.8	37.0	26.0	11.0	42.1	11.8
6	4.5	22.7	36.4	25.6	10.8	42.1	11.5
6	5.3	23.7	35.8	25.2	10.6	42.2	11.3
5	2.8	17.4	29.2	21.2	8.0	43.5	8.6
5	3.4	19.9	33.0	23.8	9.2	43.2	9.8
4	5.3	19.6	28.6	20.8	7.8	43.6	8.3
4	6.6	21.0	28.8	21.2	7.6	44.2	8.1
3	3.0	14.7	23.4	17.4	6.0	44.6	6.4
3	3.5	17.2	27.4	20.2	7.2	44.3	7.7
2	5.8	17.0	22.4	17.2	5.2	46.0	5.6
2	5.5	16.1	21.2	16.2	5.0	45.8	5.4
1	3.4	13.3	19.8	15.4	4.4	46.5	4.7
1	6.0	16.2	20.4	15.6	4.8	46.0	5.1

Run 24 100/125 Cu-H_2O
0.199" Square Orifice

Static Level #	Initial Reading cc	Apparent Total cc	F_t cc/min	F paste cc/min	F excess cc/min	η o/o	Re,o	Remarks
9	6.0	17.0	22.2	19.2	3.0	52.0	0.28	
9	4.9	16.8	23.8	20.4	3.4	51.3	0.31	
8	4.2	20.6	32.8	27.8	5.0	50.8	0.46	
8	5.5	17.7	24.4	21.2	3.2	52.0	0.29	
7	3.5	13.0	19.0	17.0	2.0	53.7	0.18	
7	5.0	15.8	21.6	19.0	2.6	52.9	0.24	
6	4.0	14.1	20.2	17.6	2.6	52.0	0.24	
6	4.9	15.0	20.2	17.8	2.4	53.0	0.22	
5	4.8	17.3	25.0	21.8	3.2	52.2	0.29	
5	5.9	15.7	19.6	17.4	2.2	53.2	0.20	
4	7.1	15.6	17.0	15.4	1.6	54.1	0.15	
4	4.2	15.2	22.0	19.2	2.8	52.2	0.26	
3	4.5	12.2	15.4	14.0	1.4	54.5	0.13	
3	5.7	13.8	16.2	14.6	1.6	54.0	0.15	
2	3.5	10.9	14.8	13.6	1.2	55.2	0.11	
2	4.4	11.3	13.8	12.6	1.2	55.0	0.11	
1	6.0	12.3	12.6	11.8	0.8	56.1	0.074	

Run 25 60/80 Glass Beads - H_2O
0.149" Tapered Orifice

9	3.2	24.7	129.0	112.2	16.8	52.0	4.33
8	3.1	24.1	126.0	109.2	16.8	52.0	4.33
8	2.8	23.6	124.8	108.6	16.2	52.1	4.18
7	3.9	21.8	107.4	94.2	13.2	52.6	3.40
7	4.8	22.3	105.0	91.2	13.8	52.0	3.56
6	5.2	22.8	105.6	93.6	12.0	53.1	3.10
6	4.8	22.0	103.2	91.8	11.4	53.4	2.94
5	3.4	19.6	97.2	85.8	11.4	53.0	2.94
5	5.2	20.2	90.0	79.8	10.2	53.1	2.63
4	4.4	18.8	86.4	77.4	9.0	53.7	2.3
4	4.4	18.6	85.2	76.2	9.0	53.7	2.3
3	4.9	23.3	73.6	65.2	8.4	53.1	2.2
3	4.7	22.8	72.4	64.4	8.0	53.5	2.1
2	3.4	18.3	59.6	53.2	6.4	53.7	1.7
2	3.0	19.1	64.4	57.2	7.2	53.2	1.9
1	4.7	17.2	50.0	44.8	5.2	53.8	1.3
1	5.0	18.4	53.6	48.0	5.6	53.8	1.4

Run 26 230/325 Glass - H_2O
0.149" Tapered Orifice

Static Level #	Initial Reading cc	Apparent Total cc	F_t cc/min	F paste cc/min	F excess cc/min	η o/o	Re,o	Remarks
9	4.8	16.8	24.0	22.4	1.6	56.0	0.099	
9	6.0	15.3	18.6	17.4	1.2	56.0	0.074	
5	7.1	15.7	17.2	16.4	0.8	57.1	0.050	
5	6.9	13.2	12.6	12.0	0.6	57.0	0.037	
1	5.8	12.0	12.4	12.0	0.4	58.0	0.025	
1	7.5	13.2	11.4	11.0	0.4	57.8	0.025	

Run 27 100/125 Glass - H_2O
0.199" Tapered Orifice

9	3.2	17.2	84.0	78.0	6.0	55.8	0.55	
9	4.1	17.5	80.4	74.4	6.0	55.6	0.55	
5	4.5	19.2	58.8	54.4	4.4	55.6	0.41	
5	5.8	21.0	60.8	56.0	4.8	55.2	0.44	
1	4.8	21.3	33.0	31.0	2.0	56.2	0.18	
1	4.5	20.5	32.0	31.2	0.8	56.6	0.074	

Run 28 230/325 Cu-Ethylene Glycol #1
0.149" Tapered Orifice

9	5.9	10.6	2.3	~2.3	~0	56	~0	Effluent bed
9	5.2	7.8	1.3	~1.3	~0	56	~0	density 0.56
5	8.3	11.0	0.9	0.9	0	56	0	
5	7.0	9.2	0.7	0.7	0	56	0	
1	6.5	8.3	0.6	0.6	0	56	0	

Run 29 60/80 Cu-Ethylene Glycol #2
0.149" Tapered Orifice

9	6.0	12.1	6.1	5.6	0.5	51	0.52	Effluent bed
9	4.0	10.4	6.4	5.8	0.6	51	0.62	density 0.56
5	3.8	8.5	4.7	4.4	0.3	53	0.31	
5	4.5	9.2	4.7	4.3	0.4	51	0.41	
1	6.5	12.6	3.0	2.8	0.2	52	0.29	
1	8.2	14.4	3.1	2.9	0.2	52	0.29	

Run 30 60/80 Cu-Ethylene Glycol #3
0.149" Tapered Orifice

Static Level #	Initial Reading cc	Apparent Total cc	F_t cc/min	F paste cc/min	F excess cc/min	η o/o	Re,o	Remarks
8	5.0	18.4	26.8	23.2	3.6	48	10.8	Effluent bed
8	5.3	17.7	24.8	21.4	3.8	48	11.4	density 0.56
5	5.2	13.4	16.4	14.6	2.0	50	6.0	
5	6.5	15.0	17.0	15.0	2.0	49	6.0	
1	6.2	11.6	10.8	10.0	0.8	52	2.4	
1	6.3	10.6	8.6	8.0	0.6	52	1.8	

Run 31 100/120 Al_2O_3 - H_2O
D_o = 0.296" D_t = 5/8"

Static Level #	Original Reading cc	Apparent Total cc	$F_t/2$ cc/min	F paste/2 cc/min	η o/o	Remarks
2	55.0	87.5	32.5	26.8	49.5	Tapered orifice
2	58.5	90.5	32.5	27.0	49.7	Nonspherical
2	Nonwetted		34.5	26.3	45.9	
2	Nonwetted		29.0	23.0	47.5	
4	61.7	87.5	25.8	22.1	51.2	
4	63.5	97.5	34.5	28.1	50.1	
4	Nonwetted		36.0	28.0	46.8	
4	Nonwetted		39.0	31.0	47.7	

Run 32 100/120 Al_2O_3 - H_2O
D_o = 0.296" D_t = 1/2"

2	65.6	83.1	17.5	17.0	58.2	Tapered orifice
2	62.2	78.0	14.8	14.2	57.6	Nonspherical
2	Nonwetted		23.0	18.1	47.7	
2	Nonwetted		22.5	18.5	49.3	
4	62.9	85.4	22.5	19.2	51.2	
4	63.6	86.5	22.9	20.1	52.9	
4	Nonwetted		24.9	19.1	46.1	
4	Nonwetted		26.0	21.0	48.3	

Run 33 100/120 Al_2O_3 - H_2O
D_o = 0.296" D_t = 3/8"

Static Level #	Original Reading cc	Apparent Total cc	$F_t/2$ cc/min	F paste/2 cc/min	η o/o	Remarks
2	57.8	73.0	15.2	14.2	56.0	Tapered orifice
2	51.1	64.1	13.0	12.1	55.0	Nonspherical
2	Nonwetted		13.6	11.2	49.5	
2	Nonwetted		14.0	12.0	51.5	
4	54.4	68.0	13.6	13.0	57.1	
4	48.5	62.0	13.6	12.2	53.9	
4	Nonwetted		15.1	12.5	49.6	
4	Nonwetted		14.8	12.1	49.1	

Run 34 100/120 Al_2O_3 - H_2O
D_o = 0.296" D_t = 3/4"

Static Level #	Initial Reading cc	Apparent Total cc	$F_t/2$ cc/min	F paste/2 cc/min	η o/o	Remarks
2	48.0	92.6	44.6	38.0	51.0	Tapered orifice
2	48.6	94.6	46.0	38.9	50.6	Nonspherical
2			49.7	39.9	48.0	
2			50.0	39.3	47.2	
4	48.0	96.0	48.0	41.0	51.1	
4	47.4	93.1	45.7	38.0	50.0	
4			56.5	43.0	45.7	
4			57.5	44.4	46.3	

Run 35 100/120 Al_2O_3 - Ethylene Glycol
D_o = 0.296" D_t = 1/2"

4	62.0	68.5	6.5	6.2	57.1	Tapered orifice
4	58.8	66.2	7.4	7.1	55.5	Nonspherical
4	65.7	74.9	9.2	8.2	53.3	Nonwetted
4	28.8	37.2	8.4	8.0	57.1	Nonwetted

Run 36 100/125 Cu-H_2O
D_o = 0.296" D_t = 1/2"

Static Level #	Initial Reading cc	Apparent Total cc	F_t cc/min	F paste cc/min	η o/o	Remarks
4	59.2	70.7	23.0	22.0	57.4	
4	59.6	73.1	27.0	25.0	55.5	
4	58.8	68.0	18.4	19.8	55.9	Nonwetted
4	7.1	15.0	15.8	15.6	59.0	Nonwetted
2	56.6	81.0	24.4	22.5	55.5	
2	54.7	84.2	29.5	27.1	55.5	
2	22.0	43.5	21.5	19.9	55.7	Nonwetted
2	28.1	48.2	20.1	18.2	54.2	Nonwetted

Run 37 100/125 Cu-H_2O
D_o = 0.296" D_t = 1.00"

4	166.0	215.0	49.0	43.0	52.6	
4	161.5	208.6	47.1	41.0	52.2	
4	166.5	225.5	59.0	51.0	51.9	Nonwetted
2	162.0	201.0	39.0	34.5	53.0	

Run 38 100/125 Cu-H_2O
D_o = 0.296" D_t = 3/4"

2	54.1	86.6	32.5	29.0	53.2	
2	55.5	89.8	34.3	30.5	53.3	
2	52.0	90.0	38.0	33.1	52.3	Nonwetted
2	46.2	84.8	38.6	33.3	51.7	Nonwetted
4	60.0	93.5	33.5	29.6	53.0	
4	55.1	92.2	37.1	32.5	52.5	
4	56.9	98.0	41.1	36.0	52.4	Nonwetted
4	29.7	75.4	45.7	39.6	52.0	Nonwetted

Run 39 100/125 Cu-H_2O
D_o = 0.296" D_t = 3/8"

2	54.3	75.9	21.6	20.1	55.9	
2	58.1	83.1	25.0	23.1	55.5	
2	53.8	69.1	15.3	13.6	53.2	Nonwetted
2	54.8	69.5	14.7	13.6	55.5	Nonwetted
4	52.8	74.7	21.9	20.6	56.5	
4	56.0	78.1	22.1	20.5	55.7	
4	59.4	73.9	14.5	13.1	54.2	Nonwetted
4	56.5	73.0	16.5	15.0	54.6	Nonwetted

Run 40 100/125 Cu-H_2O
D_o = 0.296" D_t = 5/8"

Static Level #	Initial Reading cc	Apparent Total cc	F_t cc/min	F paste cc/min	η o/o	Remarks
4	62.4	93.0	30.6	27.2	53.2	
4	59.0	93.0	34.0	29.9	52.9	
4	38.0	54.6	16.6	15.0	54.0	Nonwetted
4	22.6	41.0	18.4	16.2	53.9	Nonwetted
2	61.2	91.2	30.0	26.4	52.9	
2	60.0	86.1	26.1	23.2	53.4	
2	17.0	46.0	29.0	25.1	52.0	Nonwetted
2	28.0	69.5	41.5	35.2	50.9	Nonwetted

APPENDIX IV

VARIANCE

The variance denoted by σ^2 is defined as $\sigma^2 = \frac{\Sigma (x - \bar{x})^2}{n - 1}$ where $\bar{x}$ is the mean of the variable x, and n is the number of observations.

The above expression for the variance can be written as the following algebraically equivalent formula

$$\sigma^2 = [\Sigma (x^2) - \frac{(\Sigma x)^2}{n}] / n-1$$

This form was used in the calculations of variances. From the data shown in Page 36, one can calculate as follows:

(1) Square the individuals and add.

$(52.0)^2 + (51.3)^2 + \cdots\cdots\cdots + (51.1)^2 = 31503.82$

(2) Obtain the total for each row, square these totals, sum these squares, and divide this total by the number of individuals in each row.

$\{(52.0 + 51.3 + \cdots)^2 + (51.6 + 52.4 + \cdots\cdots)^2\} / 6 = 31498.30$

(3) Repeat (2) for each column this time.

$\{(52.0 + 51.6)^2 + \cdots\cdots\} / 2 = 31501.94$

(4) Obtain the grand total for all individuals, square this grand total, and divide by the grand total number of individuals.

$(52.0 + 51.3 + \cdots\cdots)^2 / 12 = 31498.25$

These values were used in obtaining the table of variances as shown in Table V.

BIBLIOGRAPHY

1. Abbott, T. S., Use of Slide Angles for Calculation of Bulk Materials Remaining in Hopper Cars, Chemical Processing, page 206, October 1952.

2. Belden, D. H., and Kassel, L. S., Pressure Drops Encountered in Conveying Particles of Large Diameter in Verticle Transfer Lines, Industrial Engineering Chemistry, 41 page 1174, (1949).

3. Boeza, Walter J., A Course in Powder Metallurgy, Reinhold Publishing Corporation, New York, 1943.

4. Bonilla, Charles F., Fluid Flow in Reactor Systems, Nuclear Engineering Handbook, Section 9, McGraw Hill Book Company, 1958.

5. Box, G. E. P., and Wilson, K. B., On the Experimental Attainment of Optimum Conditions, J. Royal Stat. Soc., 13, No. 1 (1951).

6. Box, G. E. P., The Exporation and Exploitation of response Surfaces: Some general considerations and examples., Biometrics, 10, No. 1, (1954).

7. Brownell, L. E., et. al., Flow of Fluids Through Porous Media, Chem. Engr. Prog. 43, page 537, (1947).

8. Brownlee, M. A., Industrial Experimentation, Chemical Publishing Co. Inc., New York 1953.

9. Calvert, Seymour, et. al., Summary Report on a Preliminary Study of the Flow of Paste, E.R.I., U. of M., 2396-1-P, September 1955.

10. Calvert, Seymour, et. al., Summary Report on Continuation of the Study of the Flow of Paste, E.R.I., U. of M., 2396-5-P, January 1956.

11. Calvert, Seymour, et. al.,, Summary Report on the Study of the Flow of Paste, E.R.I., U. of M., 2396-13-P, November 1956.

12. Calvert, Seymour, et. al., Flow of Dense Pastes in Vertical Tubes, Ind. and Eng. Chem., 50, page 1793, (1958).

13. Churchill, Ruel, V., Introduction to Complex Variables and Applications, McGraw Hill Book Company, 1948.

14. Fluid Flow Through Packed Beds, Chemical Engineering Report, Chemical Engineering, May 1949.

15. Dallavalle, J. M., Micromeritics, second edition, Pitman Publishing Corporation, New York, 1948.

16. Dennis, R. C., The Determination of Optimum Conditions, "The Method of Steepest Ascent," Atomic Power Development Associates, Inc., Detroit.

17. Eirich, F. R., Rheology, Vol. 1 and 2, Academic Press, Inc., 1956.

18. Ellis, Richard B., Personal Communication, March 1959.

19. Farbar, Leonard, Flow Characteristics of Solids - Gas Mixtures in a Horizontal and Vertical Circular Conduit, Ind. Eng. Chem. 41, page 1184, (1949).

20. Gillard, E. R., et. al., Gas and Solid Mixing in Fluidized Beds, Ind. Eng. Chem., 41, page 1191, (1949).

21. Goulden, C. H., Method of Statistical Analysis, John Wiley & Sons, Inc., New York, 1956.

22. Hammitt, Frederick G., Brown, E. M., Natural Convection Flow in Liquid-Metal Mobile-Fuel Nuclear Reactors, Preprint Paper No. 58, Nuclear Engr. & Sci. Conf., EJC, April 4-7, 1960, New York, N.Y.

23. Happel, John, Pressure Drop due to Vapor Flow Through Moving Bed, D. Sc. Thesis, Polytechnic Institute of Brooklyn, September 1948.

24. Happel, John, Pressure Drop due to Vapor Flow Through Moving Bed, Ind. Eng. Chem., 41, page 1101, (1949).

25. Hermans, J. J., Flow Properties of Disperse Systems, North-Holland Publishing Company, Amsterdam, 1953.

26. Lapidus, Leon, et. al., Mechanics of Vertical-Moving Fluidized Systems, A.I. Ch. Eng. Journal, 3, page 63, (1957).

27. Lapple, C. E., et. al., Fluid and Particle Mechanics, University of Delaware, March 1951.

28. Lewis, W. K., et. al., Characteristics of Fluidized Particles, Ind. Eng. Chem., 41, page 1104, (1949).

29. Leva, M., et. al., Fluid Flow Through Packed and Fluidized Systems, U. S. Bureau of Mines, Bulletin No. 504, 1951.

30. Leva, M., et. al., Flow Through Packings and Beds, Part 2 Fixed and Moving Beds, Chem. Eng., July through September 1957.

31. Lowenstein, J. G., For Horizontal Flow of Slurries, Design So Solids Cannot Settle Out, Chemical Engineering, January 1959.

32. Matheson, G. L., et. al., Characteristics of Fluid-Solid System, Ind. Eng. Chem., 41, page 1099, (1949).

33. McCune, L. K., et. al., Mass and Momentum Transfer in Solid-Liquid System: Fixed and Fluidized Beds, Ind. Eng. Chem., 41, page 1124, (1949).

34. Morse, R. D., Fluidization of Granular Solids Fluid Mechanics and Quality, Ind. Eng. Chem., 41, page 1147, (1949).

35. Musket, M., et. al., Flow of Gas Through Porus Media Physics, 1, pages 27 through 34, (1931).

36. Oliver, R. C., Goldstein, A., et. al., System Evaluation of the Flowable Solids Reactor, Phase 1. FLR-1 Summary Report - Fuel Study.

37. Prandtle, L., Tietjens, O. G., Applied Hydro and Aeromechanics, McGraw Hill Book Co., Inc., New York, 1934.

38. Schoenborn, E. M., et. al., Pressure Drop and Flooding Velocity in Packed Towers with Viscons Liquids, Trans. Am. Inst. Chem. Eng., 40, page 51, (1944).

39. Schwarzkopf, Paul, Powder Metallurgy: Its Physics and Production, Macmillian Company, 1947.

40. Quarterly Technical Report to Atomic Power Development Associates, Inc., on Uranium-Sodium Paste. Southern Research Institute project 834, report 1 through 24, April 1956 to April 1958.

41. Streeter, Victor, L., Fluid Mechanics, McGraw-Hill Book Company, New York, 1958.

42. Wulff, John, Powder Metallurgy, American Society for Metals, 1942.

43. Zenz, F. A., How Solid Catalysts Behave, Petroleum Refiner, page 173, April 1957.

44. Zwikker, C., Physical Properties of Solid Material, Interscience Publishers, Inc., New York, 1954.